Re-interpretation of the geology of the Cape Breton Highlands using combined remote sensing and geological databases

by

Martin Ethier

B.A. Mount Allison University (1997)

Advanced Diploma in Remote Sensing, Centre of Geographic Sciences (1998)

Thesis

submitted in partial fulfilment of the requirements for

the Degree of Master of Science (Geology)

Acadia University

Spring Convocation 2001

Table of Contents

List of Figures

List of Tables

Acknowledgements

I would like to thank the people that made this project possible. Foremost Dr. Sandra Barr for her assistance, advice, encouragement, and financial support through her research grant from the Natural Sciences and Engineering Research Council of Canada. Additional financial support was provided by the Department of Geology, partial graduate assistantships from Acadia University, and a Geomatics Canada Scholarship from the Canadian Institute of Geomatics.

Discussions with Dr. Robert Raeside, both in and out of the truck during ground-truthing, proved especially helpful. Thanks to Dr. Barr and Dr. Raeside for their patience and many comments throughout the duration of course work and the writing of the thesis. I would like to thank Tim Webster for his support and suggestions, and providing me with data. Also I am grateful to faculty at the Centre of Geographic Sciences for providing me with the skills to complete this project.

I thank Dr. Alan Macdonald, Dr. Cliff Stanley and Dr. Ian Spooner for their helpfulness and assistance in and out of the classroom, and also Ken Ford of the Radiation Geophysics Section Mineral Resources Division of the Geological Survey of Canada for providing me with airborne gamma-ray spectrometry data.

Last, but not least, I would like to thank Nisha Dubey for her encouragement and support throughout the project.

Abstract

Relationships among the varied rock units of the Cape Breton Highlands as revealed by geological mapping are not everywhere clear, in part due to limited exposure and also to difficulty of access in some areas. This study was undertaken to try to improve on the geological interpretation of the highlands, especially in those problematic areas, by combining geological and remote sensing databases.

The geological database was assembled based mainly on published maps. Remotely sensed information used in the study included Radarsat S7, Landsat TM, gravity, magnetic (vertical gradient and total field) and radiometric data. A Digital Elevation Model (DEM) was constructed from 174 Nova Scotia 1:10,000-scale contour map sheets. The geological, geophysical, and remotely sensed data were integrated into a Geographical Information System, and the resulting database was used to evaluate the various geological interpretations of the highlands. The combined DEM and vertical gradient image and a classified image based on radiometric data proved most useful in the interpretation process.

The key result of the study was to demonstrate how the combined data sets can lead to improved geological interpretation, in particular with respect to geological contacts between known map units in poorly exposed areas, and in the location of major faults and postulated terrane boundaries. Granitoid map units were best detected and distinguished with the radiometric data.

Chapter 1. Introduction

1.1 Purpose of the Study

The Cape Breton Highlands of northern Cape Breton Island, Nova Scotia are underlain by rocks that range in age from more than 1200 Ma to less than 360 Ma, and display a wide range in composition. Relationships among these varied rocks as revealed by geological mapping are not everywhere clear, in part due to limited exposure and also difficulty of access in some areas.

In Nova Scotia we are fortunate to have a wide variety of digital geological and geophysical information. For example, a large geological database exists for the highlands based on detailed mapping, much of it at 1:10,000 scale, during the 1980's by faculty and students at Acadia University and, in the western highlands, Dalhousie University. Additional mapping in some areas was done more recently by Lynch and Tremblay (1992), Lynch and Brisson (1996), Lynch and Giles (1995) and Lynch (1996). Three different digital geological interpretations of the Cape Breton Highlands have been published: Barr & Raeside (1992), Lynch et al. (1997) and Keppie (2000). Remotely sensed data available for the highlands include Radarsat S7, Landsat TM, gravity, magnetic (vertical gradient and total field) and radiometric. Although much of this material has been available for a few years, it had not been combined and evaluated in an organized and consistent way, and then used to further evaluate geological interpretations.

Hence, the goal of this study was to integrate geological, geophysical and remotely sensed data within a Geographical Information System (GIS), and use the results to evaluate the various geological interpretations of the Cape Breton Highlands.

A key goal of the study was to improve on the geological interpretations, in particular with respect to the distribution of major faults and postulated terrane boundaries.

This thesis represents the first project done within the framework of the collaborative MSc. program between the Department of Geology at Acadia University and the Centre of Geographic Sciences (COGS).

1.2 Study Area

The study area encompasses the northern part of Cape Breton Island and includes parts of Victoria and Inverness counties and a small portion of northwestern Cape Breton County (Fig. 1.1). It includes seven full National Topographic Data Base (NTS) 1:50,000 map sheets (11K/03, 11K/02, 11K/06, 11K/07, 11K/11, 11K/10 and 11K/15) and parts of six additional sheets (11K/01, 11K/08, 11K/09, 11K/15, 11K/16, 11N/02 and 11N/01) (Fig. 1.1). The area also includes 174 Nova Scotia Topographic Database (NSTDB) 1:10,000 scale map sheets (Fig. 1.2).

1.3 Methods

Remote sensing and geographic information systems has a role to play in virtually all aspects of this thesis. Designed to store and manipulate spatially referenced information, and able to access and utilize data from a variety of external sources, the GIS can quickly analyze large volumes of data that are time and cost-prohibitive using manual methods. The GIS requires a degree of consistency and structure in the initial database construction; updating geographic information and adding new information follows a predetermined structure ensuring a degree of data quality and control. Within

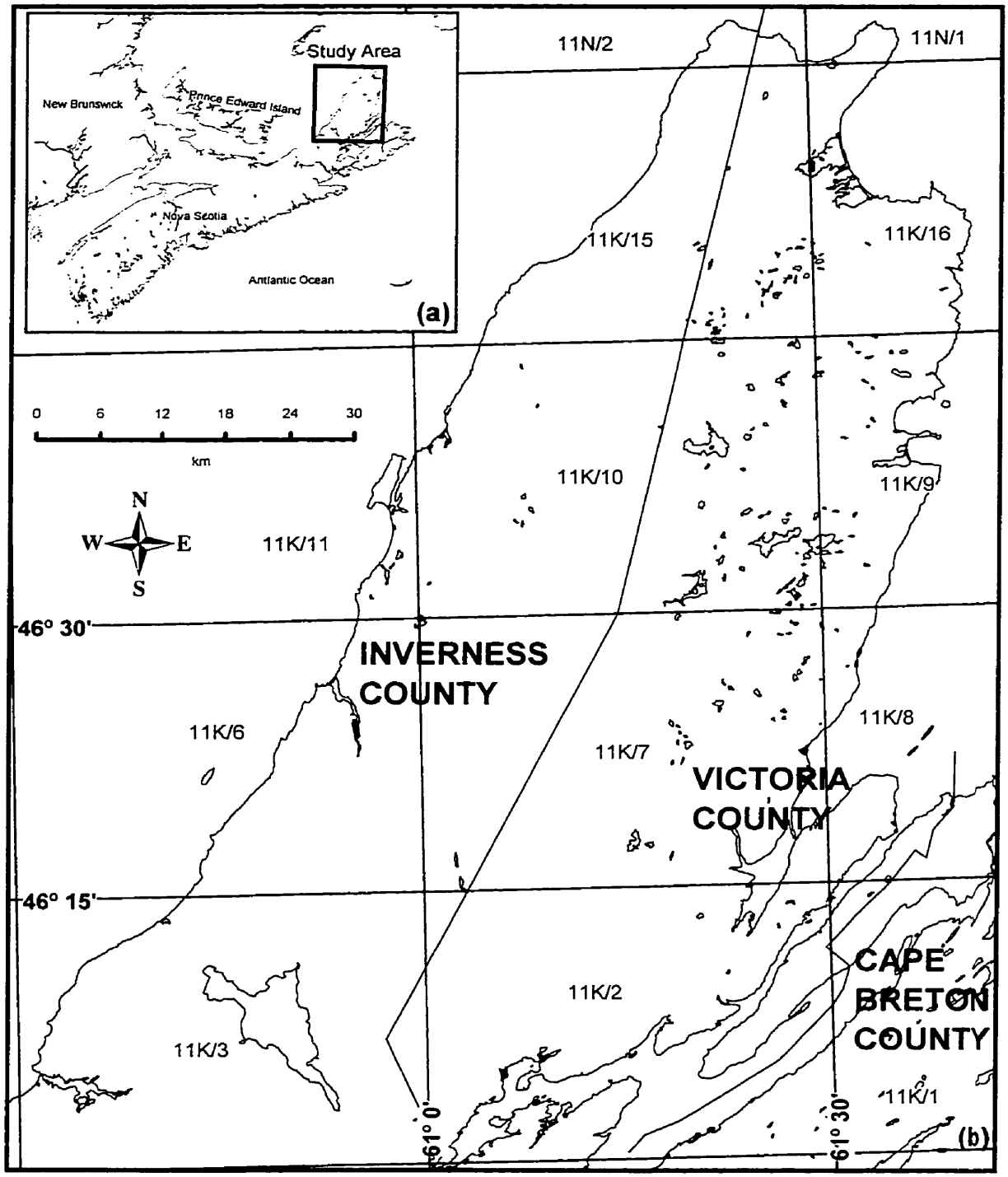

Figure 1.1 (a) Location of the study area in northern Nova Scotia. (b) Outline map of northern Cape Breton Island, showing counties and National Topographic Data Base (NTDB) boundaries.

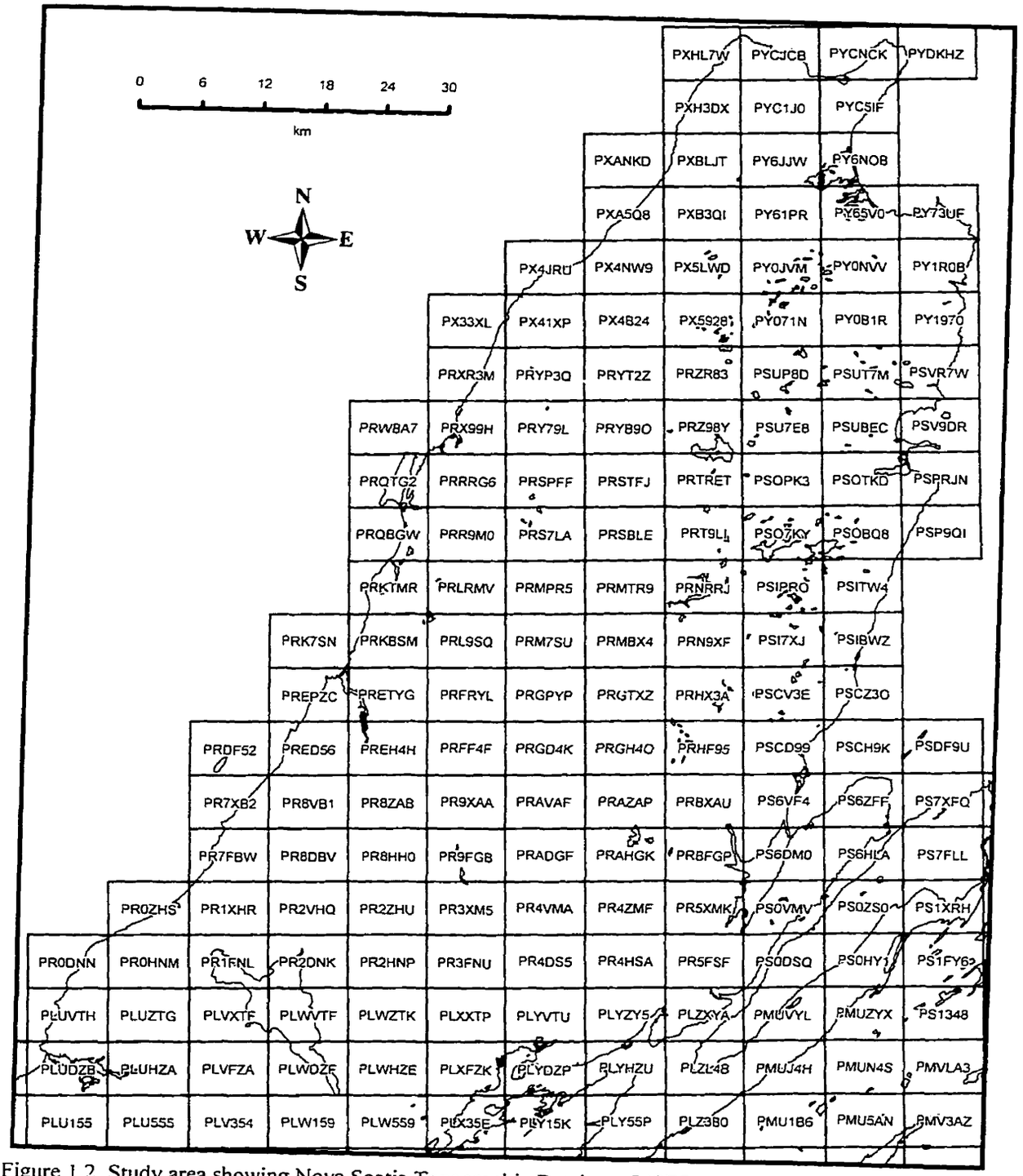

Figure 1.2 Study area showing Nova Scotia Topographic Database (NSTDB) 1:10,000 scale digital maps.

this study, the GIS emphasis was on the generation, organization, and analysis of data sets. The strength of a GIS is the ability to merge spatial datasets from quite different sources and map projections. Displaying and manipulating these combinations typically leads to an understanding and interpretation of spatial occurrences that are not apparent when these data were viewed by themselves. For example, by superimposing several digital geological maps at the same map projection, areas of agreement and disagreement between maps were apparent. Also, after superimposing the interpreted geology on a satellite image, elevation model or airborne geophysical map, it became apparent whether or not a particular lithology had a distinctive texture or spectral response.

Remote sensing methodologies also have a role to play, including non-intrusive data generation (e.g. lineament interpretation, image classification) and data registration and fusion (e.g. Intensity, Hue and Saturation (IHS) transform combinations of geophysical data and SAR imagery or elevation model allowing simultaneous interpretation of diverse data sets) (Harris et al. 1994). The process of data visualization and information dissemination was performed by both geographic information and image analysis systems.

Because of the large size of the study area, detailed geological information was examined only for selected areas and then ground truthed. Candidate areas were chosen based on their geological importance and relative degree of disagreement between published information. On a regional scale, structural and lithological domains were compared and evaluated with the processed imagery and GIS layers. The methods used are described in more detail in Chapter 2.

1.4 Computer Software

The principal image analysis system used in this study is the PCI Geomatics suite of remote sensing software, including EASI, XPACE, IMAGEWORKS and GCPWORKS. In order to incorporate all raster and vector data sets in the GIS, certain fundamental pre-processing operations were performed as indicated above. The main GIS used was MapInfo with the Vertical Mapper extension. The workstation was principally a Pentium II 400 with 192 megabyte RAM and 10 gigabyte of hard drive, along with a complimentary 4x4x24x CD burner.

1.5 Geological Framework

The Cape Breton Highlands lie within the Appalachian orogenic belt, and the study area includes portions of four contrasting crustal segments, according to Barr and Raeside (1989) and Barr et al. (1995, 1998). They are the Blair River Inlier in the northernmost part of Cape Breton Island, the Aspy and Bras d'Or terranes in the central part, and the Mira (Avalon) terrane in the southeast (Fig. 1.3). The significance of these four divisions in Cape Breton Island has been the subject of some controversy. Some other workers have interpreted Cape Breton Island to be entirely part of the Avalon terrane, and attribute geological differences to varying levels of exposure within a composite Avalon terrane (e.g. Murphy et al. 1990; Lynch 1996; Keppie et al 1992), whereas some workers have taken intermediate positions and recognized two or three contrasting terranes (e.g. Lin 1993)

A key goal of the study was to improve the understanding with respect to the distribution of major faults and postulated terrane boundaries. In the interpretations

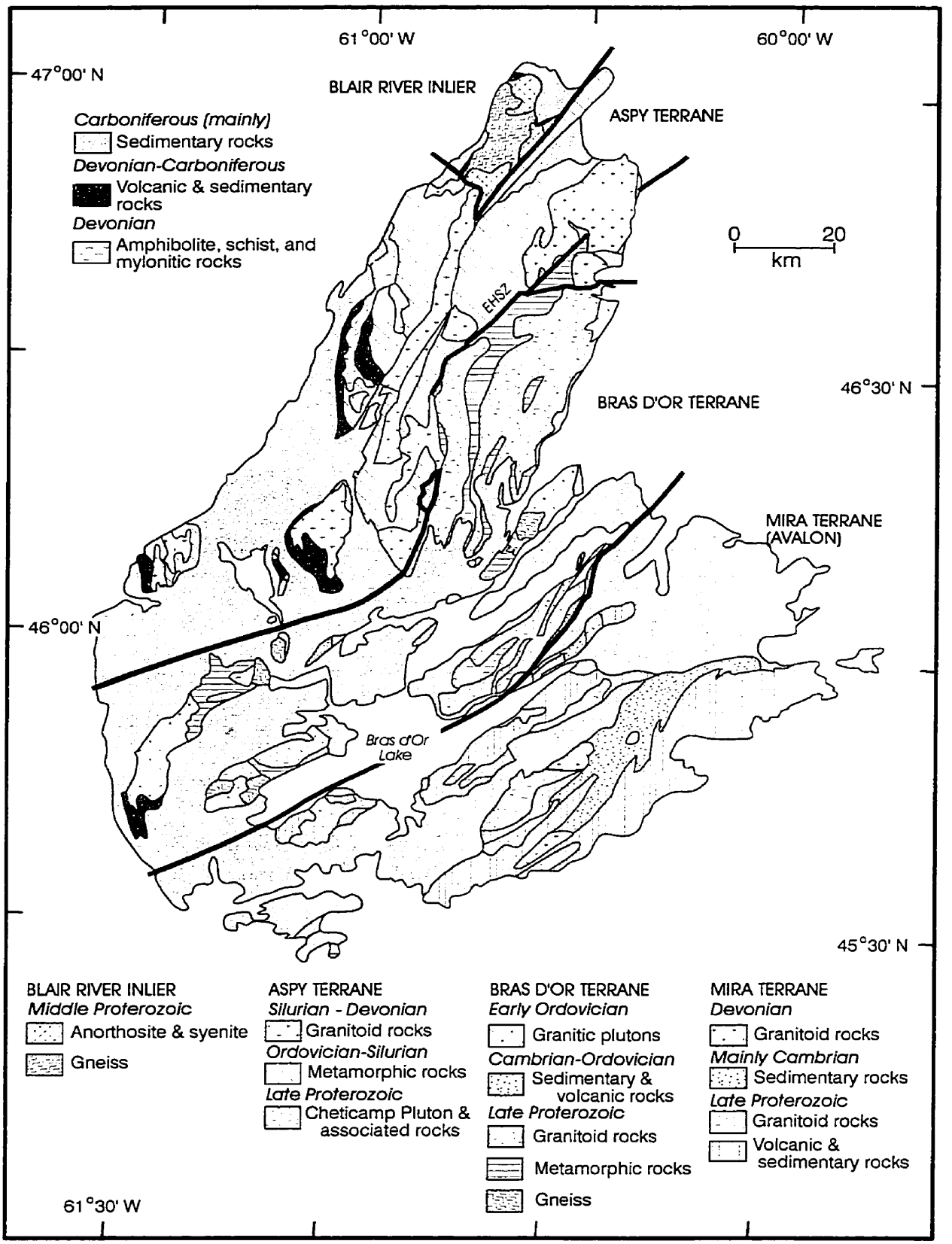

Figure 1.3 Terranes and terrane boundaries in Cape Breton Island, Nova Scotia (after Barr and Raeside, 1989). EHSZ: Eastern Highlands shear zone.

mentioned above, large bounding faults occur at the margins of terranes or linking various levels of crustal exposure. Relatively little research has been directed toward identifying these major faults and terrane boundaries from a geomatics point of view. The potential of the approach was demonstrated by Webster (1996) and Webster et al. (1998) who produced a new interpretation of the Late Carboniferous evolution of part of the Avalon-Meguma terrane boundary using remote sensing and geographic information system analysis, complemented by geological mapping.

Barr et al. (1995, 1998) presented evidence that the Blair River Inlier and the Aspy, Bras d'Or and Mira terranes have distinct and separate histories. The Blair River Inlier (BRI) is made up of mostly of ca. 1 Ga gneiss, syenite and anorthosite and displays compositional and metamorphic similarities to the Grenville province of the Canadian Shield (Miller et al. 1996, Miller and Barr 2000). The Wilkie Brook-Red River fault zones border the BRI on the southeast and southwest.

The Aspy terrane is characterized by metamorphosed Ordovician and Silurian sedimentary and volcanic rocks that were affected by a strong thermal event in the Devonian, producing granitic magmatism (Barr and Jamieson 1991). The Eastern Highlands shear zone is a wide zone of mylonitic rocks that separates the Aspy and Bras d'Or terranes.

The Bras d'Or terrane consists mainly of late Proterozoic metamorphic rocks and abundant plutonic rocks. Much of the boundary between the Bras d'Or and Mira terranes is inferred to lie beneath Bras d'Or Lake, except on the Boisdale Peninsula where the present boundary is placed at the Georges River fault (Barr et al. 1995). The Mira terrane is characterized by late Precambrian, predominantly volcaniclastic

assemblages and overlying Cambrian rocks, separated by northeast-trending faults and intruded by varied granitoid plutons.

Lin (1993) identified the Cape Breton Highlands to be composed of those terranes, but proposed that the Aspy and Bras d'Or terranes are not two tectonically juxtaposed terranes (cf. Barr and Raeside 1989). In this interpretation, the Eastern Highlands shear zone is not a terrane boundary and the original relationship between the Aspy and Bras d'Or terranes was depositional.

In contrast to the divisions of Barr, Raeside, and co-authors, Lynch (1996) proposed that a major part of the Cape Breton Highlands is part of a once-contiguous nappe (Cabot nappe) and is allochthonous. Three distinct domains were identified within this nappe, the Blair River Inlier of Barr and Raeside (1989), the Pleasant Bay Complex of Currie (1987) and the southern lobe (see Fig 1.4).

The Blair River Inlier was interpreted by Keppie et al. (1990) and Lynch (1996) to be part of Avalon basement. The Pleasant Bay Complex is separated from the BRI by the Red River shear zone which could be responsible of partial denudation of the BRI at a higher structural level within the Cabot nappe (Lynch, 1996).

These clearly different geological interpretations of the Cape Breton Highlands were investigated during this study, with the aim of integrating these models with geological, geophysical and remotely sensed data within a Geographical Information System and using the results to determine which model best correlates with the combined data.

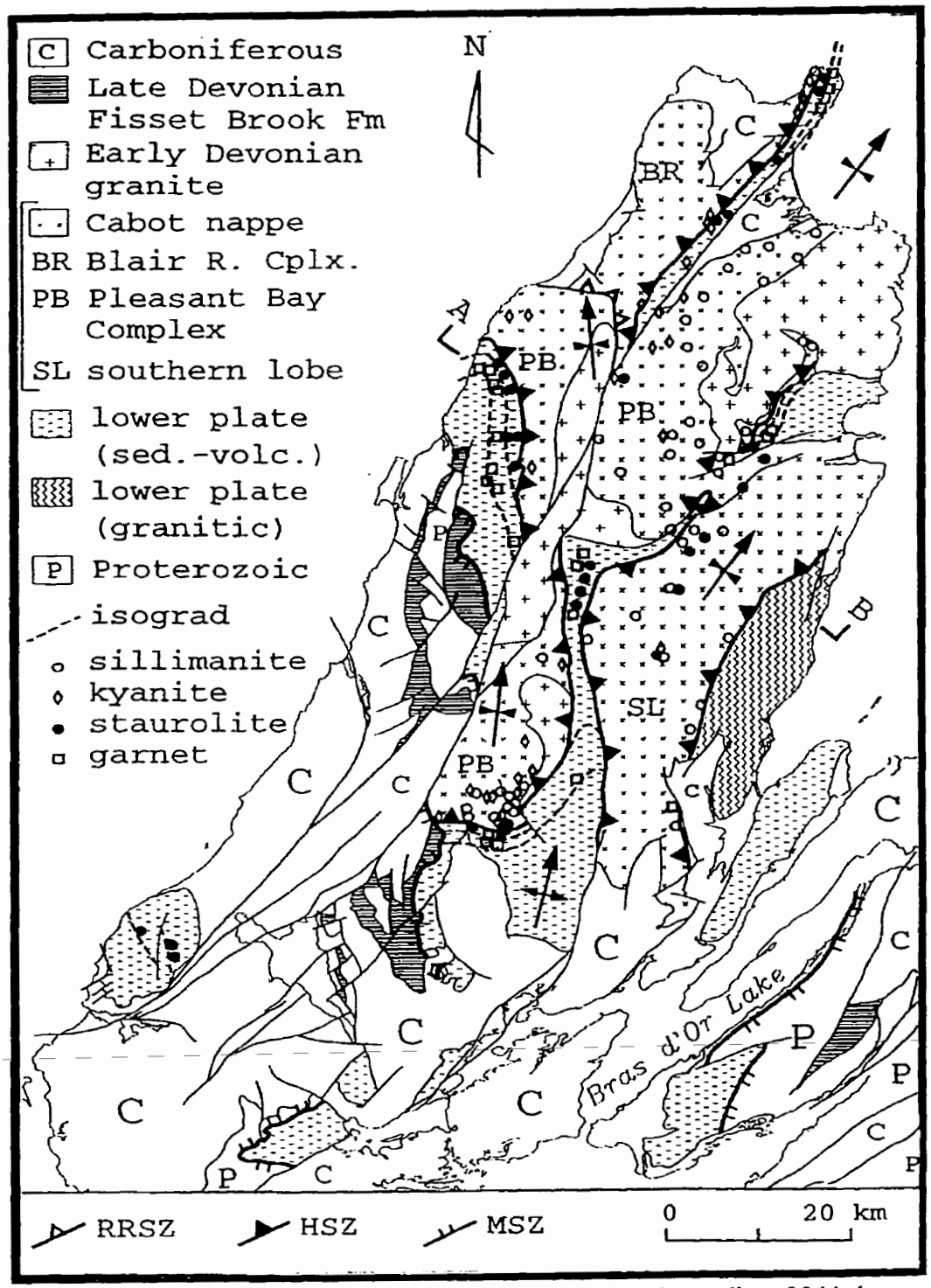

Figure 1.4 Geological map of the Cape Breton Highlands showing outline of folded Cabot nappe and bounding Highlands Shear Zone (from Lynch 1997).

Chapter 2. Data Processing and Preparation

2.1 Introduction

The GIS, in this case MapInfo with the Vertical Mapper (VM) extension, can use two types of data structure to store and display objects: vector models and raster models. In raster models, the map is divided into grids cells or pixels. Information is then displayed on the map by associating a value for each layer with each and every grid cell. Each grid cell represents a discrete area. In other words, the grid cell is the unit of observation. This approach is useful for spatial operations such as overlays and area and slope calculations. Vertical Mapper and the PCI Geomatics suite of remote sensing software were used interchangeably to manipulate the raster data in this study. For example, tasks such as gridding point values for the geophysical data and DEM were accomplished with Vertical Mapper, whereas the PCI Geomatics suite of software was used for the more complicated tasks such as classifying several image grids and geometric correction of the satellite imagery.

In the vector model, objects are displayed as points, lines, or polygons. A point is represented by its x-y coordinate, the line is represented by a sequence of x-y coordinates that form the nodes and verticies of the line, and the polygon is a closed loop of verticies and node coordinates, with the first and last x-y coordinate the same. MapInfo was used to manipulate, query, change or update attributes, and most importantly, to display and manage the data. Data from several sources were used in this study, in both digital and paper formats (Table 2.1). Much of the information had to be reformatted from one file format to another. For example, map projection and datums had to be transformed to Universal Transverse Mercator (UTM), North

American Datum 1983 (NAD83). The purpose of this chapter is to describe the procedures used to produce this large inventory of data.

Table 2.1 Dataset and image layers used in the study.

Data Set	*Source*	*Resolution*	*Comments*
RASTER		**Pixel**	
RADARSAT-1 radar S7 (1996) and S2 (1998).	Canadian Space Agency via Centre of Geographic Sciences (COGS)	30 m	Processed at COGS with PCI Geomatics
Two Landsat TM Bands 1-5.7 (1986, 1992).	Radarsat International via COGS	30 m	Processed at COGS and Acadia with PCI Geomatics
Airborne magnetics (Total Field) (Vertical Gradient)	Geological Survey of Canada	100 m	Processed at Acadia with Vertical Mapper
Gravity (Bouguer)	Nova Scotia Research Foundation Corporation (point files) Open File Report 95-005.	100 m	Processed at Acadia with Vertical Mapper
Radiometrics (Exposure, K, eU, eTh, eU/eTh, eU/K, eTh/K and Ternary Radioelement)	Geological Survey of Canada Radiation Geophysics Section *http://gamma.gsc.nrcan.gc.ca/index_e.html*	100 m	Processed at Acadia with Vertical Mapper and PCI Geomatics
Digital Elevation Model (DEM)	Derived from NSTDB via COGS	10 m	Processed with Vertical Mapper
Bouguer Gravity	Mineral Resources Division, Nova Scotia Department of Natural Resources (point file) OFR 95-005.	100 m	Processed with Vertical Mapper
VECTOR		**Scale**	
Geological Map of the Province of Nova Scotia, version 1, (2000).	Nova Scotia Natural Resources Minerals and Energy Branch *http://www.gov.ns.ca/natr/meb/index.htm*	1: 500 000	Compiled by J. D. Keppie, 2000.
Geological map of northern Cape Breton Island, Nova Scotia	Nova Scotia Natural Resources Minerals and Energy Branch *http://www.gov.ns.ca/natr/meb/index.htm*	1:100 000	Compiled by S. M. Barr, R. A. Jamieson, R. P. Raeside1992, Geological Survey of Canada, Map 1752a.
Geological Compilation, Cape Breton Island, Nova Scotia	Geological Survey of Canada, Open File 3159	1:250 000	Lynch, G et al. 1997
Surficial Geology Map of the Province of Nova Scotia, version 1, 1997	Nova Scotia Natural Resources Minerals and Energy Branch *http://www.gov.ns.ca/natr/meb/index.htm*	1: 500 000	Compiled by R.R. Stea, H.Conley and Y.Brown
Base Map (Roads, Water)	Nova Scotia Geomatics Centre via COGS	1:50 000	Processed at Acadia with MapInfo

2.2 Geological Database Acquisition

In order to compare different geological interpretations of the Cape Breton Highlands, vector overlays had to be done. The three different digital geological map interpretations (Barr et al. 1992; Lynch et al. 1997; Keppie 2000) had to be stored in the GIS. The *Geological Map of Northern Cape Breton Island, Nova Scotia* (Barr et al. 1992) and the *Geological Map of the Province of Nova Scotia* (Keppie 2000) were downloaded from the website of the Nova Scotia Department of Natural Resources, Minerals and Energy Branch. Both data sets were in Universal Transverse Mercator (UTM) Zone 20 projection using the NAD27 datum and were provided in ARC/INFO "E00" files. Both files were imported and reprojected to the NAD83 datum. The *Geological Compilation Map, Cape Breton Island, Nova Scotia* (Lynch et al. 1997) was obtained from the Geological Survey of Canada, Open File 3159. This compilation map shows rock units, geological boundaries, and fault lines. This map resulted from the integration of a series of maps ranging in scale from 1:50,000 to 1:250,000 from the Magdalen Basin NATMAP Onshore Geological Database. It was in UTM zone 20, NAD 27 and was provided in ARC/INFO "E00" format. The map layers were imported and reprojected in MapInfo to NAD83.

Other geological maps were digitized and integrated into this project, including (1) *Geology of Mabou Highlands* (Barr & Macdonald, 1989), (2) *Geology of the Blair River Inlier* (Miller 1997) and (3) *Structural Geology of the Southeastern Cape Breton Highlands National Park, NS* (Lin, 1992). It is important to have the same shoreline and water boundary in order to correlate and overlay information for the same study area. The shoreline and water polygon were constructed from Natural Resources Canada

National Topographic Data Base (NTDB) water layer. Thirteen NTDB (Fig. 1.1) water layers were appended together in order to create a seamless polygon. This water polygon was used to "cookie cut" or trim the raster data and provide a boundary for the vector layers such as the geological map.

In addition, information from numerous other maps from student thesis projects (e.g. Yaowanoiyothin 1988; O'Neill 1996; Price 1997) and various publications (e.g. Barr et al. 1995; Grecco and Barr 1999) were also examined and integrated into the study to varying extents.

2.3 Digital Elevation Model

A digital elevation model (DEM) was constructed from 174 Nova Scotia (NSTDB) 1:10,000-scale contour map sheets (Fig. 2.1). The data are from the Nova Scotia Geomatics Centre and obtained via copyright agreement from (COGS). In order to produce as much detail as possible, the 1:10,000 contours at 5 m interval were used. The elevation contours were selected instead of the 80-m grid points because of the inherent stepping effect caused by the contouring process of this data. The triangular irregular network (TIN) was the gridding interpolator within the MapInfo extension. Vertical Mapper (VM). The interpolating process is discussed further in Chapter 3.

The elevation contours came in AutoCAD (DXF) format. Maintaining the elevation attribute from DXF to MapInfo file format was problematic, therefore, an intermediate step had to be taken. The contour vectors were first imported to PCI IMAGWORKS and then the layer codes (LFCI, LFCO, LFDC20, LFDI20) were exported to MapInfo, maintaining their elevation attributes. The map projection used in

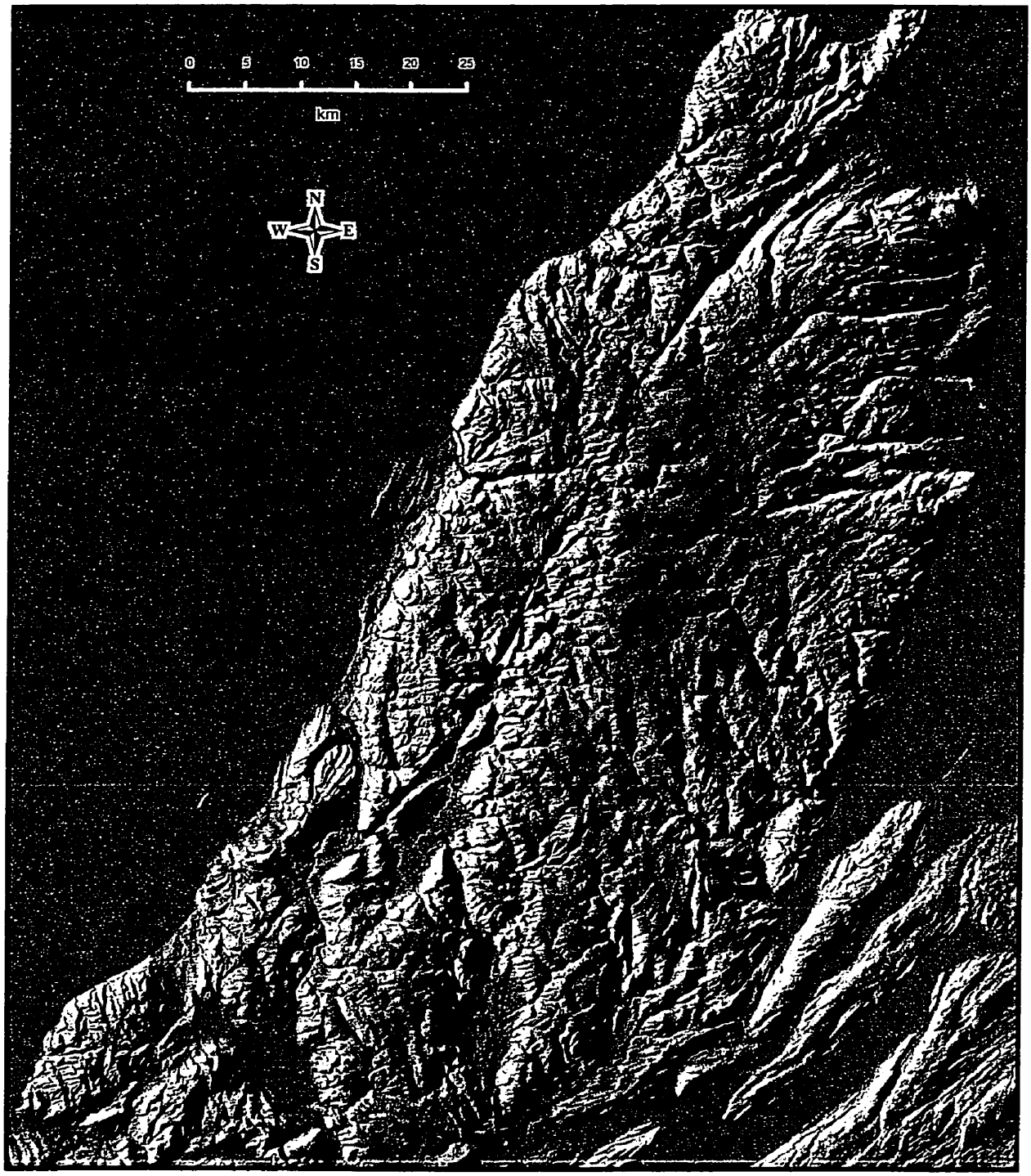

Figure 2.1 Grayscale shaded relief digital elevation model (DEM) of the study area illuminated from the northwest (azimuth 300°, inclination 30°). Gridded at 10 m cell size.

the original data was the Modified Transfer Mercator (MTM) zone 4, and the datum was the Average Terrestrial System (ATS 77) created by the Nova Scotia Geomatics Centre. The ATS 77 is the provincial standard for the topographic base mapping. The contour data were reprojected to the Universal Transverse Mercator (UTM) zone 20 projection, NAD83 datum. Within MapInfo, all the layers were appended and checked to ensure accuracy, necessary corrections were made and then all elevation and lake vectors were converted to points using the verticies and nodes. Contour elevations, point elevations, and lake elevations were utilized to produce the triangular irregular network (TIN).

An effective use of the DEM is to make a combined shaded relief model of the terrain. Several azimuth (direction from which the imaginary light sources emanates) and inclination (angle of incidence of the imaginary light source measured from a horizontal plane) combinations were chosen to effectively show structures within the topography. The effects were to visually enhance the topography of the area, allowing for a more interpretable image. An example is shown in Figure 2.1.

2.4 Remote Sensing Data

2.4.1 Landsat TM

Two seven-band Landsat Thematic Mapper "TM" scenes (summers 1986 and 1992) were geometrically rectified at COGS using the vector road network (Fig. 2.2, 2.3). The images were mainly used to identify bogs and surficial geomorphologic features. They were also an invaluable tool during the ground-truthing process in the field investigation for identifying newly created roads and clearings.

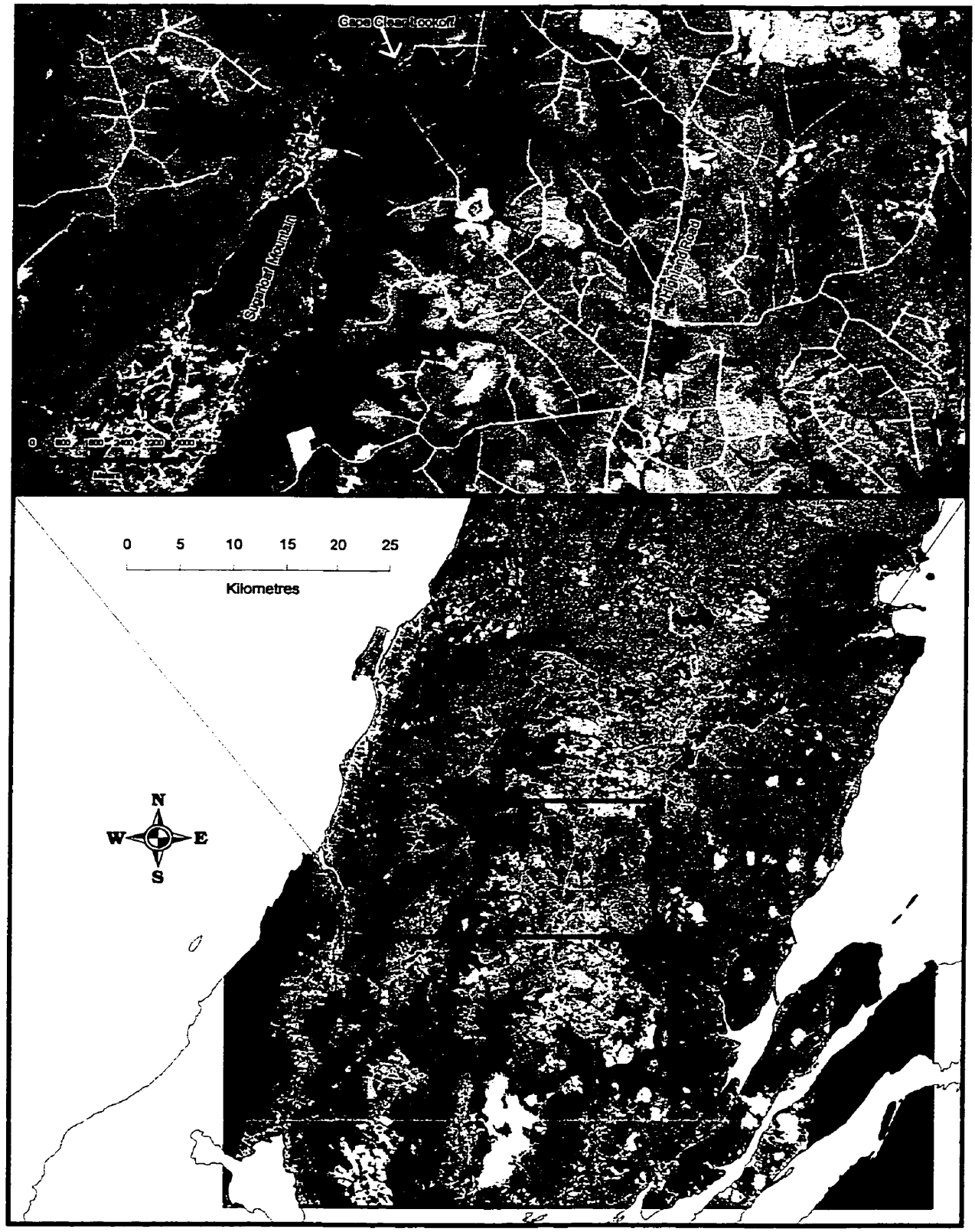

Figure 2.2 Colour composite Landsat Thematic Mapper (TM) image showing the central part of the study area. TM bands 3, 2, 1 are displayed as red, green and blue, respectively. The road network and river valleys (inset map) in the highlands are evident. (August, 1992)

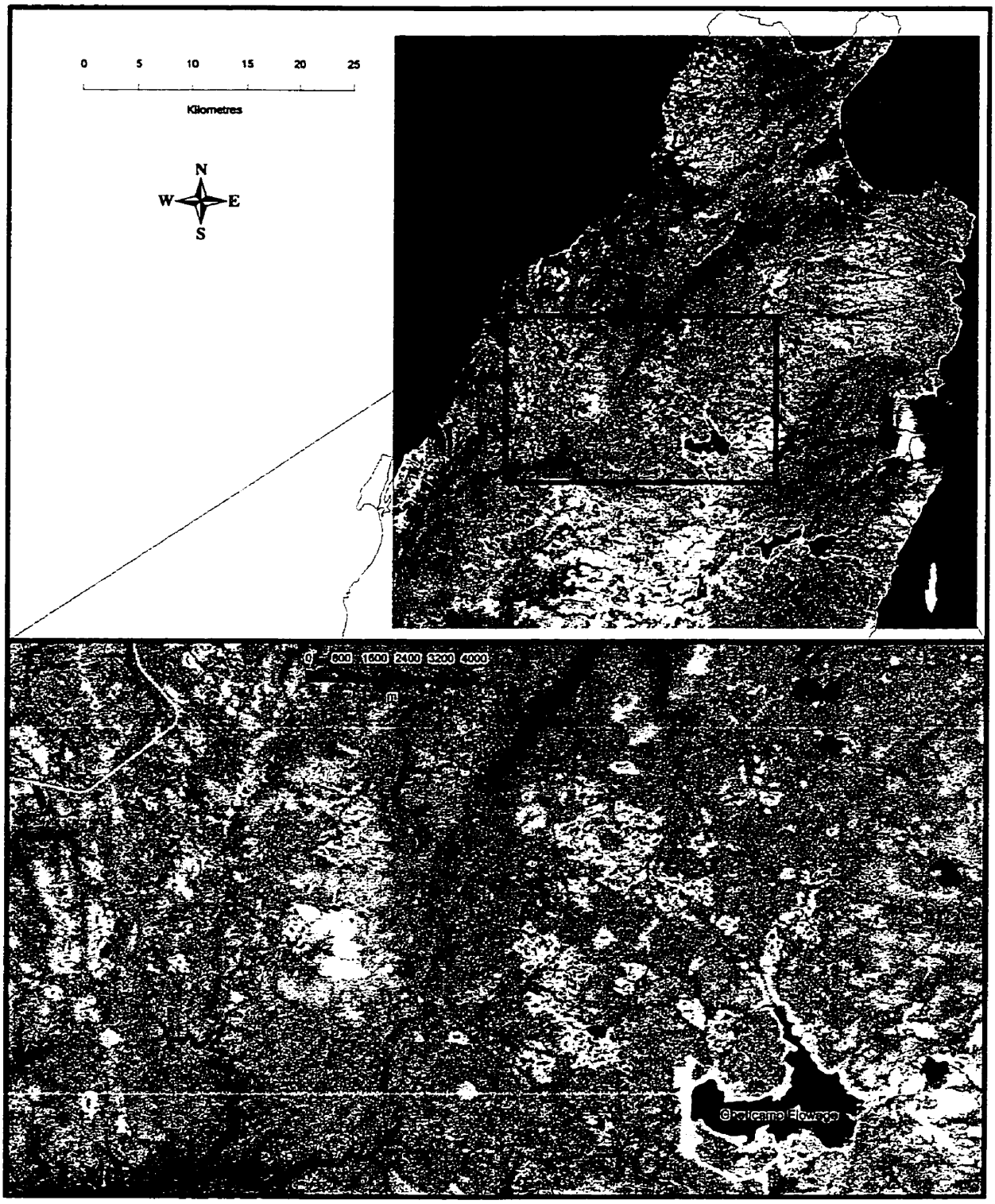

Figure 2.3 Colour composite Landsat Thematic Mapper (TM) image showing the northern part of the study area. TM bands 3, 2, 1 are displayed as red, green and blue, respectively. Areas of sphagnum moss (in pink) are evident northwest of Cheticamp Flowage. (August, 1986)

Slaney (1981), Singhoy et al. (1985), and others have examined the application of TM data for geological investigations. TM imagery also has extensive applications in landcover/landuse classification, hydrology, and forestry.

2.4.2 SAR data

Radarsat-1 synthetic aperture radar (SAR) scenes of parts of the highlands were also examined. The first SAR image is a descending standard mode beam 7 (S7) image mosaic of the entire study area, with an incidence angle ranging from 45 to 49 degrees processed by students (including the writer) at COGS in 1998-99 (Fig 2.4). The image was obtained by COGS from the Nova Scotia Geomatics Centre. The second SAR image is a mosaic of two adjacent descending standard mode beam 2 (S2) images obtained by COGS from the Canadian Space Agency (CSA). The images were orthorectified, histogram matched, filtered and appended at COGS (Fig 2.5). The mosaic covers the southern part of the study area. The production of this mosaic was part of the Radarsat Application Development and Research Opportunity (ADRO Project 656) supervised by M.S. Akhavi. Both images (S7 and S2) were in UTM Zone 20 projection using the NAD27 datum and were reprojected to the NAD83 datum.

The SAR images are more effective than optical imagery for studying features such as surface roughness and topography. This effectiveness is due to variations in radar backscatter as a function of wavelength (C-band microwaves are 5.6 cm long), incident angle, and polarization. Useful information on terrain morphology and surface relief (related to geologic structure) is provided by SAR imagery, due to the effects of radar backscatter sensitivity to slope, incidence angle and to shadow effects caused by

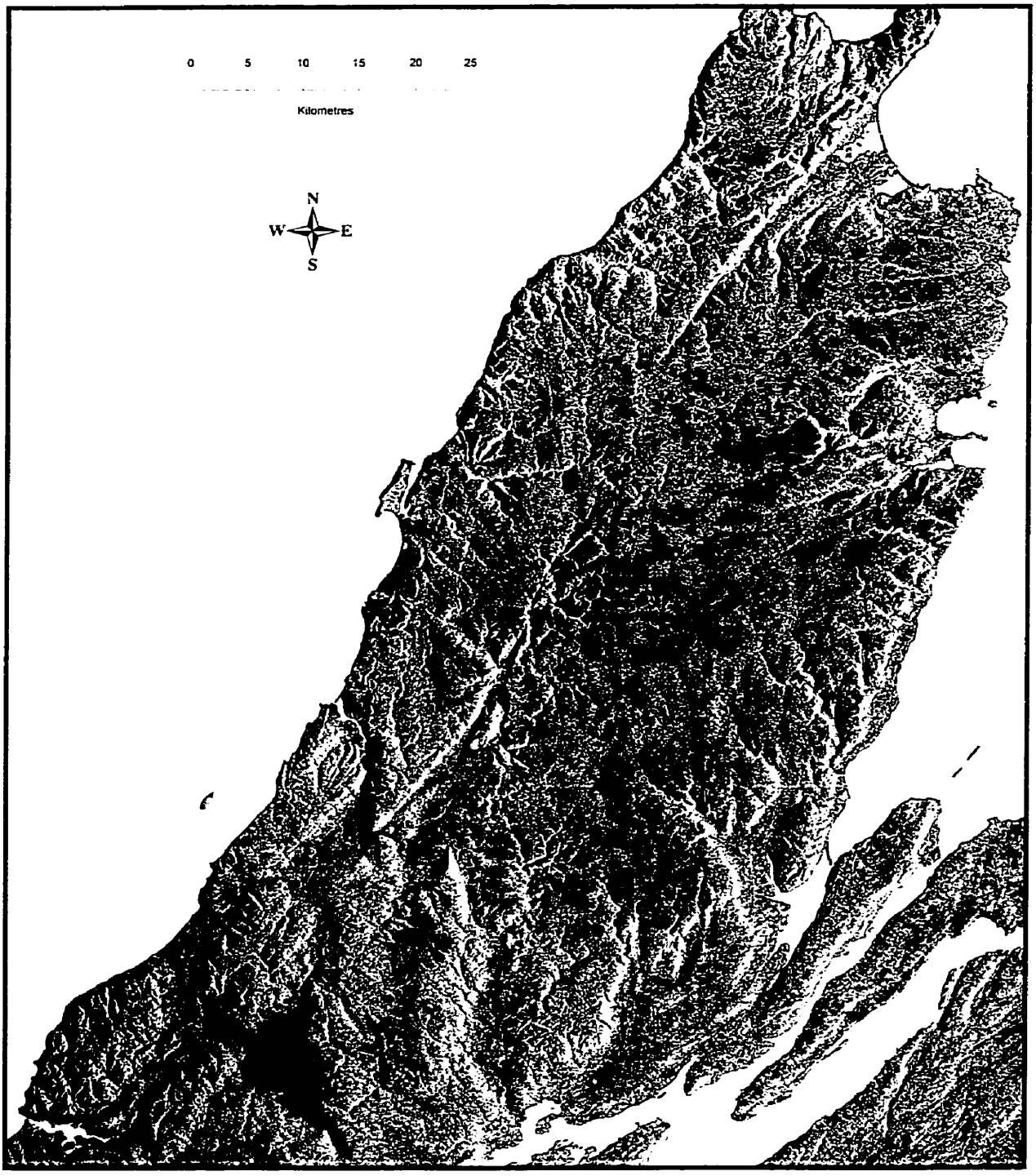

Figure 2.4 RADARSAT-1 descending standard mode S7 imagery of the study area. Incidence angle range is 45° - 49°. Radarsat data © Canadian Space Agency 1996, provided by COGS.

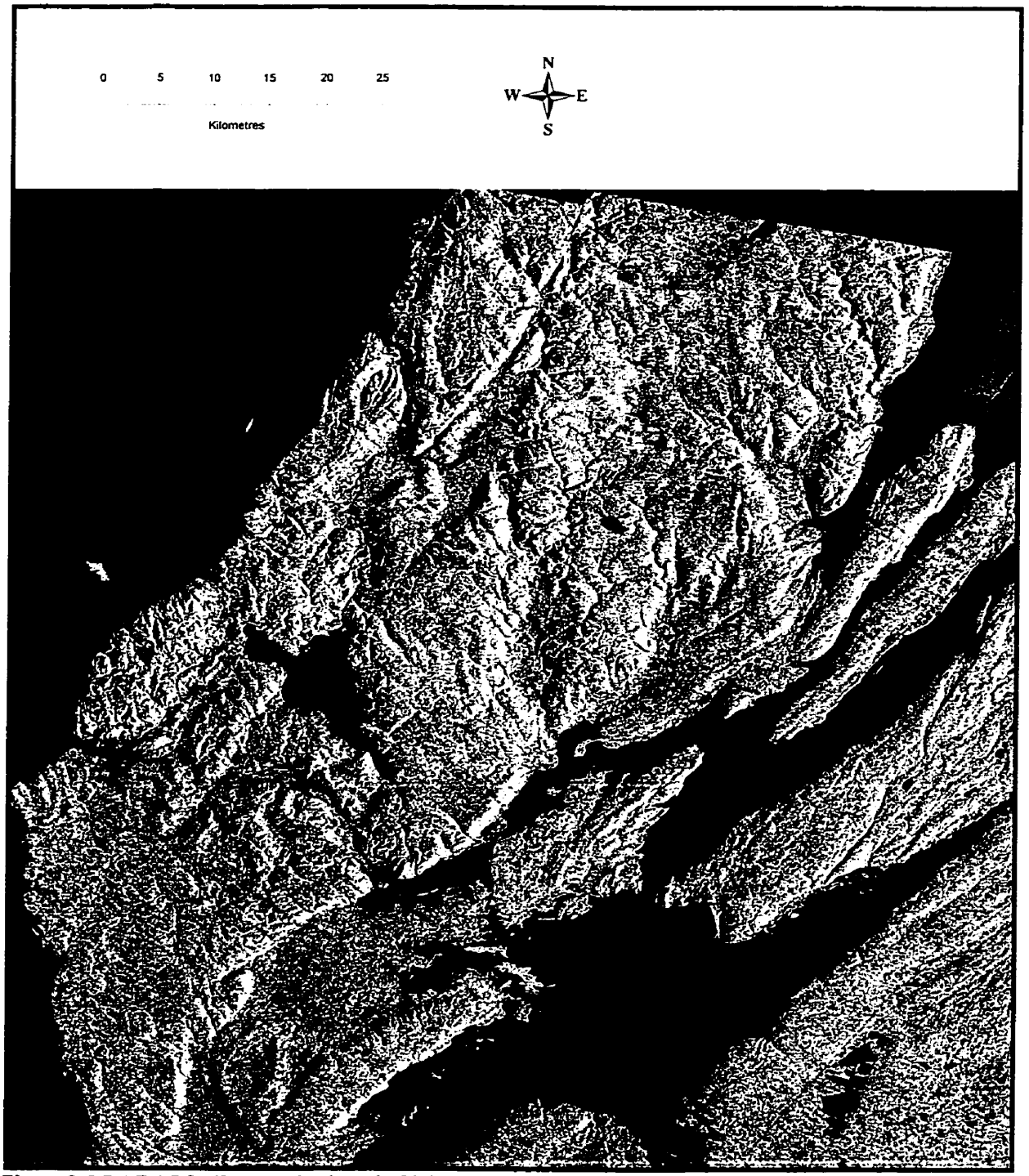

Figure 2.5 RADARSAT-1 standard mode S2 imagery of south-central Cape Breton Island, Nova Scotia. Incidence angle range is 24° - 31°. Radarsat data © Canadian Space Agency 1998, provided by COGS.

topographic relief. Singhroy et al. (1993) reviewed the contributions of SAR imagery to geological interpretation. They concluded that SAR has an important role, both in structural interpretations and in the integration of SAR with other geological and geophysical data. The S7 image was particularly important in identifying lakes and the extent of reservoirs which were not identified in the vector water layers. Knowing the spatial distribution of water and sphagnum bogs was important, mainly in the correct interpretation of the radiometric data.

2.4.3 Radiometric Data

A compilation of airborne gamma-ray spectrometry (AGRS) data for Cape Breton Island from the Geological Survey of Canada Radiation Geophysics Section was used (Fig 2.6). These data were compiled from 3 separate surveys flown with 1-km line spacing at a mean terrain clearance of 120 metres. GSC provided eight grids (Exposure, K, eU, eTh, eU/eTh, eU/K, eTh/K and Ternary Radioelement) with a cell size of 100 m. These grids were in Surview format (Grant 1993), a Geological Survey of Canada software, therefore, each layer had to be exported to PCI and VM and reprojected to the NAD83 datum from NAD27.

Terrestrial gamma-rays emanate from the ground surface, not from depth. About 60 cm of overburden, including soil, are typically sufficient to absorb 100% of the emissions from the rocks beneath. Therefore, unlike the aeromagnetic method, the radiometric method is capable of yielding information only on what lies at the ground surface. The value of radiometric data as a geological mapping device is that it has the ability to provide chemical information on rock outcrop by remote sensing. Even though

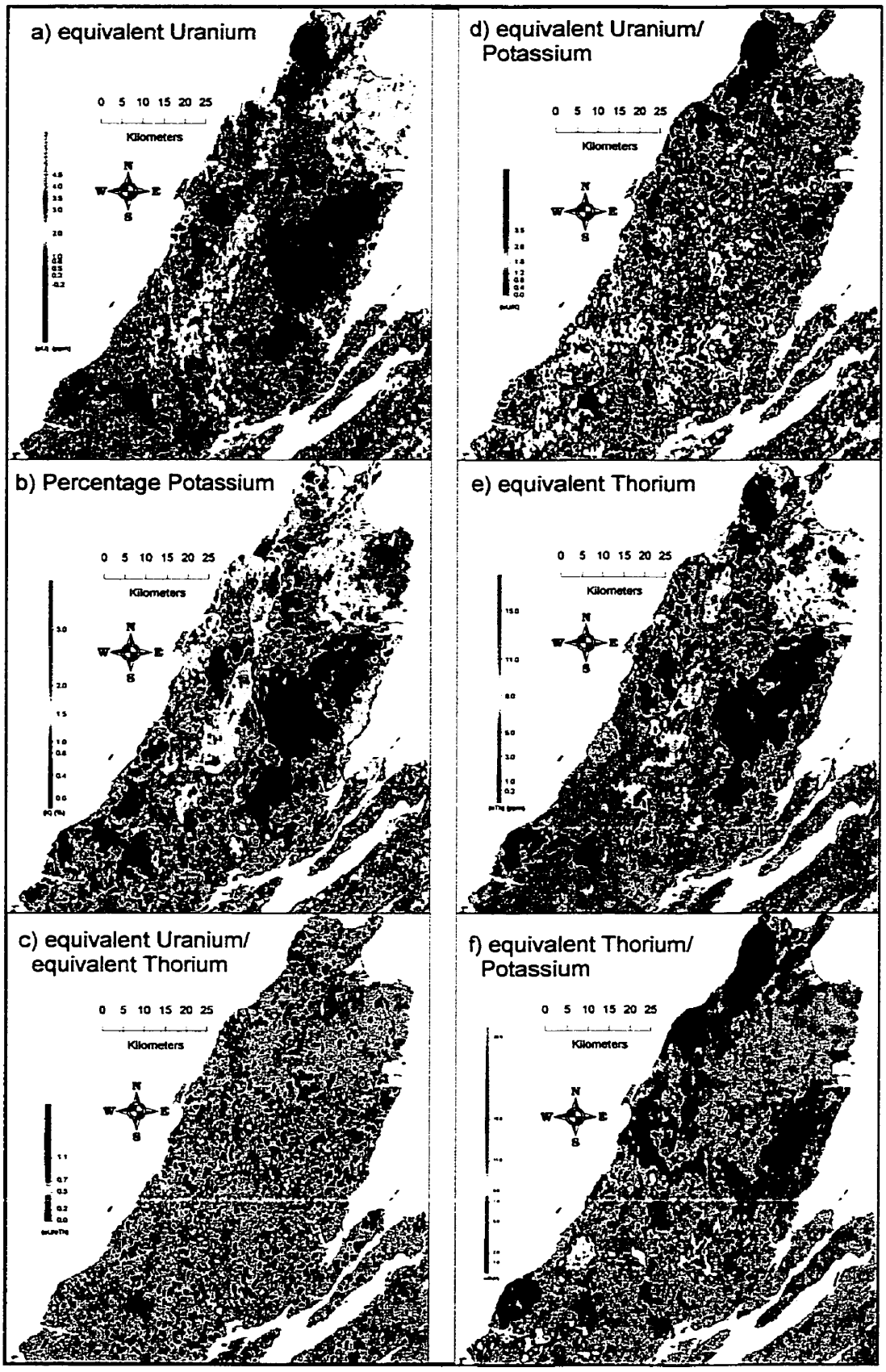

Figure 2.6 Airborne gamma-ray spectrometry data, gridded at 100 m cell size.

residual soils which have not been moved retain only some of the radioactive elements that were present in their parent rocks, their relative abundance tends to remain indicative of the parent, and thus the underlying parent rock can in some cases be mapped through a thin layer of residual soil. As a regional mapping tool, the airborne gamma-ray spectrometry technique is probably more useful than any other single airborne geophysical or remote sensing technique in providing information directly interpretable in terms of surface geology (Darnley & Ford 1987).

2.4.4 Magnetic data

Total magnetic field (TMF) and vertical magnetic gradient (VMG) surveys of the Cape Breton Highlands have been flown by the Geological Survey of Canada. These data measure local changes in the Earth's magnetic field and are largely a function of variations in the magnetite content of the rock units. Mapping the changes in TMF is useful for delineating lithologic units and potential fracture zones. The VMG survey utilises two sensors with a 2-m vertical separation. This technique removes diurnal changes and regional gradients in the Earth's magnetic field and is useful in emphasising anomalies generated by near-surface (as opposed to more deeply buried) features.

The magnetic data were obtained from COGS via the Geological Survey of Canada. The data was in an ASCII grid file format for both the total field and vertical gradient. The magnetic data were gridded at 100 m cell size resolution and projected to NAD83 from NAD27 (Fig 2.7 and 2.8). The magnetic values ranged from –580 to 550 nanotesla for the TFM and –0.4 to 0.47 nanotesla/m for the VMG.

Figure 2.7 Colour total field magnetic (TFM) data gridded at 100 m cell size.

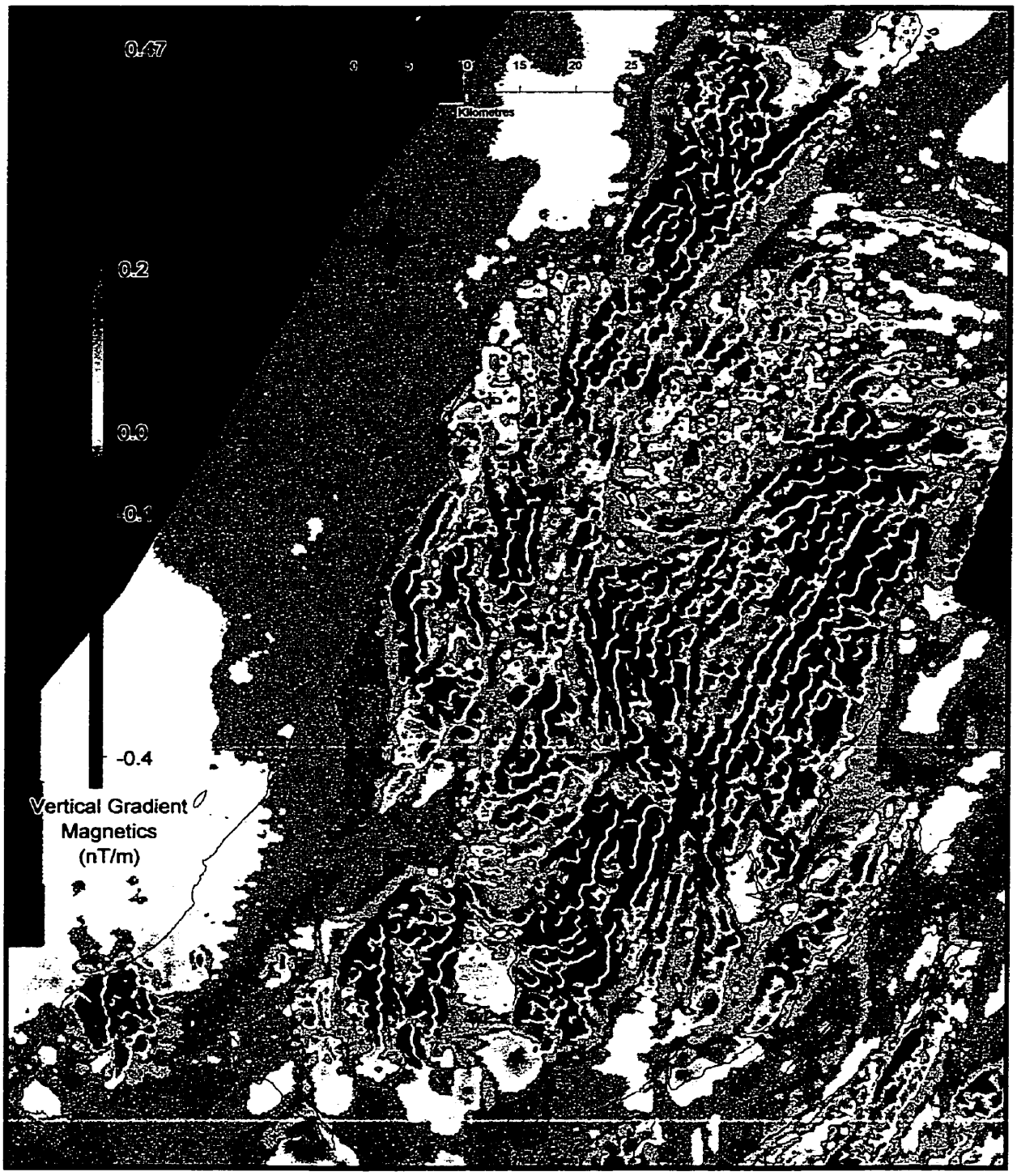

Figure 2.8 Colour vertical gradient magnetic (VMG) data gridded at 100 m cell size.

2.4.5 Gravity

Gravity data for this study were obtained from Nova Scotia Research Foundation Corporation (NSRFC), Nova Scotia Department of Natural Resources Open File Report 95-005. The initial data consisted of an irregular distribution of gravity station measurements in the form of an ASCII file consisting of longitude and latitude projection NAD27 datum. As with the magnetic data, this file was read into MapInfo and projected to UTM zone 20 NAD83. The point spacing is considered to be fairly coarse (5 km in the Cape Breton Highlands), although the data for this region have a regular grid point reference compared to the Cape Breton Island lowlands. After the file was cleaned for erroneous data, checked to ensure accuracy and necessary corrections made, it was gridded to 100 m pixel using the final Bouguer gravity (FG) attribute table (Fig 2.9). The real values of the data range from –50 to 50 milligals.

The gravity method is used extensively for the investigation of large-to medium-scale structures. On the large scale, most of the major features on the Earth's surface can be mapped. A medium-scale survey can reveal the form of subsurface structure such as igneous intrusions (Robinson and Çoruh 1988). Sedimentary basins normally produce negative anomalies. Such anomalies can locate and provide important information regarding mechanisms of basin formation (Webster et al. 1998). For this reason, gravity surveying is extensively used by the petroleum industry for the location of sedimentary basins and hydrocarbon traps, although the vast improvement and efficiency of seismic surveying has lead to the decline of gravity as a primary exploration tool.

Figure 2.9 Stepped colour shaded relief Bouguer gravity data with station point locations. Illuminated from the northeast (azimuth 45°, inclination 45°).

Chapter 3. Data Integration and Image Products

3.1 Introduction

Geologists have traditionally used a range of geographic data to assist with geological interpretation. These data include information on surface elevation represented by contours, hydrology as lines, outcrops as point symbols, and landuse and ownership generally associated with conventional topographic or orthophoto maps. The unifying factor among all these types of information is that they are geographic in nature. They relate to point, lines, or areas on the Earth's surface expressed in various cartographic coordinate systems. In paper form, such data present a number of problems in manual assembly. For example, they may be at a variety of scales and in different map projections. Even as transparent overlays, the space required and the finite ability of the geologist to mentally retain information impose limits to integrating the information properly. The strength of the GIS and Image Processing System is the ability to organise this information digitally in the same map projection and displaying it at a common scale.

After the image layers discussed in the previous chapter were corrected, processed and clipped to coincide with the study area, the next step was to manipulate the data to maximise their interpretation and integrate them. This chapter describes the ways in which the data were integrated to generate image products in order to visually provide as much geological information as possible.

3.2 Digital Elevation Model

3.2.1 Image Model Generation

In order to represent data that vary continuously in space, such as elevation, magnetic or gravity data, a mechanism is needed to provide continuous coverage such that any location can be queried and a meaningful value obtained. For this project, the surface of the elevation model was created by a triangular network method whereby all data points were connected in space by a network of triangular faces, drawn as equilateral as possible. The points were connected based on a nearest neighbour relationship (the Delaunay criterion) which states that a circumference circle drawn around any triangle will not enclose the vertices of any other triangle (Bonham-Carter 1994). A smooth grid surface was then applied and fitted to the triangular network using a bivariate fifth-order polynomial expression in the X and Y direction for each triangle face (Northwood Geoscience Ltd. 1999). Use of this expression assured continuity and smoothness of the surface. The surface thus generated passes through all of the data points while generating some degree of overshoot above local high values and undershoot below local values because it is not reasonable to assume that the data points were collected at the absolute top (or bottom) of each local rise (or depression) on the terrain surface.

The resulting surface with elevation attributes is adequate for querying the values and slope calculations, but visually the information is not portrayed effectively. The effectiveness is enhanced by assigning colour values to the surface, a standard method of presenting quantitative data in a continuous gridded surface. This method was used with the elevation data, and was also applied to the other continuous data

(vertical gradient and total field magnetic and gravity). In addition to assigning colour values to the surfaces, variation in light and shadow was also applied. Shaded relief in combination with colour is a very effective visualization tool to create 3D-like images (Fig. 3.1). The procedure calculates light and shadow effects based upon the angle of incidence of a selected point source of light to produce grayscale or colour images.

The gradient colour values are commonly represented by blue for low or "cold" values and red for high or "hot" values. However, in this case where the study area is surrounded by water, it was more effective to use dark green for low values on land and blue colours for the water. In parallel, the specific colour gradient chosen for the DEM images was modelled to work with 3-D "ChromaDepth ™" glasses. The innovative "ChromaDepth" glasses cause the image to display in a dramatic 3-D like image. Viewing the topography in this way provided another visualization tool to assist in the interpretation of the Cape Breton Highlands.

Several colour shaded relief images were produced from the DEM to highlight all major structural trends. The images were shaded using an angle of inclination of 45° for the imaginary light source, measured from the horizontal plane, and the azimuth direction was incremented from angles of 0°, 45°, 90°, 135°, 180°, 225°, 270° and 315°. Producing eight separate images was challenging because of the extremely large file size. Each file was approximately 500 megabytes, and hence 4 gigabytes of storage was needed. With such large image files, file management and image compression were very important.

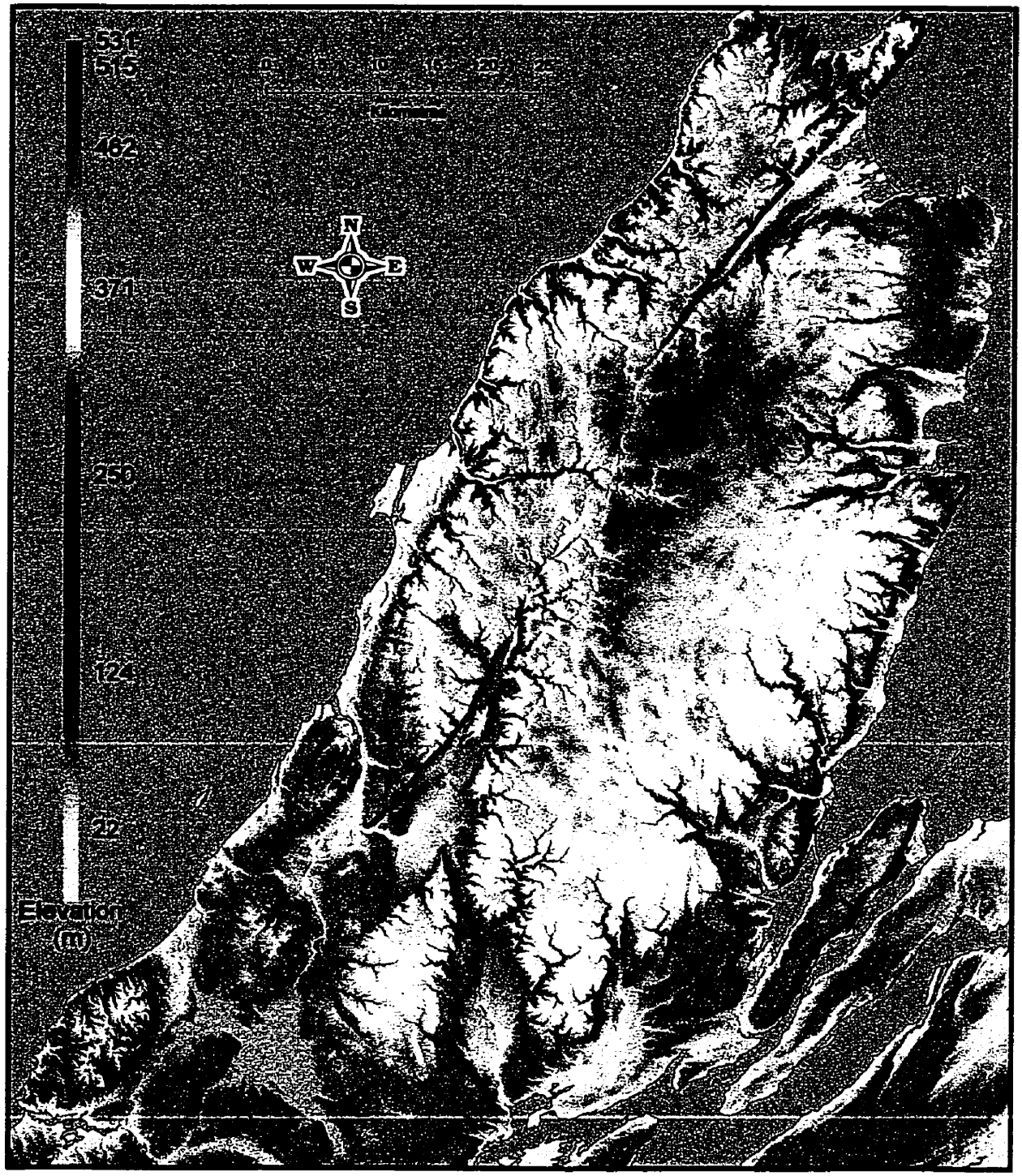

Figure 3.1 Colour shaded relief digital elevation model (DEM) illuminated from the west (azimuth 270°, inclination 45°). Gridded at 10 m cell size.

3.2.2 Image Compression Alternatives and Image Storage

Numerous methods have been developed for the compression of digital image data. The principal criteria for the evaluation of compressed versus uncompressed imagery are whether the difference between the images can be detected. Traditionally, two categories of compression are used: lossless and lossy (Simon 1993). Lossless compression means that a certain compression factor is achieved but it is still possible to exactly reproduce the original image. Generally, lossless compression images are still too large to manage. Lossy compression (for example, .gif and .jpeg) on the other hand results in some loss, but has the potential for much larger compression. For this study, the lossy compression types were considered unacceptable. The objective for the DEM images was not to lose any visual information, and therefore none of the previous compression agents were adequate.

Instead, a new software package was used called Enhanced Compression Wavelet (ECW) v2.0 from Earth Resource Mapping, Inc. This package was designed to compress images. The compression is achieved by transforming them into *wavelet space* using Discrete Wavelet Transformations (DWT) and then quantitizing and encoding the wavelet space images (Earth Resource Mapping Inc., 2000). Quantitization reduces information content, so that the encoding phase can compress the imagery. The DWT process is a 2D-filtering process. As mentioned earlier, this has meant historically that large images could not be compressed, as the computer required as much RAM as the size of the image being compressed, making it impractical to compress very large images. The ECW v2.0 eliminates the need for large amounts of RAM during compression, thus enabling very large images to be

compressed. The Enhanced Compression Wavelet (ECW) v2.0 from Earth Resource Mapping, Inc. was used in this study, mainly because it is free for files that are smaller than 500 megabytes. In addition to reducing storage requirements, it also provides free imagery plugins for popular GIS such as MapInfo. Because of this, the DEM can be visualized in a real world coordinate system and related to the geological layers. Compressing the DEM images to a *.ECW file was very beneficial for saving time when viewing and interpreting, because the computer only needed to process 5 megabytes instead of 500 megabytes. Most of the images were compressed from 400 to 500 megabytes to 5 to 10 megabytes using this method.

3.3 Airborne gamma-ray spectrometry (AGRS)

3.3.1 Introduction

Airborne gamma-ray spectrometry, or radiometric data, is basically an airborne representation of ground potassium (K), thorium (Th), and uranium (U) composition. The radiometric dataset obtained from the Geological Survey of Canada included data for %K, eU, eTh, Exposure, eU/eTh, eU/K, eTh/K and Ternary Radioelement. The potassium (K) units were measured in unit of concentration by weight %, whereas equivalent uranium (eU) and equivalent thorium (eTh) were weighted by the concentration of part per million (ppm). The spectrometer directly measured ^{214}Bi, ^{208}Tl, which is an indirect measure of uranium and thorium respectively. Potassium concentration is determined directly from ^{40}K. Exposure is the natural exposure computed from K (%), eU (ppm), eTh (ppm) concentrations. The formula is expressed as Exposure = 1.505 K + 0.625 eU + 0.31 eTh measured as micro Roentgen/hour

(μR/h). The difference between exposure and the traditional total count is that exposure excludes radiation from man-made contaminants (http://gamma.gsc.nrcan.gc.ca, 2001).

Calculating ratios of %K, eU and eTh are useful for interpretation. By gridding the eTh vs K, eU vs K or eU vs eTh, one can determine which area on the map could be rather enriched or depleted in one of the radioelements, due to either primary causes (i.e. magmatic) or secondary causes (i.e. alteration related to magmatic, hydrothermal or weathering processes). It also reduces the effect of wet areas that attenuate the radiation.

Different types of rocks and regolith have particular radiometric "signatures" associated with them, where a "signature" is a combination of high and low densities of different data. Representing these signatures with other continuous data in a gridded surface has become the standard approach (Drury 1993), but different methods of presenting the radiometric surface have been used.

The simplest approach is to present the individual gridded layers separately in a colour gradient such as with the DEM (Fig. 2.6). This method is advantageous only if one needs to see one element a time, and is limited if there is a need to represent the parent material and regolith attributes which are distinguished through combinations of %K, Th and U rather than individual unique signals. In this study, the data were combined as described below.

3.3.2 Ternary Radioelement Map

Because of the generally strong correlation between the radioelements due to their similar geochemical behaviour, maps of the natural radioisotopes are similar. A good method to increase the contrast and with it the interpretability of an image is called "histogram equalization" (Lillesand and Kiefer 1994). After histogram equalization every colour covers the same area on the map in theory. The visual impression of such a representation is optimal. As a consequence the colour scale becomes non-linear.

The histogram equalization method is particularly useful to produce ternary maps. In this representation the maps of potassium, uranium and thorium are merged into a single map. The colour red is assigned to the potassium values. Uranium and thorium are coloured green and blue, respectively. Regions with high relative potassium content will appear in red colour shades on the map. Correspondingly areas with high relative uranium or thorium content will appear in green or blue shades. Regions with equally balanced radioisotopes will be plotted as grey or white shades depending on the total activity. In fact, the ternary map has become so popular that, along with contour maps of the total count and of each of the element abundance, it has become a standard method of presenting data for the Geological Survey of Canada.

Although useful, the ternary map also has limitations, especially in grouping a set of values that correlate with a specific rock type. The ternary map displays a full range of the 8 bit data for the red, blue and green bands, from 0 to 255 DN multiplied by 3 bands, which means that the eye must differentiate between 16.7 million shades of

colours. Lithological edges and lineaments were subdued on the normal ternary image, and therefore, an infrequency histogram stretch was applied.

3.3.3 Infrequency brightening of the ternary image

This image is similar to the ternary map, but the function is derived from an inverted "upside down" histogram of the input image data values (Fig. 3.2). The infrequency brightening is also termed "histogram inversion" and produces an image in which the high "bright" pixels represent those grey levels in the original image that were infrequent and accounted for a small proportion of the entire image. This function is useful for highlighting rare or small features in the image that may otherwise go unnoticed. The infrequency enhancement "brightens" these features so that they become more obvious. While this enhancement was useful in the detection of lineaments and lithological edges, it also has limitations, such as the inability to quantify the amount of K, Th and U.

3.3.4 Unsupervised Classification of Gamma-Ray data

With radiometric data, parent material and regolith attributes are distinguished through combinations of K, Th and U rather than individual unique signals. This section deals with one aspect of a new interpretation methodology, developed during this study using data analysis techniques to examine relationships among variables such as K, eTh and eU (Harris 1989).

Interpreting with a multivariate data suite, manual or visual methodology presented some difficulties. In particular, the number of geophysical and non-

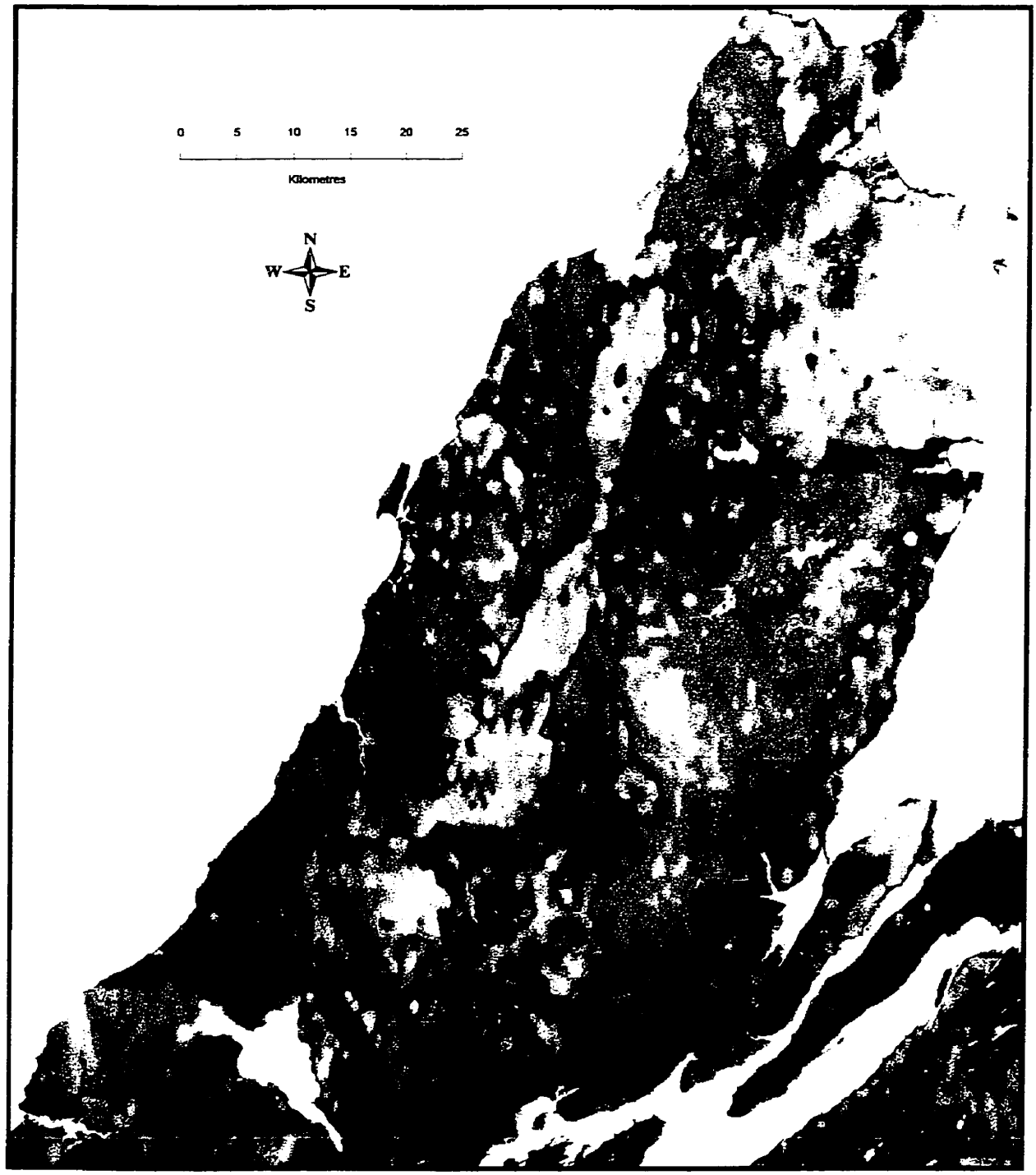

Figure 3.2 Infrequency brightening ternary image of radiometric data. Percentage potassium, equivalent thorium and equivalent uranium are in red, green and blue, respectively, with the infrequency stretch applied.

geophysical variables made it likely that potentially important relationships between data sets were not being identified and thus the full value of the data was not being realised. The large quantity of data made it difficult to effectively extract information. Unsupervised classification, such as that commonly applied to remotely sensed imagery, was chosen as the analysis technique for this part of the study to help alleviate this problem.

Unsupervised classification is a method which examines a large number of unknown pixels and divides them into a number of classes based on natural groupings present in the image values (Drury 1993). The resultant classes are spectral classes. the identity of which is initially unknown. In this case, they were compared to reference data (geological maps) to determine their identity. PCI's ImageWorks offers two different clustering algorithms that serve the purpose of unsupervised classification. K-Means Clustering and Isodata Clustering

K-Means Clustering is the simplest and most fundamental clustering algorithm. Although the number of spectral clusters to be located in the data and the initial mean vector for each cluster or class can be specified, if they are unspecified. then the algorithm arbitrarily selects seed or start positions for the "K" clusters. Each pixel of the image data is then assigned to the cluster with a mean vector closest to the pixel vector. A new set of class mean vectors is then calculated from the results of the previous classification and the pixels are reassigned to the new cluster vectors. The procedure continues until no significant change occurs in pixel assignments from one iteration to the next, or until the number of iterations has reached a maximum number specified by the user.

The Isodata algorithm is basically an extension of the K-Means algorithm. As with K-Means, the number of desired clusters is specified and the initial set of cluster mean vectors is optimally specified. Unlike K-Means, however, after each iteration, Isodata statistically examines each cluster and applies cluster splitting, merging, or discarding according to some criteria. This may lead to a category number that does not agree with the number initially specified by the user.

The choice of unsupervised classification in preference to supervised classification was based on two factors. First, the purpose of this analysis was to determine what information is contained in the data. Generally, this approach is used near the beginning of the interpretation process to help understand and represent the spatial correlations between the available geophysical and non-geophysical variables. At the first stage of manipulating geophysical variables for the Cape Breton Highlands, training data (in digital format) on which to base a supervised classification were insufficient. Several geological maps were available in digital format, but the selection of the appropriate training data is difficult when dealing with radiometric data because of overburden materials. Second, the geological maps contain a strong element of interpreted information, and this interpretation could bias the results of a supervised classification.

The unsupervised clustering algorithm used was the EASI/PACE histogram clustering process, Isodata clustering (ISOCLUS). ImageWorks, a module of EASI/PACE, was used to display and compare the output of the ISOCLUS with the raw data bands. The output clusters were colour-coded using a pseudocolor table (PCT). In general, the initial clustering of %K, eTh and eU was not sufficient to

completely distinguish between classes. This process was repeated until a satisfactory discrimination was achieved. The ISOCLUS output clusters were then assigned to the classes. Trial and error determined that approximately fifteen classes represented the variability in the data sufficiently without making interpretation of those classes too complicated (Fig 3.3 and 3.4). Their correlation with geological features is described and discussed in chapters 4 and 5.

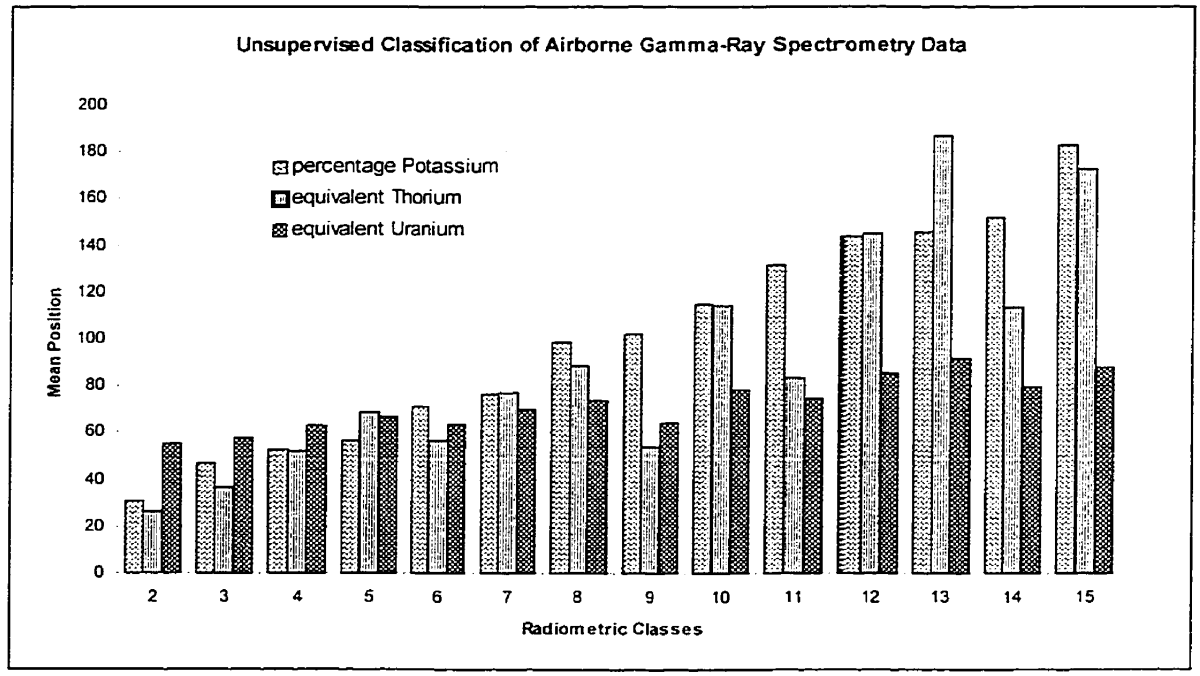

Figure 3.3 A graph showing 15 radiometric classes based on the relative abundance of radiometric elements (%K, eTh and eU). Class 1 is water. The distribution of the classes in the study area is shown in Figure 3.4.

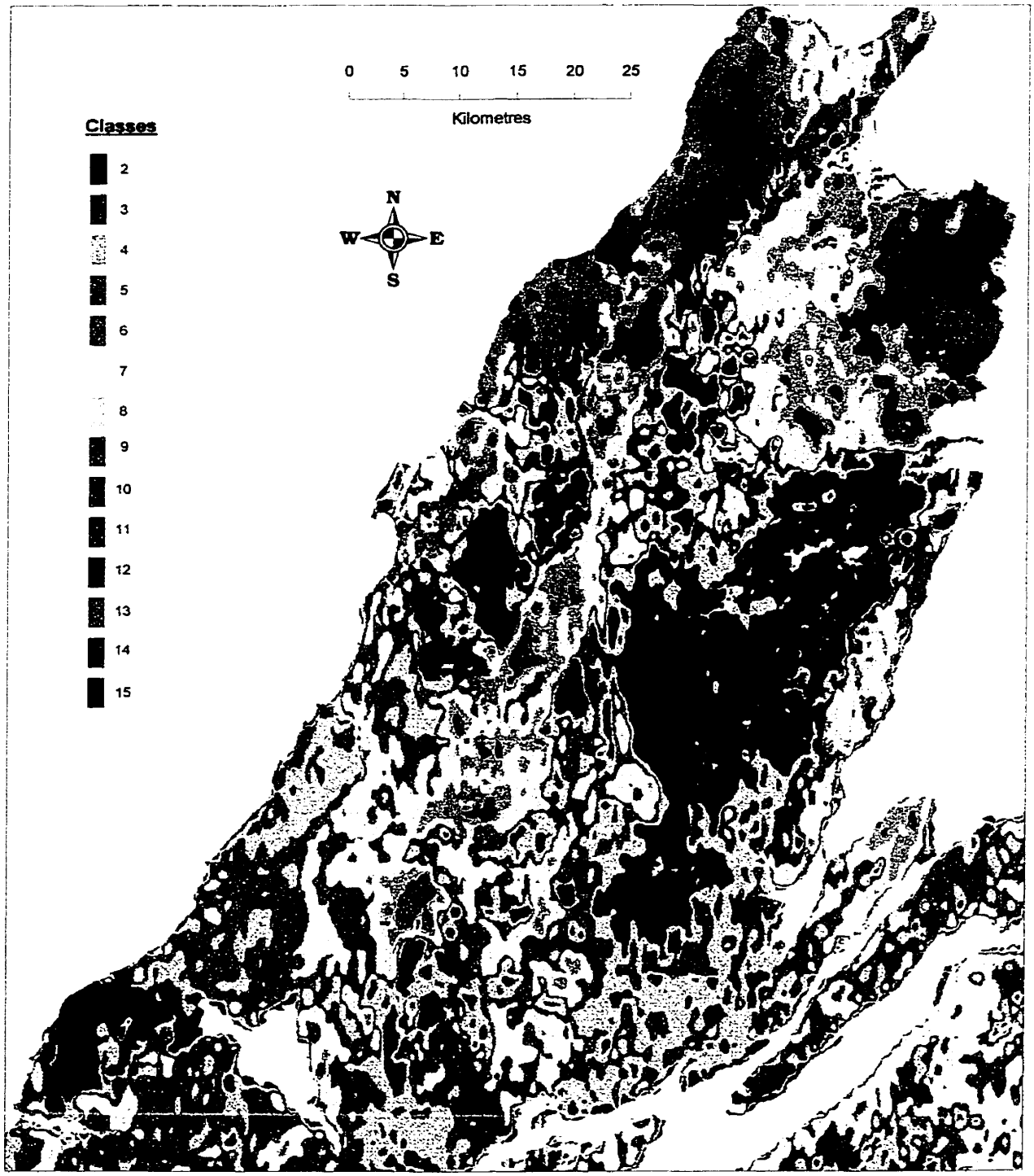

Figure 3.4 Unsupervised classification of radiometric data (%K, eTh and eU). Class definitions are shown in Figure 3.3.

3.4 Colour Display Transforms – IHS

Data integration using colour display transformations is a proven data integration technique used in image processing (Harris et al. 1994; Webster et al. 1998). This colour model technique is referred to as the IHS (Intensity, Hue and Saturation). The IHS system is based on the colour sphere system of primary colours (red, green, and blue, or RGB system) in which the vertical axis represents intensity, the radius is saturation, and the circumference is hue (Fig. 3.5). The intensity (I) axis represents brightness variations and ranges from black (0) to white (255); no colour is associated with this axis. Hue (H) represents the dominant wavelength of colour. Hue values starts with 0 at the midpoint of red tones and increase counter-clockwise around the circumference of the sphere to conclude with 255 adjacent to 0. Saturation (S) represents the purity of colour (i.e. amount of white light) and ranges from 0 at the centre of the colour sphere to 255 at the circumference.

A saturation of 0 represents a completely impure colour, in which all wavelengths are equally represented and which the eye will perceive a shade of grey that ranges from white to black depending on intensity. Intermediate values of saturation represent pastel shades, whereas high values represent purer and more intense colours. Harris (1990) described the IHS system in detail.

When one-spectral band of vertical gradient magnetic data for example are combined in the RGB system, the resulting "pseudo-colour encoded" (PCE) image is represented by the original vertical gradient of the red, green and blue images (Webster 1996). The resulting PCE image can then be integrated for example with

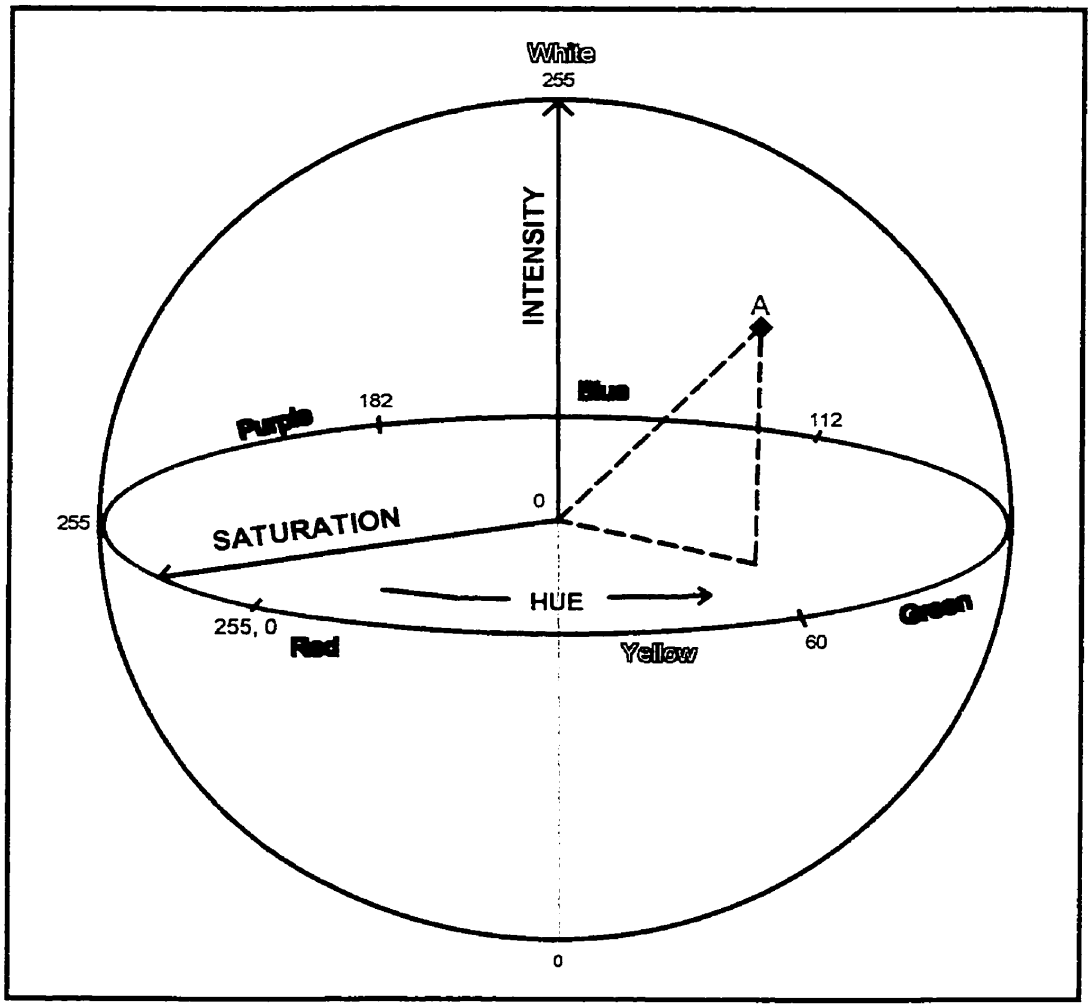

Figure 3.5 Intensity, hue, and saturation (IHS) colour coordinate system. The colour at point A has the following values: Intensity=190, hue=80 and saturation=130 (modified from Drury 1993).

topography through colour space transformation. A series of images was produced using this method, with three types of intensities. The first set depicted 3 images that used the (RGB) colours of the magnetic vertical gradient, bouguer gravity and radiometric classification fused with the shaded relief elevation model. The second set used the same previous colours but had the S7 Radarsat image as the intensity and the final set used the colours of the Bouguer gravity and radiometric classification fused with the intensity of shaded relief magnetic vertical gradient.

Five images were selected and considered the best combination for the interpretation process from the series of IHS integration. They are presented in the following figures and include: Vertical gradient magnetic (VGM) fused with shaded relief elevation model (DEM) (Fig. 3.6); total field magnetic (TFM) fused with Radarsat S7 (Fig. 3.7); gravity data fused with shaded relief elevation models (DEM) (Fig. 3.8); gravity data fused with shaded relief vertical gradient magnetic (VGM) (Fig. 3.9) and radiometric classification fused with shaded relief vertical gradient magnetic (VGM) (Fig. 3.10). These images are compared, evaluated and interpreted in Chapter 4.

3.5 Technique for Identifying Lineaments from Radarsat S7 and DEM

Radar images are important sources for identifying lineaments (Desjardins et al. 2000). Digital elevation models (DEM) have also been increasingly used to obtain geomorphic information. The purpose of this section was to develop techniques for efficient and reliable extraction of lineaments from the two data sets.

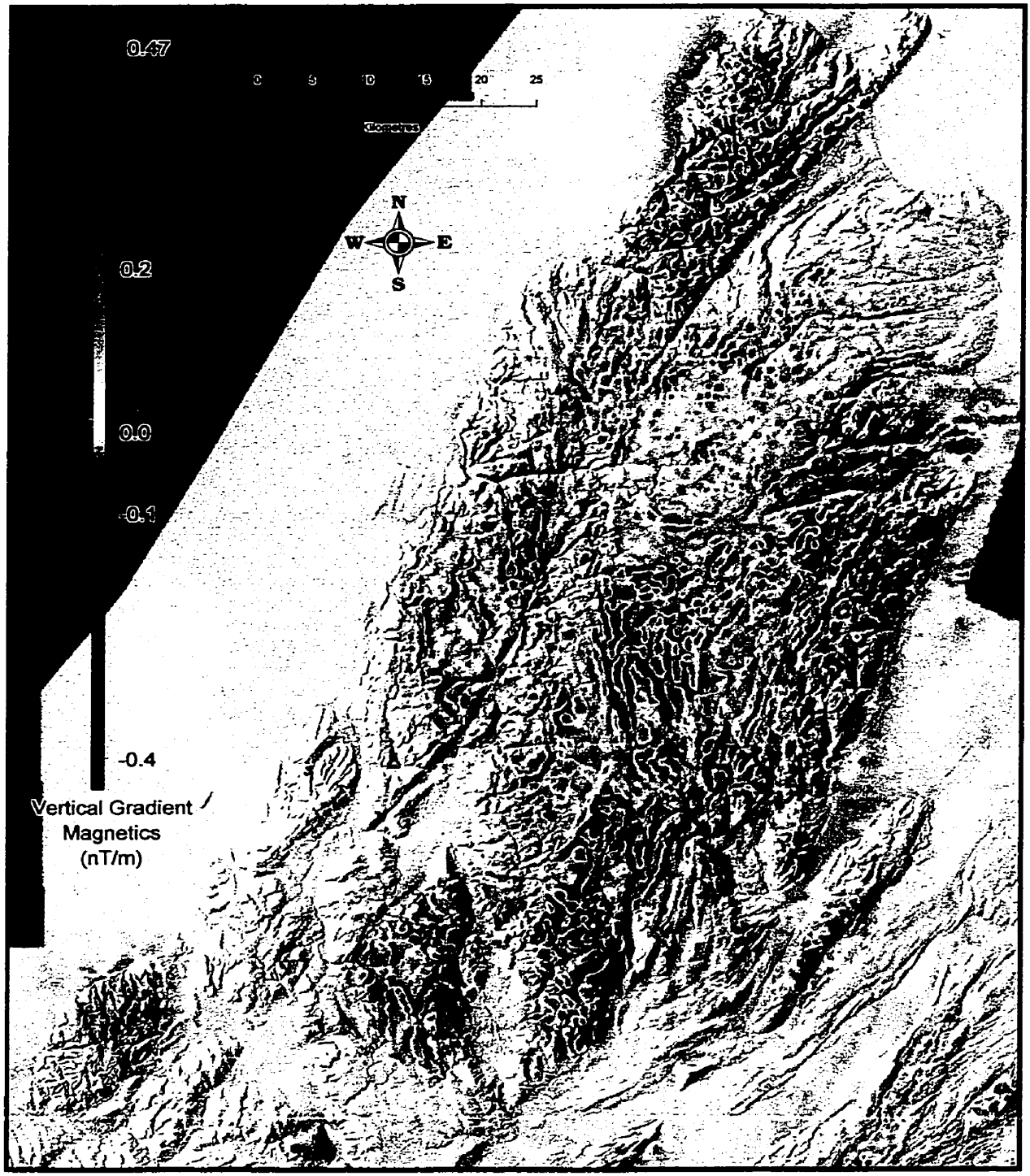

Figure 3.6 Colour coded vertical gradient magnetic data fused with shaded relief elevation model (DEM).

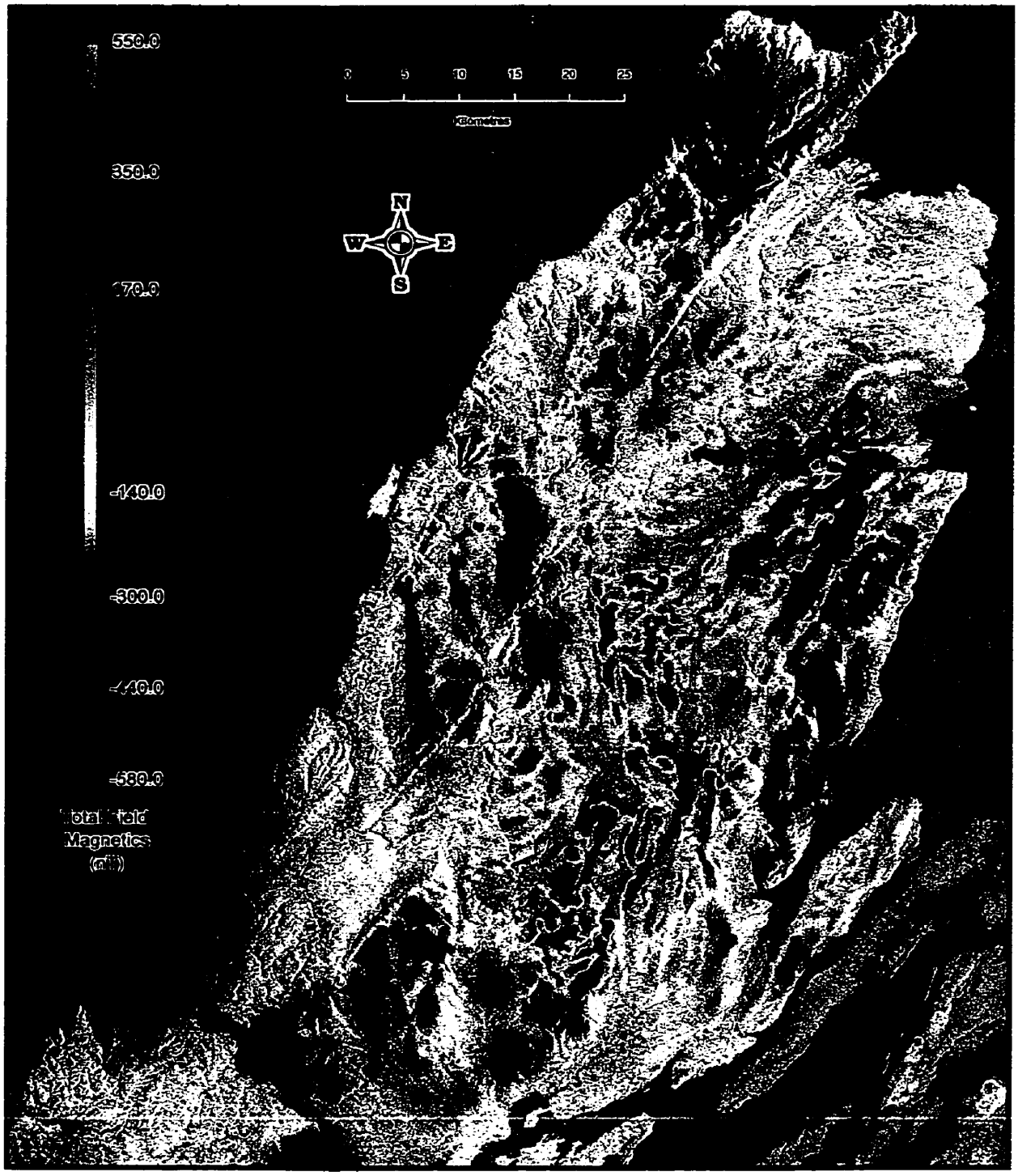

Figure 3.7 Colour coded total field magnetic data fused with Radarsat S7. Radarsat data © Canadian Space Agency 1996.

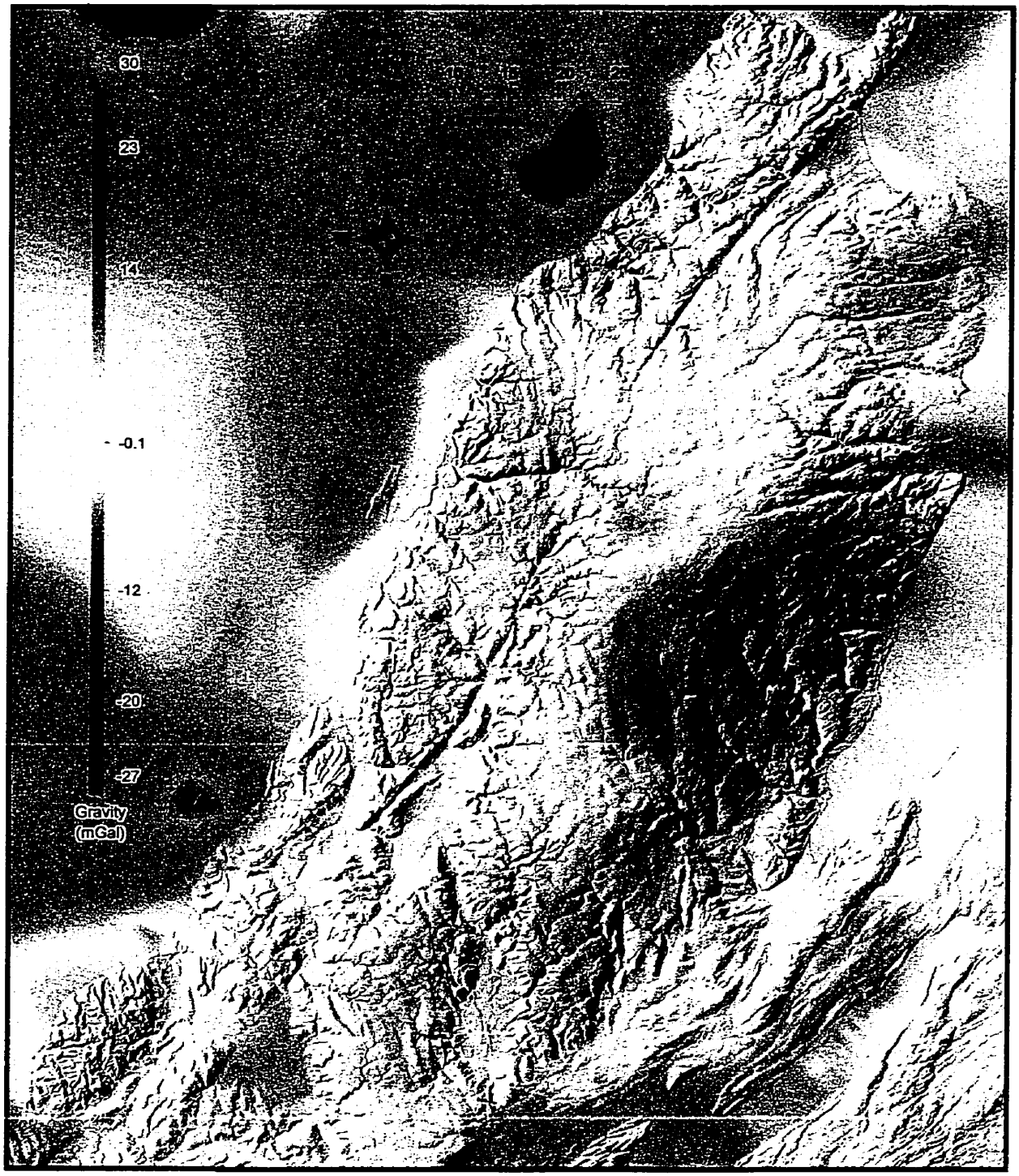

Figure 3.8 Colour coded Bouguer gravity data fused with shaded relief digital elevation model (DEM).

Figure 3.9 Colour coded Bouguer gravity fused with shaded relief vertical gradient magnetic data.

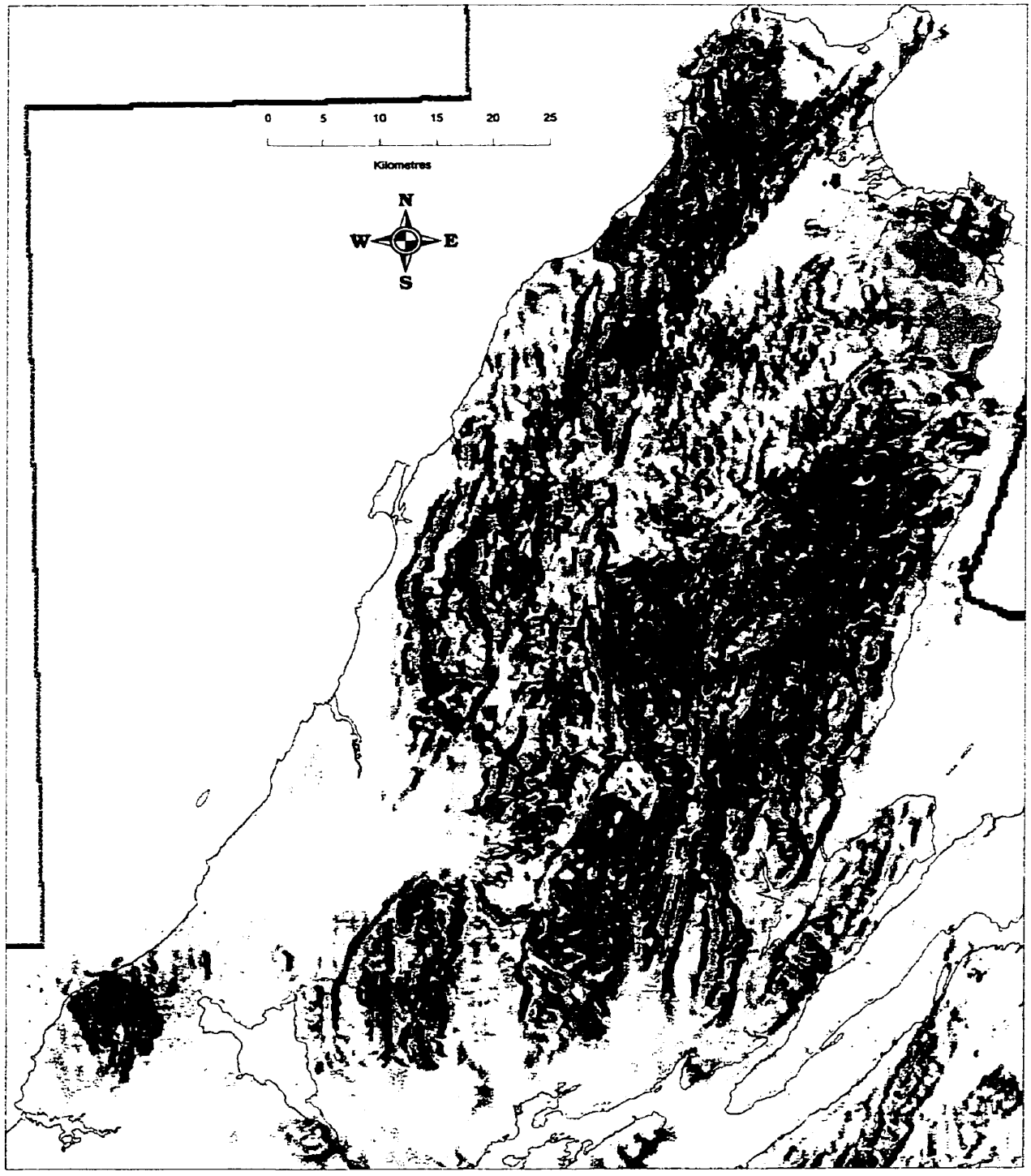

Figure 3.10 Unsupervised radiometric classification fused with shaded relief vertical gradient magnetic data.

A lineament is usually defined as a straight or somewhat curved feature in an image. In a satellite image, lineaments can be the result of man-made structures such as transportation networks (roads, canals, etc.) or natural structures such as geological structures (faults/fractures, lithological boundaries, unconformities) or drainage networks (rivers). Because many mineralization zones occur near fracture zones, lineaments are useful for locating them. The integrated study of remotely sensed data and a DEM may provide a powerful tool for structural investigations, particularly with low-resolution DEM and remote sensing images. The techniques developed in this section may contribute to solving any geologic problem that requires an assessment of regional stress and identification of major fracture sets that intercept the surface.

The Cape Breton Highlands have lineaments that reflect both glaciation and underlying regional structural trends. An automated lineament extraction procedure available in PCI Geomatics was used to detect linear features. The parameters used in the automation lineament extraction process are shown below. This methodology for mapping lineaments was used to reduce the labour-intensive task and human subjectivity in image interpretation. It is important to note that lineaments are distinguishable by the change in image intensity as measured by gradient. By applying edge detection filters to the image or extracting pixel gradient information, a numerical method for lineament detection can be constructed. This method, however, is not as good as the human visual system. The human visual system is very good at extrapolating linear features (Drury 1993). Thus, to the eye, a lineament that varies in intensity along its length may be viewed as a single long lineament whereas to a numerical method, it may appear as several short lineaments. As a result, a numerical

method for extracting lineaments has to be allow for gradual or sudden changes in gradient along the lineament, and also for minor changes in direction.

The automatic lineaments extraction parameters used on the Radarsat S7 (Fig. 3.11) and shaded relief DEM (Fig. 3.12) were:

Edge filter radius:	10 pixel
Threshold for edge gradient:	90/255 dn
Threshold for curve length:	10 pixels
Threshold for line fitting error:	3 pixel
Threshold for angular difference:	30 degrees
Threshold for linking distance:	20 pixels

A two-level integrated raster to vector approach was used, i.e. automatic line extraction from the image, and image interpretation and calculation in the GIS environment. First, the PCI Geomatics technique for extracting lines from images was applied. Topographic data and lineament vector lines were imported into MapInfo. Visual classification of linear features was carried out in the GIS interactive environment. The nature of each line (length and azimuth) was coded into the topological vector database. A program was written to extract the X and Y coordinates of the lines in order to calculate the lengths and orientations in degrees. The orientation information was then imported to a Stereonet program in order to plot rose diagrams for the selected regions. A lineament map was finally generated and rose diagrams of lineament orientations were produced for selected parts of the study area which may have the same geological significance. These data are presented in Chapter 4.

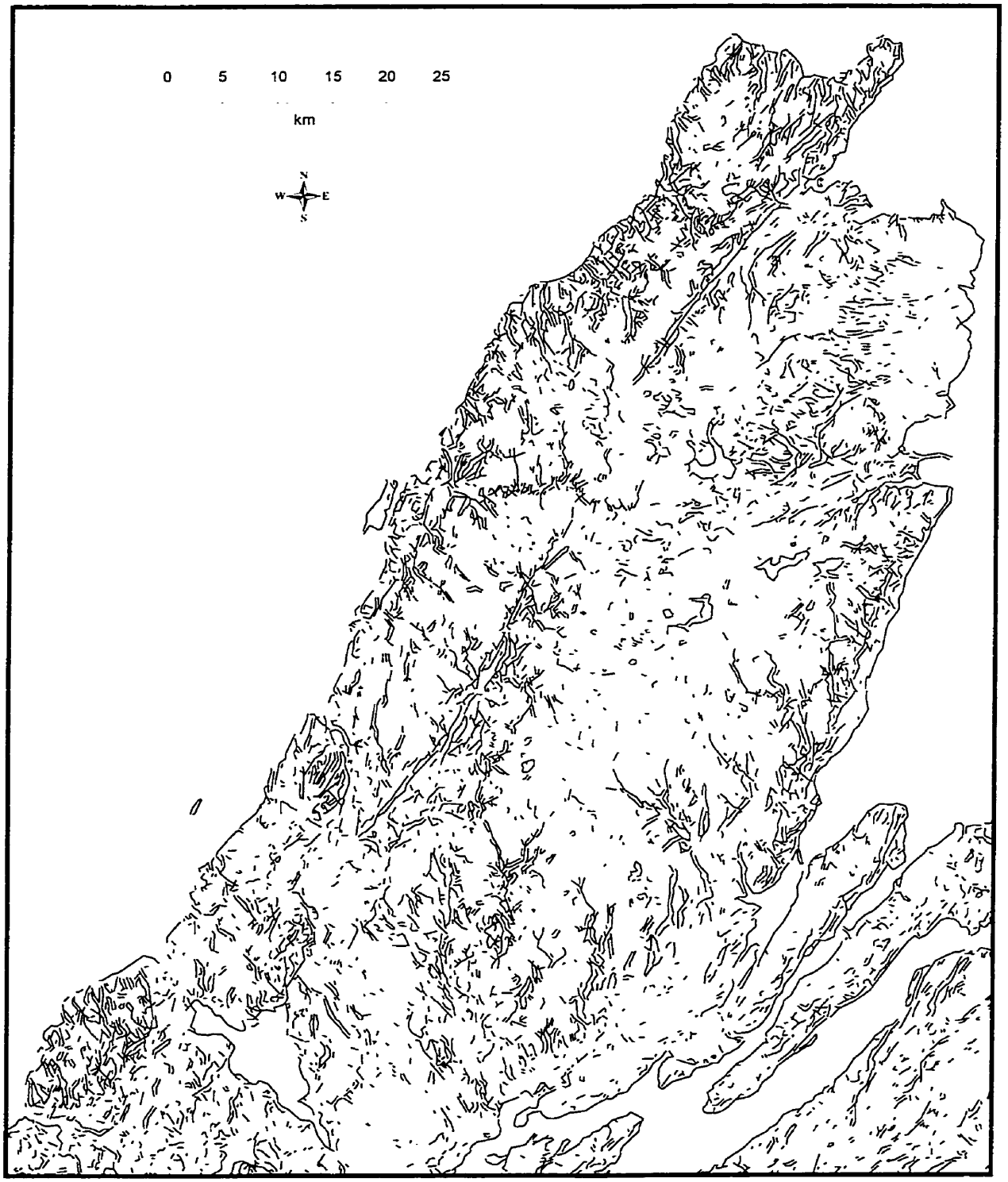

Fig 3.11 Lineaments extracted from Radarsat S7.

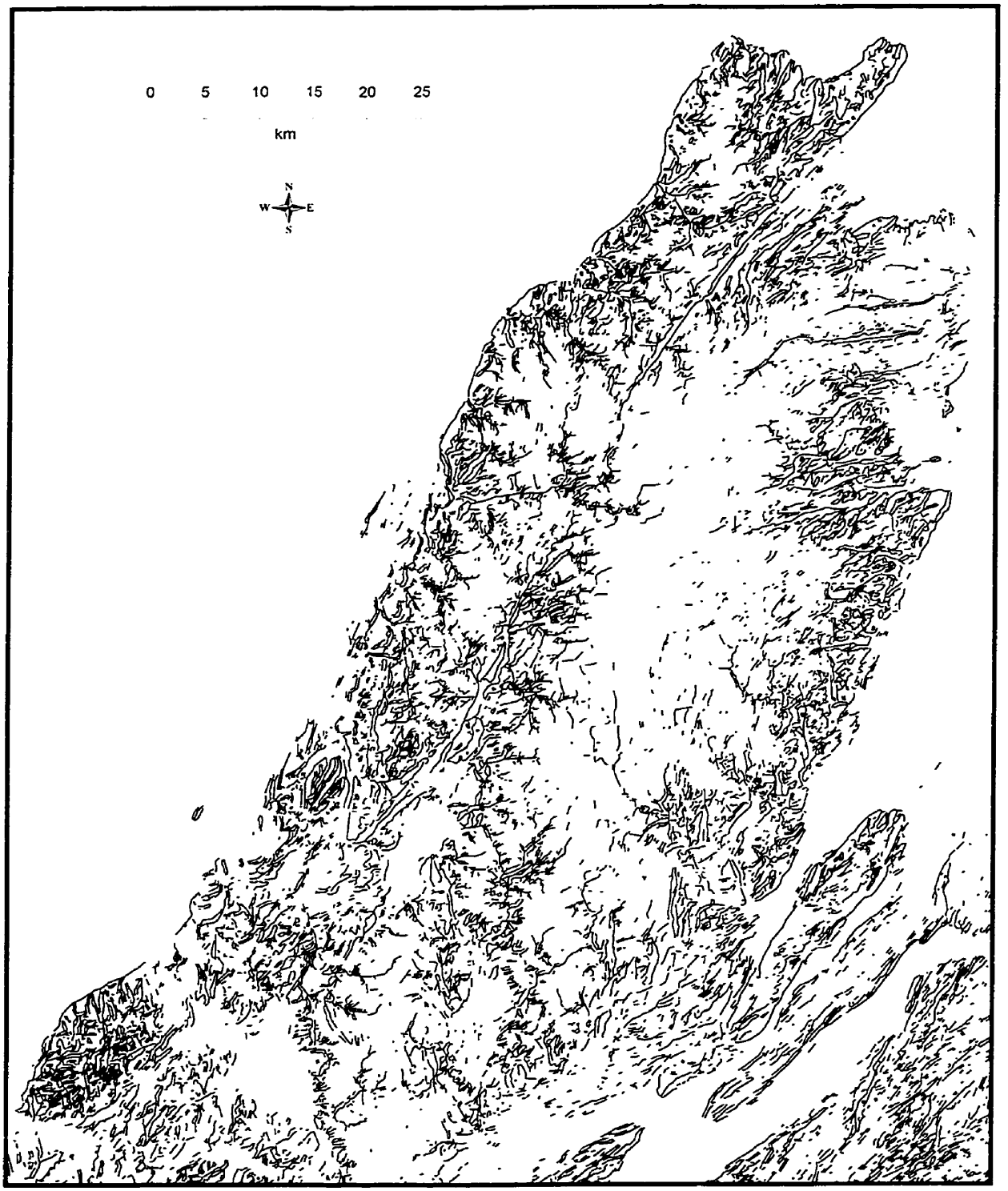

Fig 3.12 Lineaments extracted from the shaded relief digital elevation model (DEM).

Chapter 4. Regional Geological Interpretations

4.1 Introduction

The Cape Breton Highlands have been divided into five overlapping areas for the purpose of regional interpretations (Fig. 4.1). The subdivision is somewhat arbitrary but was based on convenience of size, as well as known geological characteristics and geophysical signatures. Area 1 focuses on the northern part of the highlands, specifically the Blair River Inlier and its bounding faults. Area 2 centres on the southeastern part of the study area, mainly the Bras d'Or terrane. Areas 3, 4 and 5 focus on the northeastern, western, and southern parts of the Aspy terrane, respectively.

The digital dataset presented and described in previous chapters is used here to highlight important lithological similarities and contrasts in comparison to published geological interpretations of pre-Carboniferous rock units. A new digital geological map and associated geological unit database were produced. The geological map of Barr et al. (1992) appears to provide the best agreement with the image datasets, and was used as the base for the revised map. For each area, a labelled revised geological map is presented, followed by images showing the vertical gradient magnetic data fused with the shaded relief digital elevation model and the radiometric classification, both overlain by the revised geology.

Other images in Chapters 2 and 3 are also referred to as appropriate. Within the scope of this thesis, it is not possible to discuss every map unit or feature visible on the maps. This chapter attempts to provide an overview of the usefulness of the data in assisting geological interpretations.

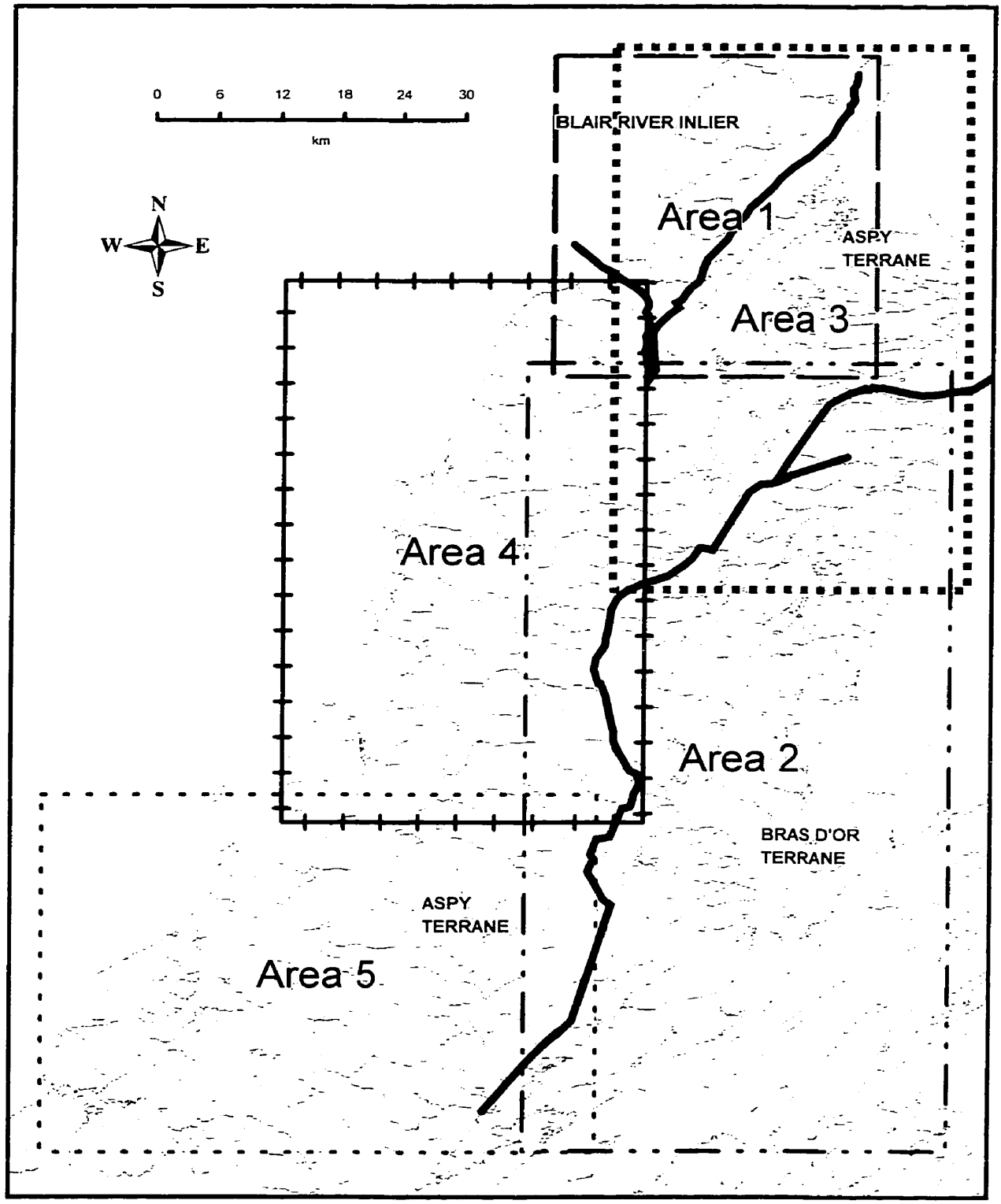

Figure 4.1 Outline map of the Cape Breton Highlands showing overlapping areas used for regional interpretations. Dark lines represent terrane boundaries.

It should be noted that the remote sensing images have limitations because of their varied resolution. The resolution ranges from 10 to 30 metres for the DEM, Landsat TM and Radarsat, whereas the geophysical data are gridded at 100 m pixels. For this reason, as well as space limitations, small features such as dykes and minor rock units are not discussed. However, Chapter 5 will focus in more detail on specific smaller areas selected as examples of the types of more focussed studies that could be done.

4.2 Area 1

Area 1 (Fig. 4.2a, b, c) contains the Blair River Inlier (BRI) which is made up of mostly Mesoproterozoic metaplutonic rocks and displays compositional and metamorphic similarities to the Grenville province of the Canadian Shield (Barr and Raeside 1989; Miller et al. 1996). The Wilkie Brook and Red River fault zones border the BRI on the southeast and southwest, respectively. The anorthosite, syenite, and granitoid plutons (ages 1100-980 Ma) of the BRI intruded the older Sailor Brook and Polletts Cove River gneiss units. In map view, the gneissic units make up close to half of the area of the BRI. The southwestern part of the BRI contains Devonian to Silurian plutonic rocks, including Sammys Barren granite, Red Ravine syenite and the Fox Back Ridge diorite-granodiorite. The BRI is overlain by Devonian to Carboniferous volcanic and sedimentary rocks and younger Carboniferous sedimentary units (Fig. 4.2a). The latter units are not discussed in the present study.

The Mesoproterozoic rocks of the BRI generally have a high TFM value of about 500 nT (Fig. 2.7), and an irregular vertical gradient magnetic pattern with a wide range

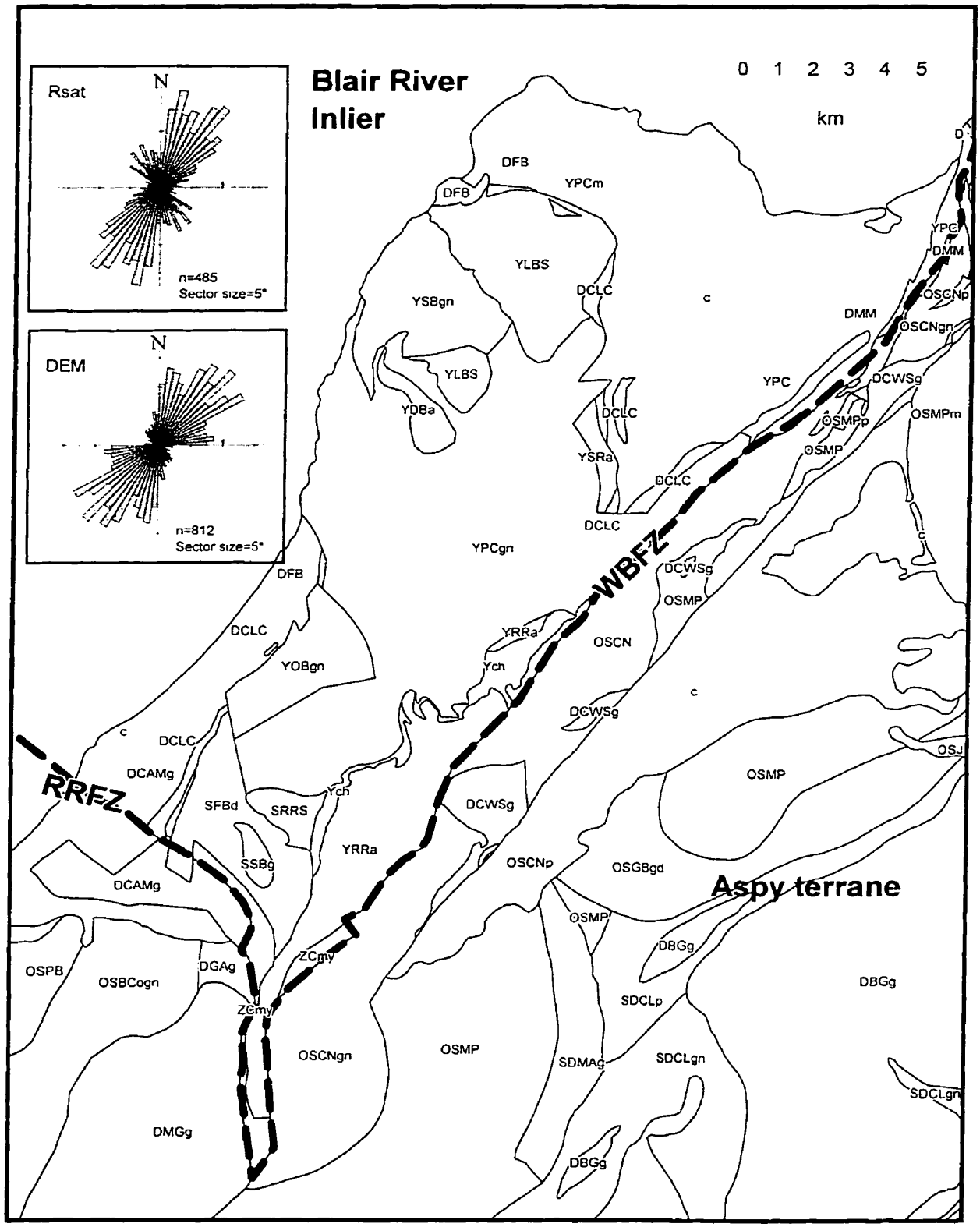

Figure 4.2a Geology of the Blair River Inlier modified from Miller (1997). Dashed line represents approximate terrane boundary. Inset diagrams show lineament orientations derived from DEM and Radarsat. Unit labels are identified in Appendix A.

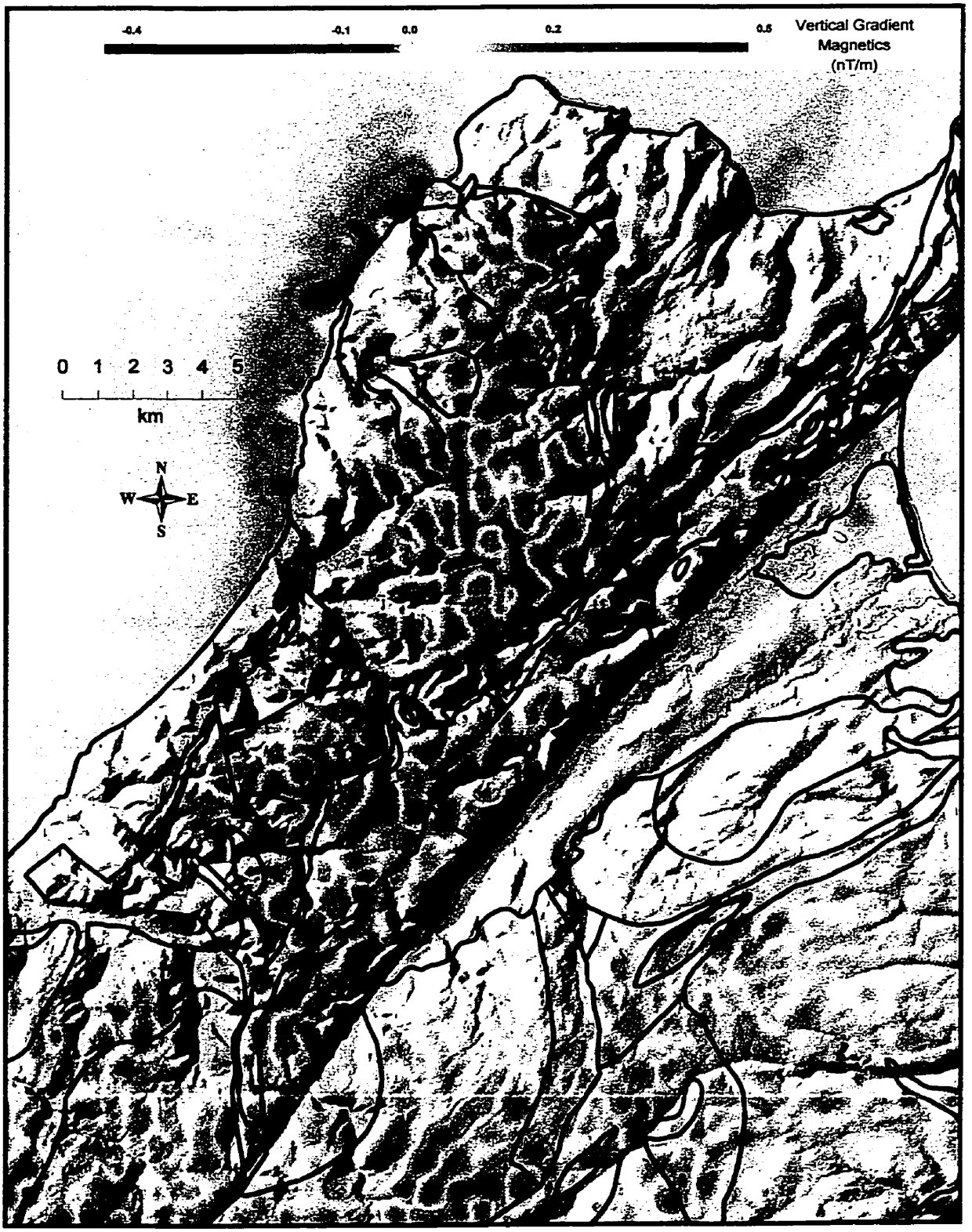

Figure 4.2b Vertical gradient magnetic data fused with shaded relief (DEM) overlain by geology from Figure 4.2a.

Figure 4.2c Radiometric classification from Figures 3.3 and 3.4, overlain by geology from Figure 4.2a.

from –0.4 to +0.5 nT/m (Fig. 4.2b). Based on the limited data, the gravity response (Fig. 2.9) for this area is moderately high for the Cape Breton Highlands, with values ranging from 2 to 7 mGal. The radiometric signature of the area is dominated by classes 2, 3, 6, and 9 (Fig. 4.2c) and contrasts with that of the surrounding Carboniferous units and units of the adjacent Aspy terrane. The differences are consistent with the rock types in the BRI, which differ significantly from those of the Aspy terrane. Lineaments derived from Radarsat and DEM trend mainly northeast to north-northeast (Fig. 4.2a inset), a pattern not readily apparent from the geological map (Fig. 4.2a) or the VGM and radiometric images (Fig. 4.2b, c).

The Otter Brook Gneiss (YOBgn) (medium- to coarse-grained, augen to flaser, biotite-garnet granitoid gneiss) has moderate (1.2% to 1.5%) K values with low eTh (1.2 ppm to 1.8 ppm) as represented by class 9. It gives a relatively high magnetic response (TFM 450 to 500 nT; VGM up to 0.5 nT/m). The Pollets Cove River Gneiss (YPC) has similar magnetic and radiometric signature (in part) but is separated from the Otter Brook Gneiss by the Polletts Cove River valley and a linear magnetic gradient anomaly. The presence of this moderately low magnetic linear suggests a faulted contact between the Otter Brook Gneiss and Polletts Cove River Gneiss. The Polletts Cove River Gneiss is mainly represented by radiometric classes 2, 3 and 6. These three classes correspond to low K (0.1 to 0.8 %), eTh (0.6 to 1.8 ppm) and eU (-0.1 to 0.45 ppm). The gravity response of the Polletts Cove River Gneiss ranges from 5 to 6.7 mGal, the highest values measured in the BRI, although data are limited (Fig. 2.9).

The anorthosite units in the BRI give magnetic and radiometric signatures similar to those of the gneissic units and are not readily distinguished (Fig. 4.2b, c). In contrast

the Lowland Brook Syenite (YLBs) appears to display lower gravity and much higher K values (2.3 to 3.2% K) than the gneissic units, consistent with high K-feldspar content in the syenite and high K_20 content in analysed samples (range 3.68 to 6.91 % K_20, average 5.56 %; Miller and Barr 2000). The Lowland Brook Syenite also exhibits low eTh and eU relative to K, and hence falls in radiometric class 11.

West of the Lowland Brook Syenite, the Sailor Brook Gneiss has moderately low magnetic values (TFM=200 to 380 nT; VGM= -0.4 to –0.2 nT/m) and has a radiometric signature of mainly class 9, indicating higher K compared to eTh and eU, although the Sailor Brook Gneiss has lower mean K values (1 to 2% K) than the Lowland Brook Syenite. Chemical analyses of samples from the Sailor Brook Gneiss confirm a lower K_20 content ranging (0.47 to 4.1% K_20, average 1.9 %; Miller and Barr 2000).

Silurian granitoid rocks, including the Sammys Barren granite (SSBg), Red Ravine syenite (SRRs) and the Fox Back Ridge diorite and granodiorite (SFBd), are characterised by radiometric signatures represented by classes 9, 11 and 14. All of these classes indicate higher K compared to U and Th. The Fox Back Ridge diorite has higher magnetic values (TFM 550 nT; VGM 0.5 nT/m) compared to the Red Ravine syenite and Sammys Barren granite (TFM -200 nT; VGM –0.3 nT/m). The ratio of eU to eTh in the Sammys Barren granite is particularly useful to mark the extent of this pluton, which has moderate amounts of each element (4 to 6 eTh and 1.2 to 1.7 eU).

The BRI is bordered by younger volcanic and plutonic rocks, including the Lowland Cove Formation (DCLC) (basalt, rhyolite and sedimentary & tuffaceous rocks) on the west the Andrews Mountain (DCAMg), Grande Anse (DGAg), and Margaree (DMPg) plutons to the south, and the Wilkie Sugarloaf (DCWSg) and related granitic

plutons to the east. Unlike the Fisset Brook Formation (DFB) in area 4 to the south, unit DCLC has low magnetic values (TFM -500 to –590 nT; VGM –0.4 nT/m). The VGM image suggests that this unit might be continuous under the water along the western edge of BRI , joining the small exposure of the unit to the north of the Lowland Brook Syenite. The Red River Fault Zone (RRFZ) separates the high magnetic signature of the BRI from the moderately low values associated with the Andrews Mountain Granite (DCAMg) to the south. Similarly, on the eastern edge of the BRI, the Wilkie Brook Fault Zone (WBFZ) marks a change from high magnetic values on the west to lower values on the eastern side associated with units of the Aspy terrane. Granite plutons east of the fault, such as Wilkie Sugarloaf (DCWSg) have high radiometric signatures (class 14) like the Andrews Mountain Granite.

4.3 Area 2

Area 2 (Fig. 4.3a, b, c) includes the Bras d'Or terrane southeast of the Eastern Highlands Shear Zone (EHSZ) of Barr and Raeside (1989). It consists of sedimentary and volcanic rocks, variously metamorphosed from relatively low grade in the south to high grade in the northern part of the area. The main metamorphic unit in the area is the McMillan Flowage Formation, the most extensive stratified unit in the Bras d'Or terrane (Raeside and Barr 1990). The metamorphic rocks are intruded by voluminous diorite, tonalite and granite interpreted to have formed in a continental margin subduction zone (Raeside and Barr 1990). The plutonic units have U-Pb (zircon) ages of 555–565 Ma (Late Neoproterozoic).

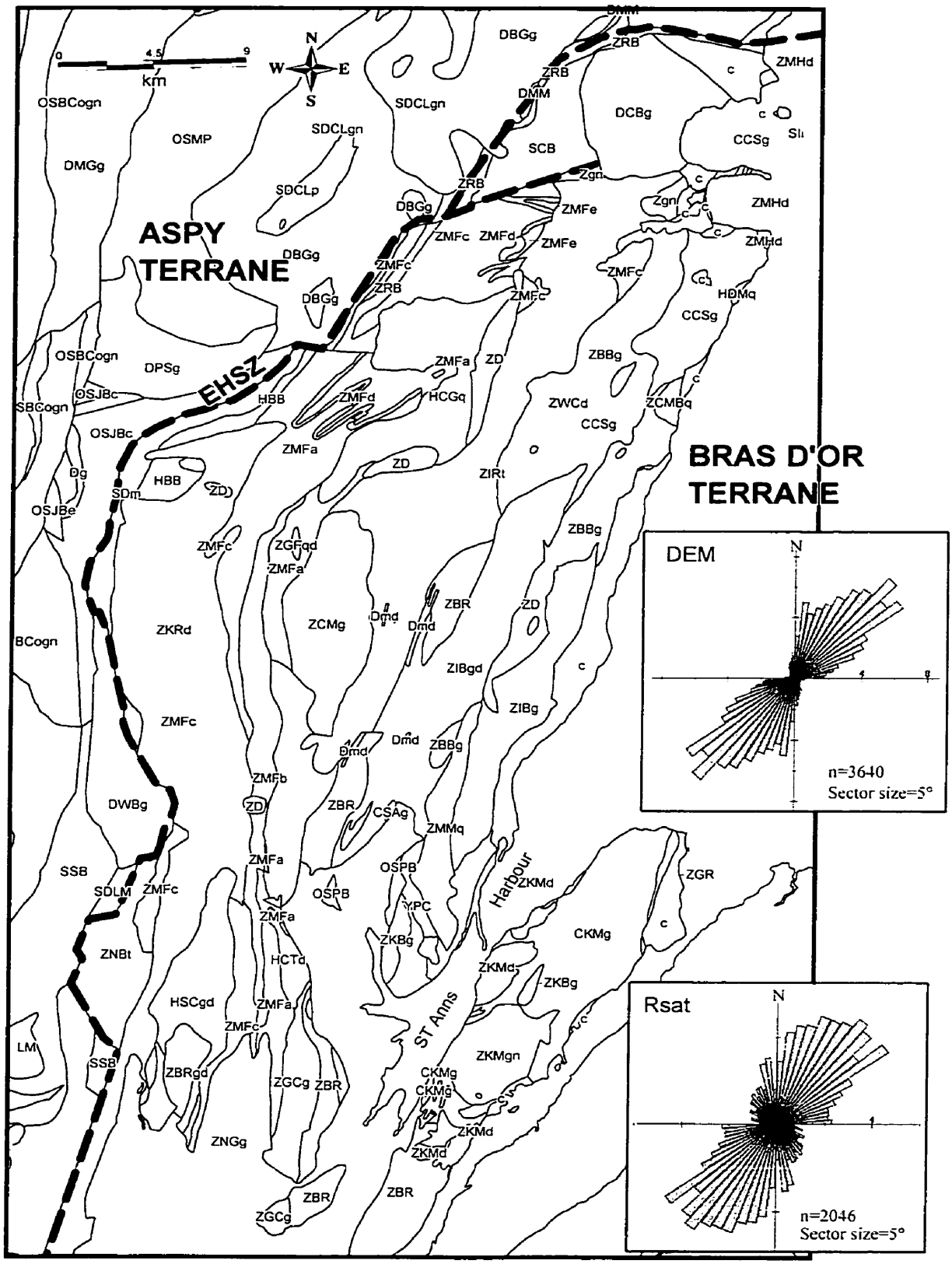

Figure 4.3a Geology of the Bras d'Or terrane modified from Barr et al. (1992). Inset diagrams show lineament orientations derived from DEM and Radarsat. Unit labels are identified in Appendix A. Dashed line represents approximate terrane boundary (Eastern Highlands Shear Zone, EHSZ).

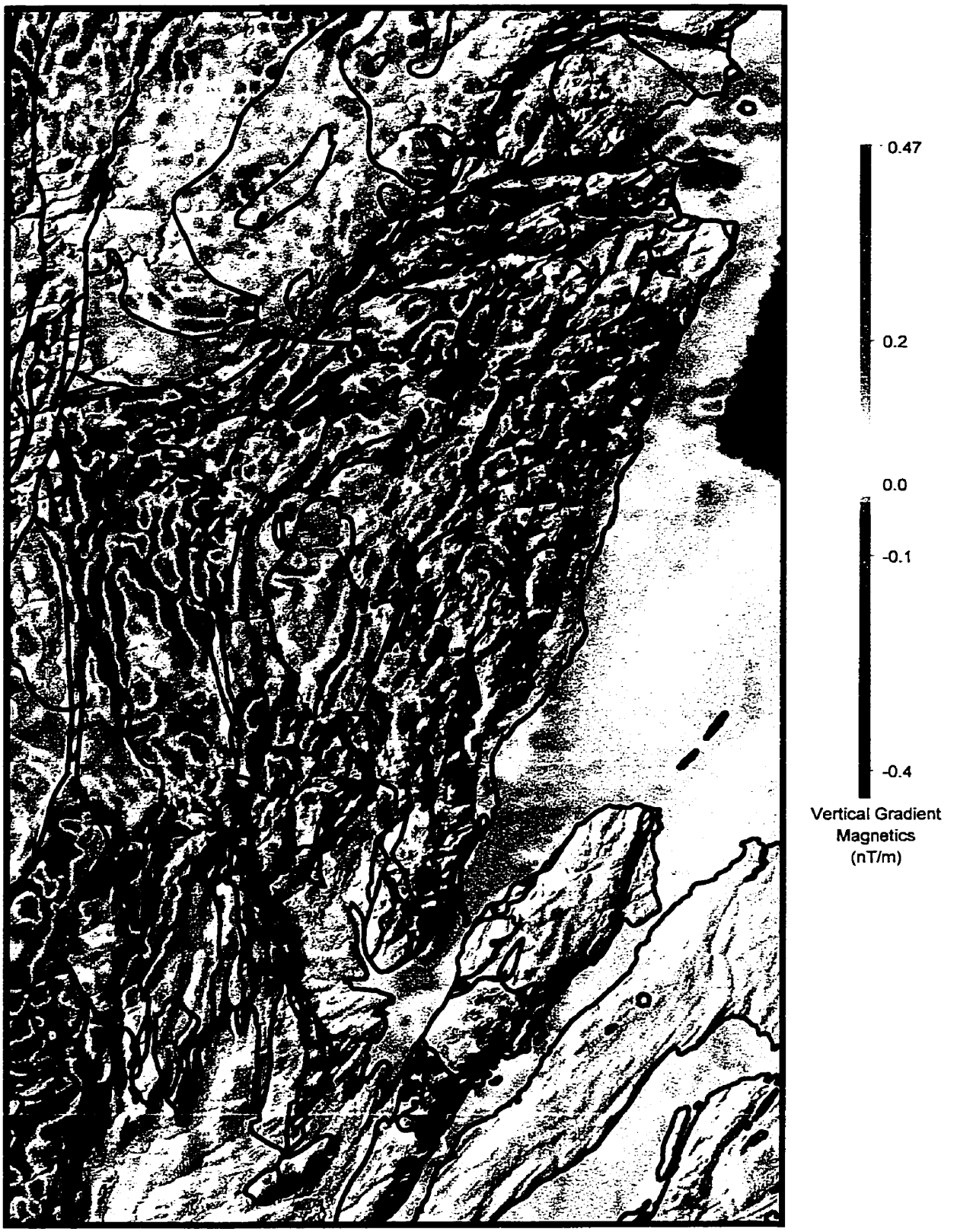

Figure 4.3b Vertical gradient magnetic data fused with shaded relief (DEM) overlain by geology from Figure 4.3a.

Figure 4.3c Radiometric classification overlain by geology from Figure 4.3a.

The western and northwestern boundary of this block of rocks is the Eastern Highlands Shear Zone. Toward the east, the EHSZ is less well defined, and appears to have been intruded by the Black Brook Granitic Suite and the Cameron Brook Granodiorite, although some faults in this area cut Carboniferous sedimentary units (Raeside and Barr 1992, Barr and Raeside 1989). Hence the northern limit of the Bras d'Or terrane is obscure in this area (Lin and van Staal 1997; Lin 1992, 1993, 1995).

Magnetic data show strong northeast-trending anomalies in the eastern part of area 2, and more disrupted but mainly north-trending anomalies in the west (Fig. 4.3b). Most of the Bras d'Or terrane is characterised by radiometric classes 2, 3 and 4 (purple tones in Fig. 4.3c), and has the highest Bouguer gravity values in the study area (Fig. 2.9). In contrast to the tonalite and diorite units in the middle, the eastern edge of the Bras d'Or terrane has higher radiometric classes (orange Fig. 4.3c) and lower gravity values (Fig. 2.9) characterising the lower density granites. Lineaments derived from shaded relief DEM and Radarsat (Fig. 4.3a, inset) indicate a dominant northeasterly trend coinciding with shore lines of the Atlantic Ocean and Great Bras d'Or Lake, and with the geological and magnetic trends. The lineations derived from Radarsat also show a weak north-northwest trend (Fig. 4.3a inset). The NE direction has variability within the 30° and 70° range. The NNW trend is in part attributed to the area of the "zone of structural complexity" discussed below.

The Ingonish River Tonalite (ZIRt), Wreck Cove Dioritic Suite (ZWCd), Murray Mountain Quartz Monzodiorite (ZMMq), and Indian Brook granodiorite (ZIBgd) and granite (ZIBg) have the highest magnetic anomalies (TFM 550 nT; VGM 0.5 nT/m) in area 2. This group of elongate plutons coincides with the area of continuous NNE

magnetic trends noted previously and with higher total field magnetic signatures compared to the Kathy Road Dioritic Suite (ZKRd) farther to the west. Furthermore, the Kathy Road Dioritic Suite and the Snake Cat Lake Granodiorite (ZSCgd) have similar class 2 radiometric signatures (Fig. 4.3c) and anomalous yellow to white colour on the infrequency brightening ternary image (Fig 3.2). Both units have low K content (0.1 to 0.2 % K). The middle part of Kathy Road Dioritic Suite has also the lowest eTh (0.1 to 0.9 ppm) content in the area, in contrast to the Snake Cat Lake Granodiorite which has a higher eTh of (1.1 to 1.6 ppm) and a generally lower magnetic values (Fig. 4.3b) compared to Kathy Road Dioritic Suite.

The linear trends displayed on the image of VGM fused with DEM (Fig. 4.3b) converge toward a focal point near the area where North River splays into the West, Middle and East branches. This area is identified as the "zone of structural complexity" (Fig. 4.4). Three linear magnetic trends occur north of the "zone of structural complexity". They surround the Cross Mountain Granite (ZCMg), forming a crude inverted triangle. The Cross Mountain Granite has a relatively low magnetic signature (TF -530 to –280 nT; VG -0.4 to –0.1 nT/m) compared to surrounding units. Based on the signature, the position of the southeastern contact of the pluton has been shifted to the northwest (where no outcrop control exists) in comparison to its position on the map of Barr et al. (1992). East of the Cross Mountain Granite, the NNE magnetic trends are very straight and continuous, but to the north and west of the granite, the NE and NNW trends follow approximately the EHZS. Similarly, the magnetic trends south of the "zone of structural complexity" converge to the north forming a "bow-tie" shaped pattern (Fig 4.4). This area will be discussed further in Chapter 5.

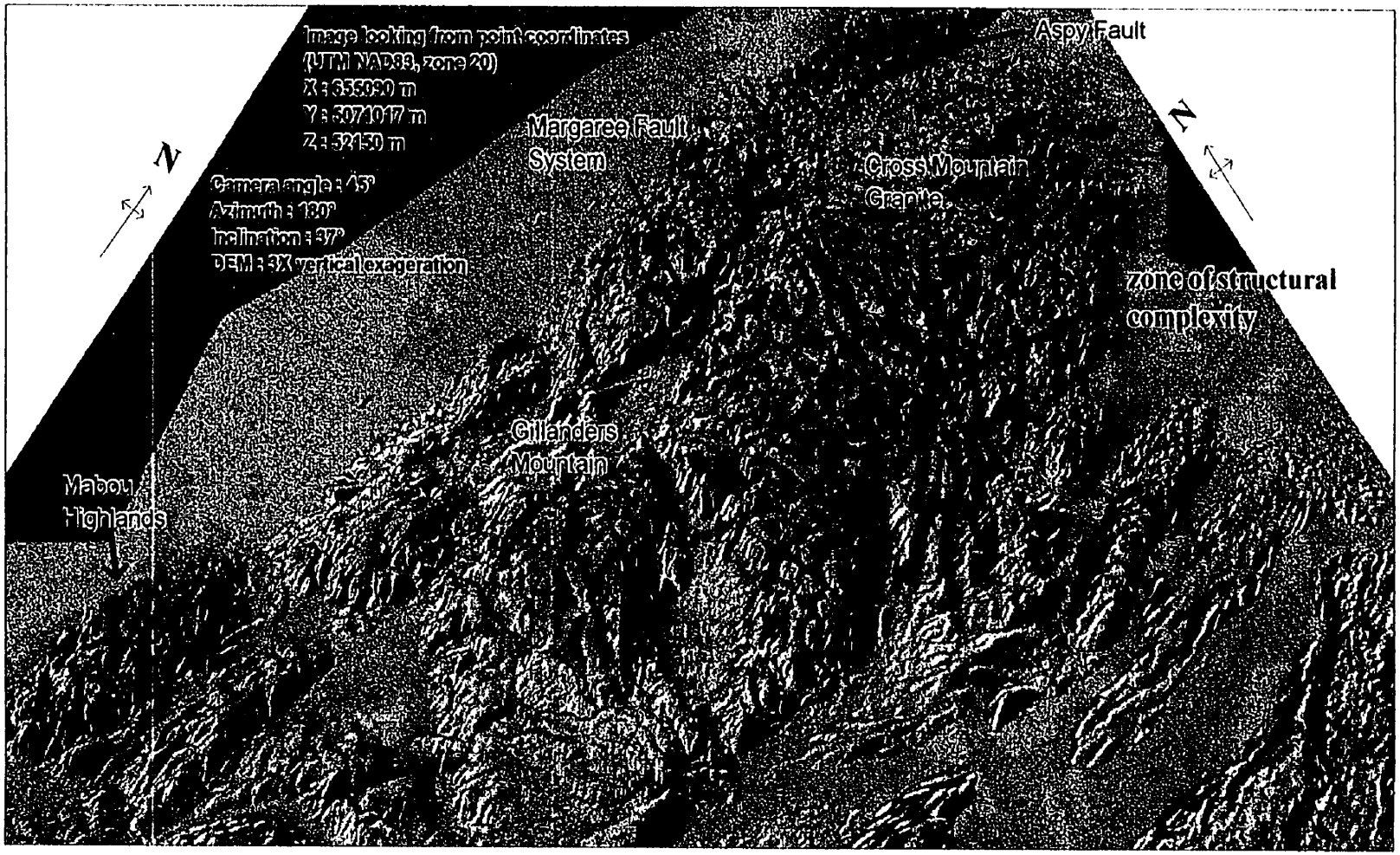

Fig. 4.4 3D view of vertical gradient magnetics draped over DEM showing the "zone of structural complexity". Dashed lines represent magnetic trends within the Bras d'Or terrane.

In the northern part of area 2 a significant magnetic anomaly surrounds the western and northern margin of the Cameron Brook Granodiorite (DCBg)and Clyburn Brook Formation (SCB) (Fig. 4.3b). The magnetic anomaly has a narrow wavelength with moderate values (TFM -200 to –120 nT; VGM 0 to 0.4 nT/m) and a quarter-circle appearance in map view. This anomaly coincides with the Eastern Highlands Shear Zone (EHSZ) including the Roper Brook amphibolite (ZRB) and chlorite schist mylonitic shear zone (SDm) of Raeside and Barr (1992). Between the Cameron Brook Granodiorite and the EHSZ, the Clyburn Brook Formation forms a triangular wedge. The Clyburn Brook Formation consists of rhyolite, andesite, tuff, volcanic and pelitic phyllite (Lin 1992; Barr and Raeside 1998) and has a radiometric response of mainly class 7 (yellow) and low magnetic amplitude (TFM -580 to –560 nT; VGM -0.1 to -0.4 nT/m). These values contrast with those of adjacent plutons, including the Cameron Brook Granodiorite that has a signature of class 13 in the south and class 10 and 12 in the north. All of these classes have a much higher ratio of K and eTh compared to eU whereas class 7 is relatively neutral, with approximately 1:1:1 ratio of K, eTh and eU. Petrochemical analysis of samples from of the Cameron Brook Granodiorite also indicate a high ratio of K and eTh (67.3-71.5 % SiO_2; 3.7-4.3 % K_2O; and 19-24 ppm Th) (O'Beirne et al. 1986), whereas samples from the Clyburn Brook Formation are dominantly mafic (46-55 % SiO_2; <2 % K_2O; and <10 ppm Th; Barr and Raeside 1998). The radiometric response of the Clyburn Brook Formation also contrasts with that of the McMillan Flowage Formation (ZMFC) and Ingonish River Tonalite to the south (Fig. 4.3c). The contrast with the McMillan Flowage Formation supports the exclusion (Barr and Raeside 1998) of the Clyburn Brook Formation from the McMillan Flowage

Formation to which it was originally assigned (Barr et al. 1992), and by implication its inclusion on the Aspy terrane, rather than the Bras d'Or terrane.

A 3 km-wide band of strong (K and Th vs U) signatures classes (8, 10, 12 and 14) coincides with the eastern margin of the Cape Breton Highlands including Kellys Mountain (Fig. 4.3c). These orange and red colours coincide with the Cape Smokey Granite (ЄCSg) in the north, Birch Plain Granite (ZBPg) in the central area, and the St. Anns (ЄSAg) and Kellys Mountain (ЄKMg) leucogranite plutons in the south. These granites also have similarities in their magnetic fabrics, with moderate values compared to the more mafic plutons to the west.

One of the elongate plutons in the southeastern highlands, the Indian Brook Granodiorite, is divided into eastern (ZIBg) and western (ZIBgd) parts by the Birch Plain Granite in the north and the Murray Mountain Quartz Monzodiorite (ZMMq) in the south. The Indian Brook Granodiorite is distinct from the Birch Plain Granite and Murray Mountain Quartz Monzodiorite because of its high magnetic amplitudes. Although both the eastern and western parts of the Indian Brook Granodiorite have high magnetic values, the western block is represented by radiometric classes 2 and 3 (low K and Th vs U) whereas the eastern part is represented by classes 8, 9 and 10 (high K and Th vs U). Petrochemical analysis also suggested differences between the two parts of the Indian Brook Granodiorite (Grecco and Barr 1999). Grecco and Barr (1999) concluded that the Indian Brook Granodiorite varies from more mafic in the northwest to more felsic in the southeast, and they suggested that the western part represents the deeper part of the pluton.

The mapped units of the McMillan Flowage Formation follow the same continuous magnetic trends discussed above, north and west of the Cross Mountain Granite. Although very continuous from the south of the Clyburn Brook Formation to Goose Cove Brook, west of St Anns Harbour, magnetic wavelengths and classification are variable. The quartzite member (ZMFb) can be readily recognised on the elevation model (Fig. 2.1) and generally has low magnetic values about (TFM -300 to –450 nT; VGM -0.1 to -0.4 nT/m).

4.4 Area 3

Area 3 (Fig. 4.5a, b, c) is dominated by the Black Brook Granitic Suite (DBGg), one of the largest plutons in Cape Breton Island. It intruded the Neils Harbour Gneiss (DNH) on the east and the Cheticamp Lake Gneiss (SDCLgn) on the west. Metasedimentary and metavolcanic rocks both northwest and southeast of the Aspy Fault, assigned to the Money Point and Cape North groups (Barr and et al. 1992) also occur in area 3. Also present northwest of the Aspy Fault are the Wilkie Sugarloaf Granite and other related small granitic intrusions, as mentioned previously.

Generally area 3 is characterised by a gradual elevation change from the lowest in the northeast along the coastline of the Black Brook Granitic Suite to highest in the southwest. The White Hill north of Cheticamp Flowage is the highest point in the Cape Breton Highlands, and the southwestern part of area 3 in the area of Park Spur Granite is the highest elevated plateau region. Furthermore, this plateau has variable radiometric signatures as a result of numerous bogs and swamps. Magnetic trends are variable, gravity values are moderate to the west and low in the northeast. Area 3 has also been

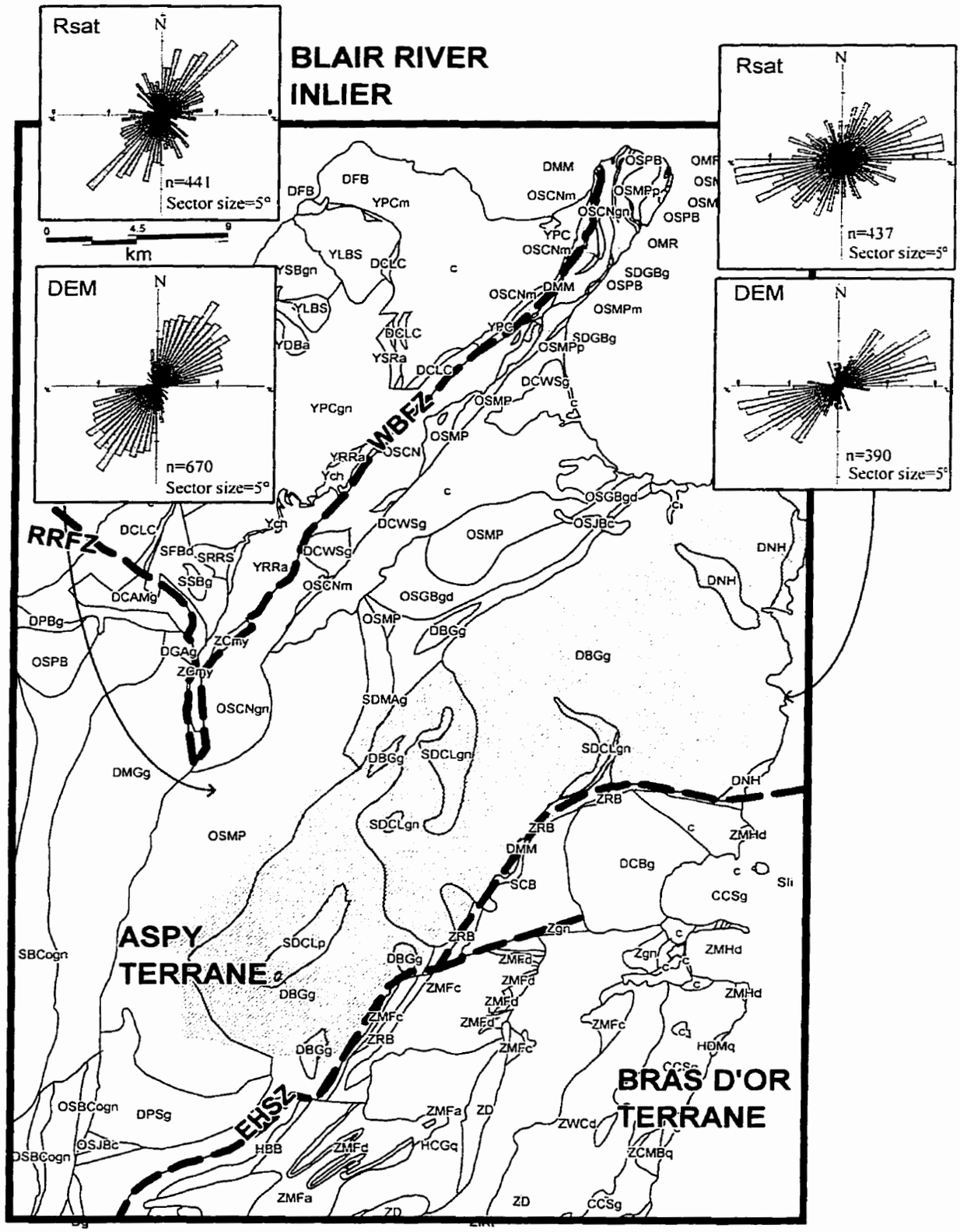

Figure 4.5a Geology of the northeastern part of the Aspy terrane modified from Barr et al. (1992). Inset diagrams showing lineament orientations within domains are derived from DEM and Radarsat. Dashed lines represent approximate terrane boundaries from Barr & Raeside (1989).

Figure 4.5b Vertical gradient magnetic data fused with shaded relief (DEM) overlain by geology from Figure 4.5a.

Figure 4.5c Radiometric classification overlain by geology from Figure 4.5a. Dashed lines represent divisions of the Black Brook Granitic Suite from Yaowanoiyothin (1991).

divided in two domains representing different lineament orientation (inset rose diagrams in Fig. 4.5a). The southeastern part of the area, mainly underlain by the Black Brook Granitic Suite, is characterised by east-to ENE-trending topographic lineaments (Fig. 4.5a), whereas the northwestern part of area 3 has mainly northeast-trending lineaments.

The Black Brook Granitic Suite has been divided into three main units based on texture and modal mineralogy (Yaowanoiyothin and Barr 1991). Two of these units correlate well with the radiometric classification. Unit 1 consists mainly of fine- to medium-grained monzogranite and forms much of the northern part of the Black Brook Granitic Suite. It coincides approximately with radiometric classes 14 and 15 (the highest content of K and Th relative to U within the classification scheme). Unit 2 consists mainly of medium- to coarse-grained granodiorite and some monzogranite, forms the eastern and western parts of the Black Brook Granitic Suite, and is represented by radiometric classes 12 and 13 (Fig. 4.5c). The Black Brook Granitic Suite has moderate to low magnetic (TFM -40 to –100 nT; VGM 0.0 to -0.1 nT/m) and Bouguer gravity (-5 to –7 mGal) response. A 15 km-long magnetic anomaly trending at 100° is visible in the northern part of the Black Brook Granitic Suite and has an unknown source. Moreover, Black Brook follows the linear trends mentioned above, in that the lower 14 km of the brook have an east-west trend whereas the upper 8 km trend southwest. In map view, Black Brook follows the same trends as the Eastern Highland Shear Zone, 5 km to the south. This similarity in shape is consistent with the interpretation of Yaowanoiyothin (1988) that the Black Brook Granitic Suite intruded while the EHSZ was active.

Much of the central region of area 3 is part of the Cape Breton Highlands National Park and both access and outcrops are limited. Radiometric data for this region are varied, mainly because numerous bogs overlie the bedrock. As shown on the colour-coded elevation model, this region has the highest elevation in the Cape Breton Highlands. The VGM fused with DEM indicates a semi-circular magnetic anomaly with the axes trending SSW within the Money Point Group and Cheticamp Lake Gneiss. The semi-circular magnetic anomaly appears to link with northeasterly trending limbs, suggesting a possible fold. If the interpreted fold is valid, then the Park Spur Granite (DPSg) intruded the nose of the fold. The extent of the Park Spur Granite is poorly constrained by outcrop data but is well constrained by moderate to low magnetic signatures (TFM -250 to –300 nT; VGM 0.0 to -0.1 nT/m) and low gravity values (-5 to –7 mGal), similar to the Black Brook Granitic Suite. This similarity supports the correlation between Park Spur Granite and Black Brook Granitic Suite proposed by Raeside and Barr (1992). It also enables refinement of the northern and southern extent of the Park Spur Granite in this area of limited outcrop.

Along the Aspy Fault, the Wilkie Sugarloaf granite and related plutons are characterised by radiometric classes 14 and 15. The radiometric data successfully distinguish units in a small region at the tip of Money Point and Cape North. Within a 24 km^2 area, the Cape North Group (class 11-green), Money Point Group (classes 8,10-orange), Gulch Brook Granite (classes 14,15-pink) and Wilkie Sugarloaf Granite (classes 12, 15-pink) are all distinguishable (Fig. 4.5c).

4.5 Area 4

Area 4 (Fig. 4.6a, b, c) focuses on the central and western Cape Breton Highlands, an area that consists of a complex assemblage of gneissic, metavolcanic, metasedimentary, and diverse plutonic rocks of Precambrian, Ordovician, Silurian, and Devonian ages (Barr et al. 1992). In the northern and western parts of the area, different geological interpretations have been published (e.g. Lynch and Tremblay 1992, Barr et al. 1992). For the purpose of this investigation, map boundaries from Barr et al. (1992) were used, as modified by Price et al. (1999).

The metavolcanic and metasedimentary rocks have been assigned to different units but mainly to the Jumping Brook Metamorphic Suite. Major plutonic units include the Neoproterozoic Cheticamp Pluton, the Ordovician-Silurian Belle Côte Road Orthogneiss and Silurian Taylor Barren Pluton, and the Devonian Margaree and West Branch North River granitic plutons.

Strong lineaments characterise area 4. Rose diagrams (Fig. 4.6a, inset) show a strong NNE and moderate NW lineament orientation. The NNE lineaments are related to the Margaree Fault system extending SW past the study area. The NW lineaments are related to NW-trending faults cutting through Carboniferous units, the Devonian Fisset Brook Formation (DFB), and Proterozoic Cheticamp pluton (Giles et al. 1997). The Radarsat image shows an E-W lineament related to the Cheticamp River Gorge. This E-W (85° trend) lineament can be traced in a straight line across to Ingonish through the Cheticamp Flowage and Ingonish River.

The radiometric classification is very effective to differentiate the Margaree, Taylors Barren, and West Branch North River granitic plutons from surrounding units.

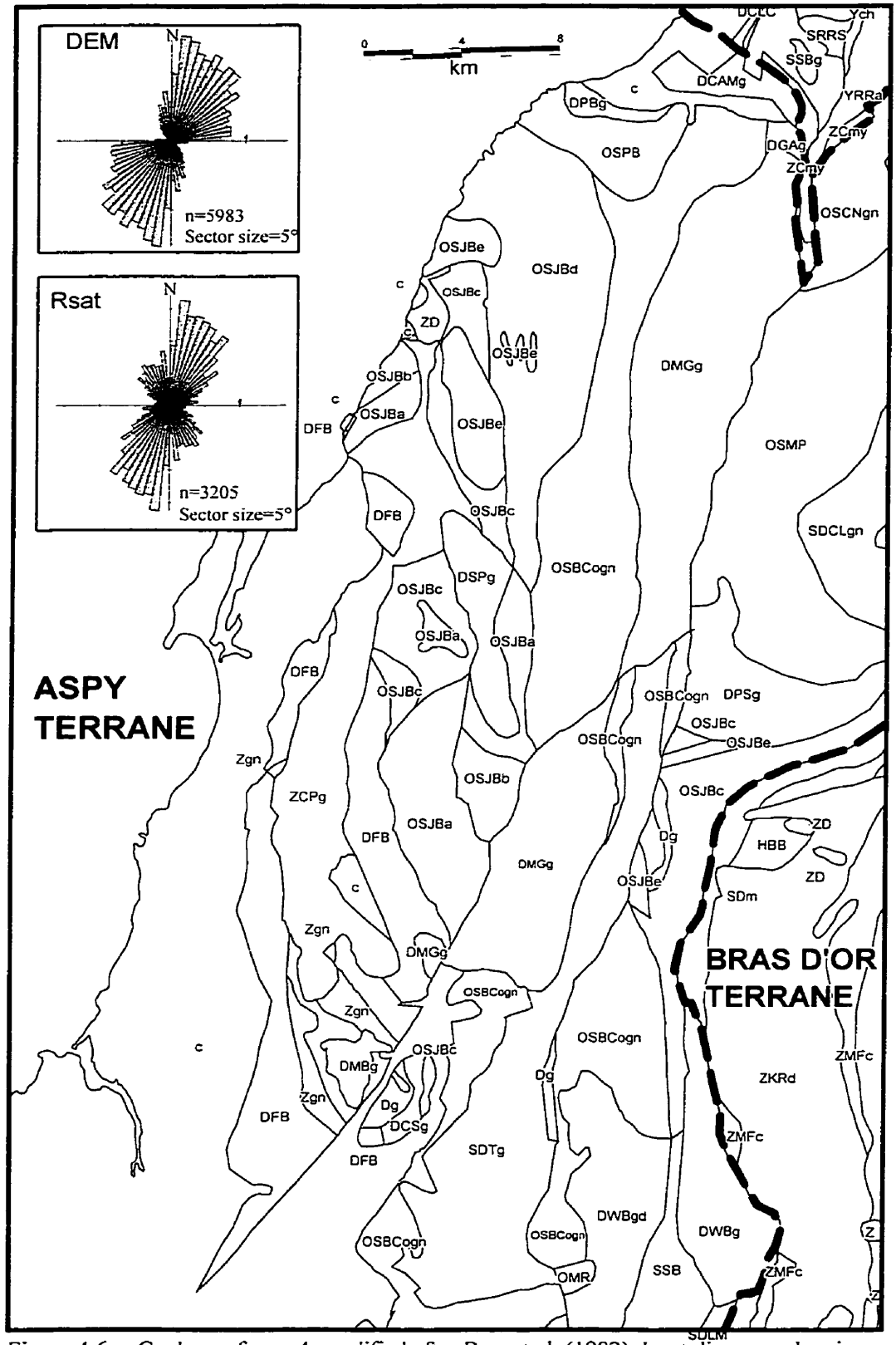

Figure 4.6a Geology of area 4, modified after Barr et al. (1992). Inset diagrams showing lineament orientations derived from DEM and Radarsat. Dashed lines represent approximate terrane boundaries from Barr and Raeside (1989).

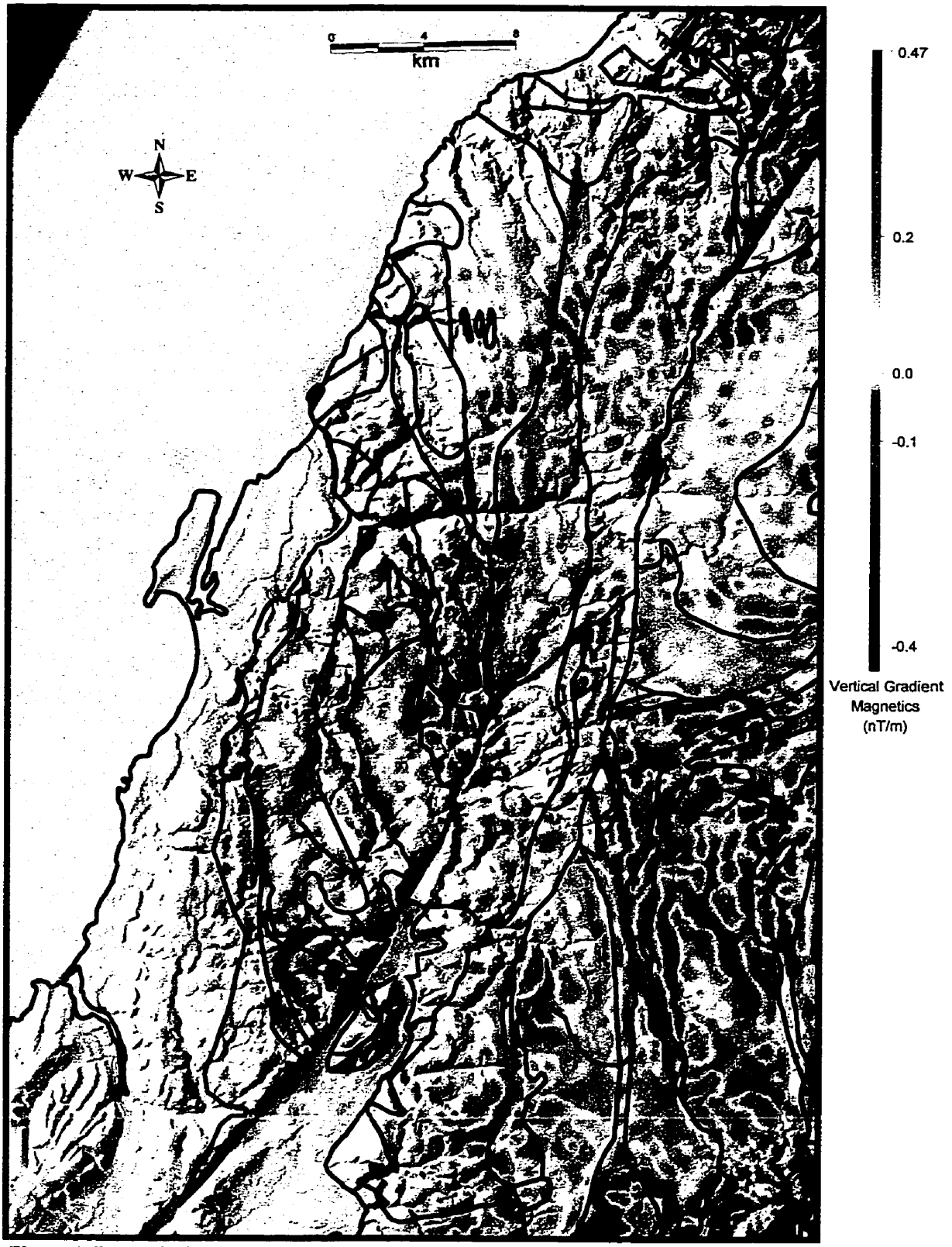

Figure 4.6b Vertical gradient magnetic data fused with elevation model (DEM) overlain by geology from Figure 4.6a.

Figure 4.6c Radiometric classification overlain by geology from Figure 4.6a.

Gravity data are again sparse for this region (Fig. 2.9), but give some control between the plutons mentioned above and surrounding rocks. Radarsat S7 (Fig. 2.4), but more so Radarsat S2 (for the southern part of the area Fig. 2.5) and the DEM (Fig 2.1 and 3.1), provide a dramatic outlook on the topographic lineaments and slopes. The VGM fused with shaded relief DEM (Fig 4.6b), and TFM fused with Radarsat S7 (Fig. 3.7) categorises particular lithological and structural patterns within specific regional blocks.

North of the westerly trending Cheticamp River, and within the Corney Brook Schist (OSJBd), two parallel elongate (north-trending) ridges are visible in the colour-coded DEM (Fig 3.1). The valley between the two ridges has a narrow, north-trending magnetic anomaly with moderate values (TFM -20 to –60 nT; VGM 0.1 to 0.2 nT/m). East of this linear anomaly, a moderately low magnetic block (TFM -230 to –330 nT; VGM -0.1 to –0.3 nT/m) is visible and has values similar to those associated with the Park Spur Granite (DPSg). The Corney Brook Schist is variable in composition from more mafic in the west to felsic in the east. The metamorphic grade also varies, and the high-grade rocks have abundant granitic and pegmatitic dykes Numerous pegmatite and felsic dykes are present in outcrop east of the linear valley anomaly (S. Barr, per comm 2001) which could explain the low magnetic block.

Apart from major lineaments displayed on the DEM and Radarsat images, the most apparent feature in area 4 on the radiometric classification are the Margaree Pluton (DMGg) and adjacent Taylors Barren Pluton (SDTg). In map view, the Margaree Pluton is made up of 2 elongate lobes and forms the central part of area 4, extending from the Red River fault zone (BRI terrane boundary) in the north across the Cheticamp River gorge, and continuing farther south to Cape Clear Lookoff. It is generally characterised

by radiometric classes 8 and 10, although variable with higher radiometric classes in the northern part of the northern lobe and the southern part of the southern lobe.

Similarly, the Taylor Barren Pluton, east of the Margaree Granite is characterised by classes 8 and 10, representing lower K content relative to eTh and eU. This similarity is consistent with petrological data from the plutons (67.82-74.55 % SiO_2; 2.64-6.76 % K_2O; and 11-39 ppm Th) in the Margaree Pluton; (O'Beirne-Ryan et al. 1986), and (66-76 % SiO_2; 4.5-7 % K_2O; and 17-36 ppm Th) in the Taylors Barren Pluton (MacDonald 1996).

As with the Black Brook Granitic Suite in the northeastern Cape Breton Highlands, the Margaree Pluton displays variations in radiometric and magnetic signatures. For example, the northern part of the northern lobe has mainly a class 14 signature and moderate magnetic values, whereas the central part has high magnetic values and mainly class 10 and 11 radiometric signature. In the southern lobe, the northern part has mainly a radiometric class 11 signature and moderate magnetic values. For the Margaree Pluton, high-K radiometric classes are associated with moderate magnetic values and low-K radiometric values are associated with higher magnetic values, probably related to variations in the ratio of K-feldspar to mafic minerals in the pluton.

The Salmon Pool Granite (DSPg) east of the Margaree pluton is also well identified by its radiometric signature, including classes 7, 8 and 10, but in the northern part of the pluton an area has a class 13 signature (eTh= 16.3 ppm; K=2.5%; eU=3.4 ppm). Unlike most granitic plutons, in the study area, the Salmon Pool Granite has high magnetic values (TFM 550 nT; VGM 0.3 to 0.4 nT/m). The magnetic signature could

be related to the presence of abundant mafic material (dykes and enclaves) in the granite (S. Barr, pers. comm. 2001). However a lower magnetic anomaly (TFM 200 nT; VGM -0.3 nT/m) is associated with the class 13 zone.

In the western part of area 4, the radiometric classification is less effective compared to the VGM fused with DEM and TFM fused with Radarsat. West of the Salmon Pool Granite, two (approximately 1.5 km wide) elongate, highly magnetic belts are separated by two (approximately 3 km wide) zones of low magnetic amplitude. The highly magnetic belts are associated with the Fisset Brook Formation (DFB) whereas the low amplitude zones are related to the older Cheticamp pluton (ZCPg) to the west and the Jumping Brook Metamorphic Suite (OSJBa, b, c) on the east. The mineralogy in the basaltic flows in both the western and eastern belts of the Fisset Brook Formation is dominated by plagioclase and clinopyroxene, with up to 5% magnetite (Barr and Peterson 1998), which could explain the magnetic signature. The colour-coded elevation model shows a triangle-shape topographic low which corresponds to Carboniferous rocks overlying the Cheticamp pluton (Fig. 3.1).

In the southeastern part of area 4, the West Branch North River Granite is also well defined by the radiometric classification. It is divided in two parts where the eastern side (DWBg) has a unique appearance in map view, circular to the south (5 km diameter), and pinching out to the north. The eastern part intruded the Kathy Road Dioritic Suite and the Eastern Highland Shear Zone, although it is cut by major faults (Barr et al. 1992) probably related to the "zone of structural complexity", in area 2. The eastern part of the pluton consists of mainly red syenogranite with radiometric signatures of classes 7, 8 and 10 and low magnetic values of TFM -350 to –500 nT; VGM -0.2 to –

0.3 nT/m. The eastern part of the pluton (DWBgd) is characterised by classes 5, 6, and 7 with relatively the same magnetic values as the eastern section of the pluton. These radiometric data show that the eastern part of West Branch North River Granite (70-74 % SiO_2; 3.62-5.09 % K_2O; and 19-54 ppm Th) has slightly higher K values compared to the western part (54-62 % SiO_2; 1.93-2.94 % K_2O; and <8 ppm Th) (O'Beirne-Ryan and Jamieson 1986). Correspondingly, as a result of detailed mapping, Horne (1995) subdivided the West Branch North River Granite, the eastern lobe as monzogranite and the western part, granodiorite.

The Belle Côte Road gneiss (OSBo) is a major component of the western Cape Breton Highlands, and extends from near Pleasant Bay in the north to the southern part of area 4. The Belle Côte Road gneiss is difficult to interpret. In general, magnetic signatures are variable from moderate to low and radiometric signatures of mainly class 2, 3, 4 and 6, similar to the tonalite and diorite rocks of the Bras d'Or terrane. East of the Taylor Barren Pluton (SDTg), the Belle Côte Road gneiss has high K content, and is represented by radiometric classes 8, 11 and 14.

4.6 Area 5

Area 5 (Fig. 4.7a, b, c) focuses on the southwestern part of the Cape Breton Highlands and includes the Mabou Highlands in the southwest, the Lake Ainslie and Gillanders Mountain areas in the central part, and the southern tip of the Cape Breton Highlands in the east. These areas are separated by Carboniferous rocks. In the southern part of the Cape Breton Highlands, rock units include metavolcanic, metasedimetary, and diverse plutonic rocks. Most of these rocks are part of the Aspy terrane of Barr and

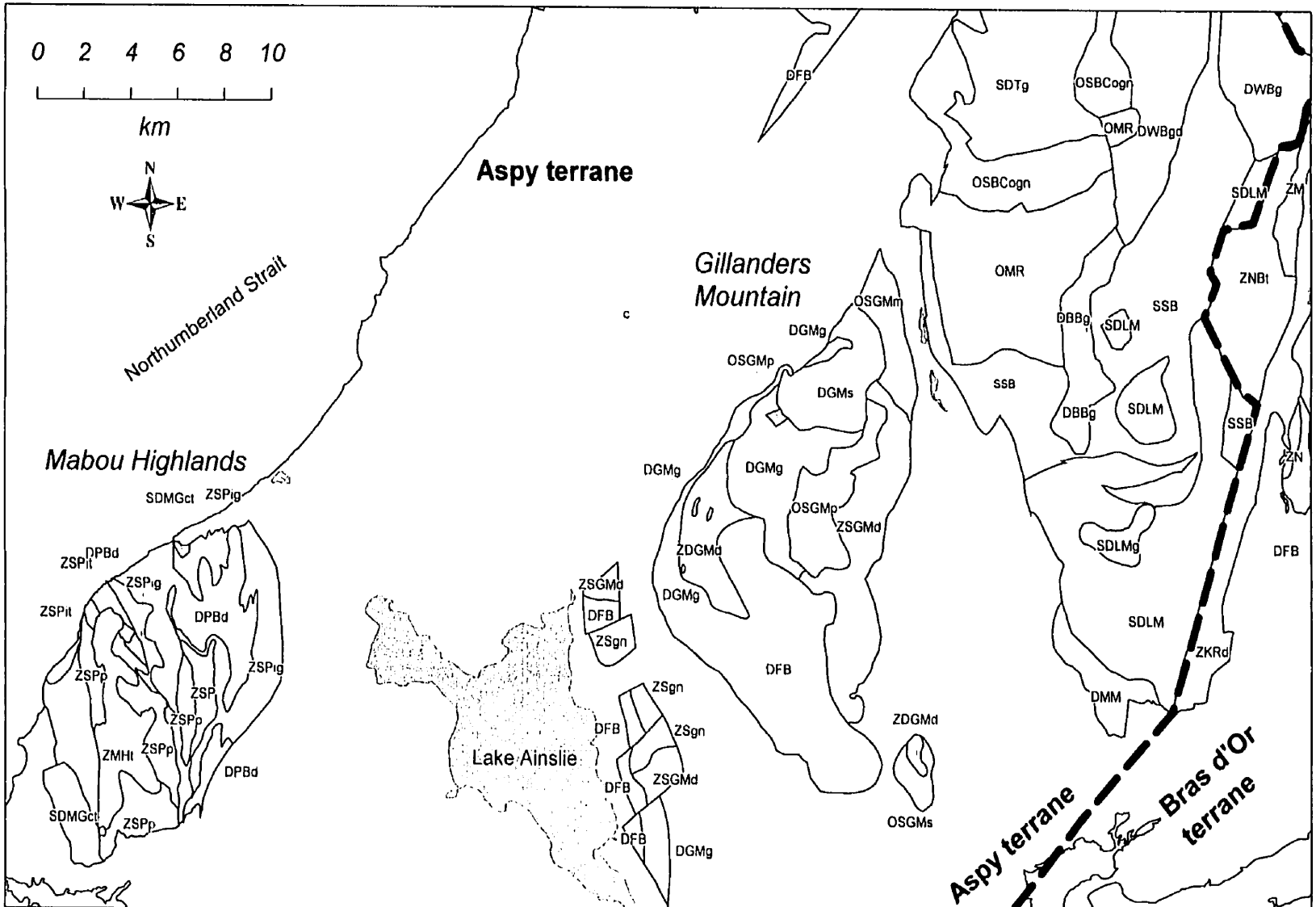

Figure 4.7a Geology of area 5, the southwestern part of the Aspy terrane. Gillanders Mountain area modified after Barr et al. (1992), and Mabou Highlands area after Barr and Macdonald (1989). Dashed line represents approximate terrane boundary.

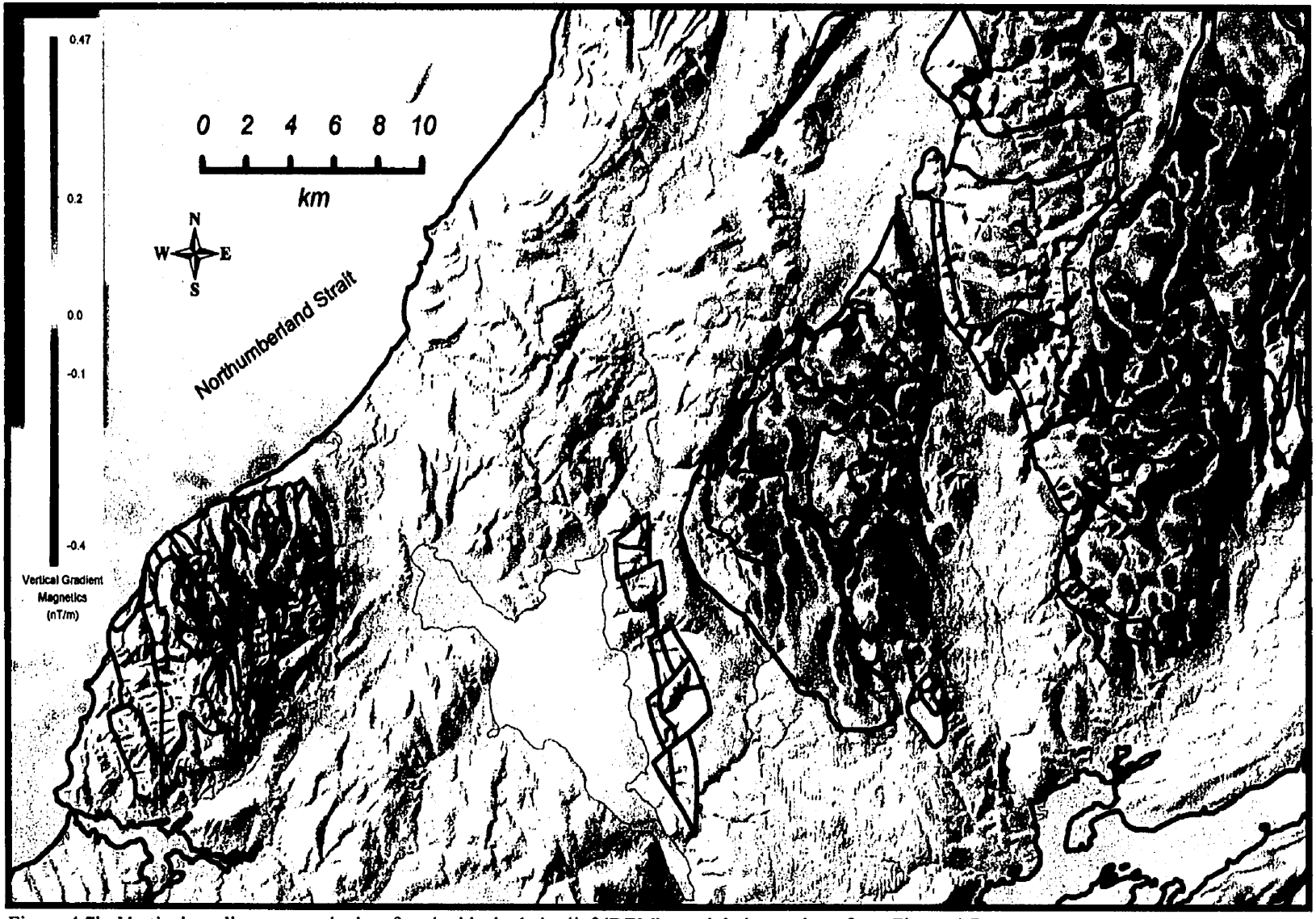

Figure 4.7b Vertical gradient magnetic data fused with shaded relief (DEM) overlain by geology from Figure 4.7a.

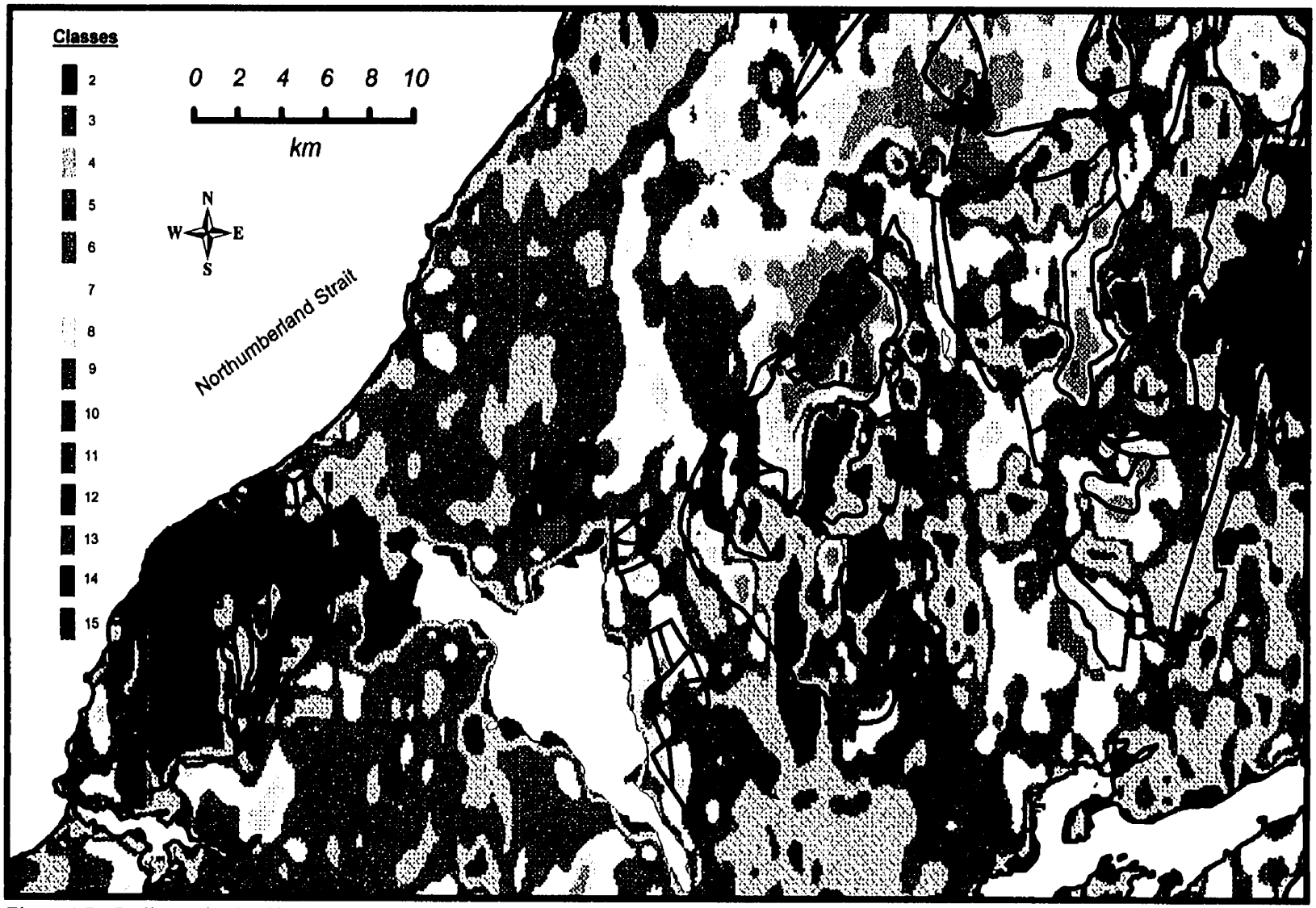

Figure 4.7c Radiometric classification overlain by geology from Figure 4.7a.

Raeside (1989) and have been assigned to several different units, including Macmillan Mountain Volcanics, Sarach Brook Metamorphic Suite, Middle River Metamorphic Suite, Leonard Brook Complex and the Bothan Brook Granite. A sliver of dioritic rocks assigned to the Kathy Road diorite unit of the Bras d'Or terrane occurs in the eastern part of the southern highlands block (Fig. 4.7a). The Gillanders Mountain and Lake Ainslie blocks of pre-Carboniferous rocks are dominated by volcanic and sedimentary rocks of the Devonian Fisset Brook Formation and Devonian and older plutonic rocks. The Mabou Highlands are underlain by Neoproterozoic metamorphic and plutonic rocks, a large Devonian diorite pluton, and possible Silurian-Devonian volcanic rocks on the western side.

In general, gravity data are lacking from Gillanders Mountain area and the Cape Breton and Mabou highlands, although having higher values compared to the surrounding Carboniferous units where data control is relatively good (Fig 2.9). The southern part of the Cape Breton Highlands is characterised by strong magnetic and topographic trends that change from northerly to westerly (Fig. 4.7b). These trends are associated with the Middle River (OSMR) and Sarach Brook (OSS) metamorphic suites (Fig 4.7a). Metamorphic fabrics, including gneissic banding and schistosity, parallel lithological layering in these units (Horne 1995), and define this concave-northward pattern. The pattern is also observed in the Belle Côte Road orthogneiss to the north, suggesting that these units were involved in a common deformation. The contact between the Middle River Metamorphic Suite and the Belle Côte Road orthogneiss is parallel to the principal fabrics in both units, implying that the contact was modified by this deformation (Horne 1995).

The concave-northward pattern is cut by the Bothan Brook Granite (DBBg) to the east. The Bothan Brook Granite was originally included as part of the West Branch North River pluton, but is more felsic than the western, granodioritic part of the West Branch North River pluton. The difference is apparent in radiometric signatures, as the Bothan Brook granite is characterised by classes 8, 10, 12, and 13, in contrast to the West Branch North River granodiorite to the north with classes 5, 6, 7, indicating lower K, eU, and eTh in the latter units. Petrochemical analysis also suggested differences between the two plutons where the Bothan Brook is the most felsic (72.35-75.76 % SiO_2; 4.97-5.81 % K_2O; and 15 – 59 ppm Th) compared the West Branch North River granodiorite (54-62 % SiO_2; 1.93-2.94 % K_2O; and less than 8 ppm Th).

The extent of the Bothan Brook Granite is well constrained by the radiometric data, and also by its low magnetic amplitudes (TFM -480 to –590 nT; VGM -0.3 to –0.4 nT/m) compared to the surrounding metamorphic suites. An intrusive relationship is indicated by the VGM fused with DEM image, which shows that the pluton cuts the pattern in the adjacent units (Fig. 4.7b). These data are consistent with field observations that dykes of the Bothan Brook Granite cut the Middle River Metamorphic Suite (Horne 1995).

The area east of the Bothan Brook Granite, mapped as the Sarach Brook Metamorphic Suite, has low potassium values (0.1 to 0.4 % K), but moderate eTh (4 to 6 ppm) and eU (1.1 to 1.6 ppm). The combination of these values gives high anomalies on the ratio images of eTh/K and eU/K (Fig 2.6f).

The Leonard Macleod Brook complex (SDLM) has variably high magnetic values surrounding a zone of lower magnetic values and radiometric classes 8 and 10.

According to mapping by O'Neill (1996), this area is underlain by pink, fine-grained granitic rocks, ranging from alkali-feldspar granite to tonalite. The rest of the "Leonard MacLeod Brook Complex" consists mainly of class 3, 4, consistent with the diorite to tonalitic rocks and of class 5 and 7 agreeing with the metamorphic rocks of O'Neill (1996). The McMillan Mountain volcanic (DMM) unit also has a distinctive radiometric signature (classes 7 and 8) compared to the adjacent Leonard Macleod Brook Complex.

The VGM fused with DEM image, and to some extent the radiometric classification image, support the interpretation of Barr et al. (1992) that Gillanders Mountain is composed of rocks separate from the Sarach Brook Metamorphic Suite and Middle River Metamorphic Suite. The northwestern part of Gillanders Mountain is characterised by a radiometric signature represented by classes 8,10, 11,12 and 13, correlating directly with the Gillanders Mountain Syenogranite (DCGs) and Monzogranite (DGMg). The syenogranite has mainly class 13 (bright pink), indicating high eTh values (14 to 16 ppm), moderate K (1.8 to 2.8 %) and eU (2.2 to 3.6 ppm) whereas the monzogranite has mainly a class 8 signature, indicating lower K and eTh content compared to the syenogranite. High magnetic values are also characteristic of the syenogranite, similar to the Salmon Pool Granite in area 4. The eastern part of the monzogranite has low magnetic values, although the western part has higher value, maybe related to the underlying mafic rocks. The boundary of the syenogranite has been modified as a result of ground-truthing using a global positioning system (GPS) unit. It was noted that the northern tip of Gillanders Mountain was not syenogranite, but more dioritic in composition, consistent with the radiometric signature (class 4) and low to moderate magnetic values (TFM 60to 90 nT; VGM 0.0 nT/m).

Furthermore, the contact between the Gillanders Mountain Monzogranite and the Gillanders Mountain Metamorphic Suite (psammitic, to pelitic schist, metabasite, minor quartzofelsdpathic augen gneiss) was more accurately located by GPS. The contrast in rocks can be noted on the radiometric image (Fig 4.7c), as the metamorphic rocks have class 2, 3 and 4 signatures (similar to those of metamorphic rocks of the Bras d'Or terrane) whereas the monzogranite is higher in K and Th.

The southern part of the Gillanders Mountain area, mapped as the Devonian Fisset Brook Formation (DFB), was interpreted as a folded structure (Barr et al. 1995). The magnetic data show two parallel north-trending high magnetic anomalies (TFM 552 nT; VGM 0.5 nT/m) and do not suggest the large-scale anticlinal fold closing toward the south inferred by Barr et al. (1995). These anomalies have values similar to those that characterise the Fisset Brook Formation in area 4. Dextral offset is suggested in the magnetic trends at Trout Brook, on strike with a major NE-trending fault in the Lake Ainslie block to the west (Fig. 4.7b). Between the linear anomalies that appear to be associated with basalt is an area of moderate to low magnetic amplitude correlating to the conglomerate, sandstone and silstone unit of the Fisset Brook Formation (Barr et al. 1995). Moderate to low magnetic values also characterise the western part of the area and a small area to the east. These areas have class 8 and 10 (high in K and eTh) radiometric signatures (Fig. 4.7c) and coincide with areas mapped as rhyolite (Barr et al. 1995).

The Fisset Brook Formation also occurs to the west in the Lake Ainslie block as a north-south array of rhombic fault blocks dextrally offset. In the southwestern part of this area class 8, 11 and 14 radiometric signatures are related to areas mapped as

rhyolite flows and tuff whereas magnetic highs are associated with areas mapped as basaltic flows (Barr et al. 1995). A north-trending magnetic linear between Gillanders Mountain and the Lake Ainslie block may indicate the presence of basaltic rocks beneath Carboniferous cover.

The Mabou Highlands appear to consist of a magnetic northeastern block and a non-magnetic southwestern block. The high magnetic anomalies (TFM 552 nT; VGM 0.5 nT/m) coincides with Devonian diorite (DPBd) and the associated injection complex (ZSPig). Within the dioritic magnetic anomaly to northeast, a moderate to low magnetic amplitude (TFM 200 to 340 nT; VGM -0.2 to –0.4 nT/m) coincides with the quartz phyllite and schist of the Sight Point Group (ZSPp). Another undivided unit (ZSP) of this group has class 6 radiometric signature in the northern part, probably relating to the presence of metarhyolite.

The southwestern block is underlain by the Mabou Highlands Leucotonalite (ZMHt) with a class 2 radiometric signature (very low K, eTh and U content) similar to that of the North Branch Baddeck River Leucotonalite (ZNBt) in area 4. The volcanic and sedimentary unit in the southwest has radiometric classes 6 and 9 and a moderate content of K (1.2 % K) compared to the adjacent units mapped as quartz-feldspar crystal tuff, rhyolite and felsic tuff (Barr and Madonald 1989).

Chapter 5. Interpretations of Specific Areas

5.1 Introduction

During the process of manipulating and interpreting the image maps produced for the Cape Breton Highlands during this study, many interesting features were noted in the geology, especially with respect to the position and nature of contacts between map units in poorly exposed areas, and in the location of major faults and postulated terrane boundaries. It is not possible to discuss all such areas within the scope of this project. The purpose of this chapter is to show the potential of the database for more detailed follow-up studies, using specific areas as examples, including the Bothan Brook Granite area, a possible strike-slip "pull-apart" basin in the Gillanders Mountain area, and the position of major faults and terrane boundaries.

5.2 Bothan Brook Granite Area

The Bothan Brook Granite area is an example of where the GIS was very useful in combining ground-truthing information using the global position system (GPS) and an overlay of different digital map interpretations. Using integrated images as a backdrop within the GIS, spatial correlation and geological control were made easier.

As indicated in the previous chapter, the Bothan Brook Granite (DBBg) was originally included in the West Branch North River Granodiorite (DWBg), but is a more felsic unit, with a higher K_2O content. It has an overall radiometric signature represented by classes 8, 10, 12 and 13 (Fig 5.1). The highest classes occur in the southern part, probably an indication of mineralogical variation in the granite. This pluton is an example of where a digital database of sample data would have been an

asset in this project. The extent of the Bothan Brook Granite is well constrained by the radiometric data (Fig. 5.1), and truncation of trends in magnetic data (Fig. 4.7b) suggest that the pluton intruded the surrounding metamorphic suites, consistent with field observations (Horne 1995).

Based on image interpretation, the extent of the Bothan Brook Granite of Barr et al. (1992) was modified and the new boundaries were checked in the field using a GPS. In hand sample the Bothan Brook Granite is typically medium- to coarse-grained, pink, and moderately equigranular to slightly megacrystic. The older surrounding rocks of the Sarach Brook and Middle River metamorphic suites contrast in appearance. The Sarach Brook Metamorphic Suite consists of variably deformed greenschist facies rocks (chlorite to garnet grade), undivided fine- to coarse- grained felsic to mafic pyroclastic rocks and flows and minor slate, locally mylonitic (Barr and Jamieson 1991; Lister 1998). The Middle River Metamorphic Suite may be the lateral and generally higher grade equivalent of the Sarach Brook Metamorphic Suite, or an unrelated older unit. The latter interpretation is suggested by the intrusive relationship between the ca. 442 Ma Belle Côte Road orthogneiss and the Middle River Metamorphic Suite, whereas rhyolite from the SBMS gave a Silurian age (ca. 430 Ma) (Price et al. 1999). The Middle River Metamorphic Suite includes greenschist to amphibolite facies phyllite, schist, gneisses, metabasite, and rare marble and metaconglomerate (Barr and Jamieson 1991).

Different interpretations of the geology in the area of the Bothan Brook Granite are shown overlain on the radiometric classification image (Fig 5.1) and DEM (Fig 5.2). The red contacts and unit labels are from the compilation map of Keppie (2000).

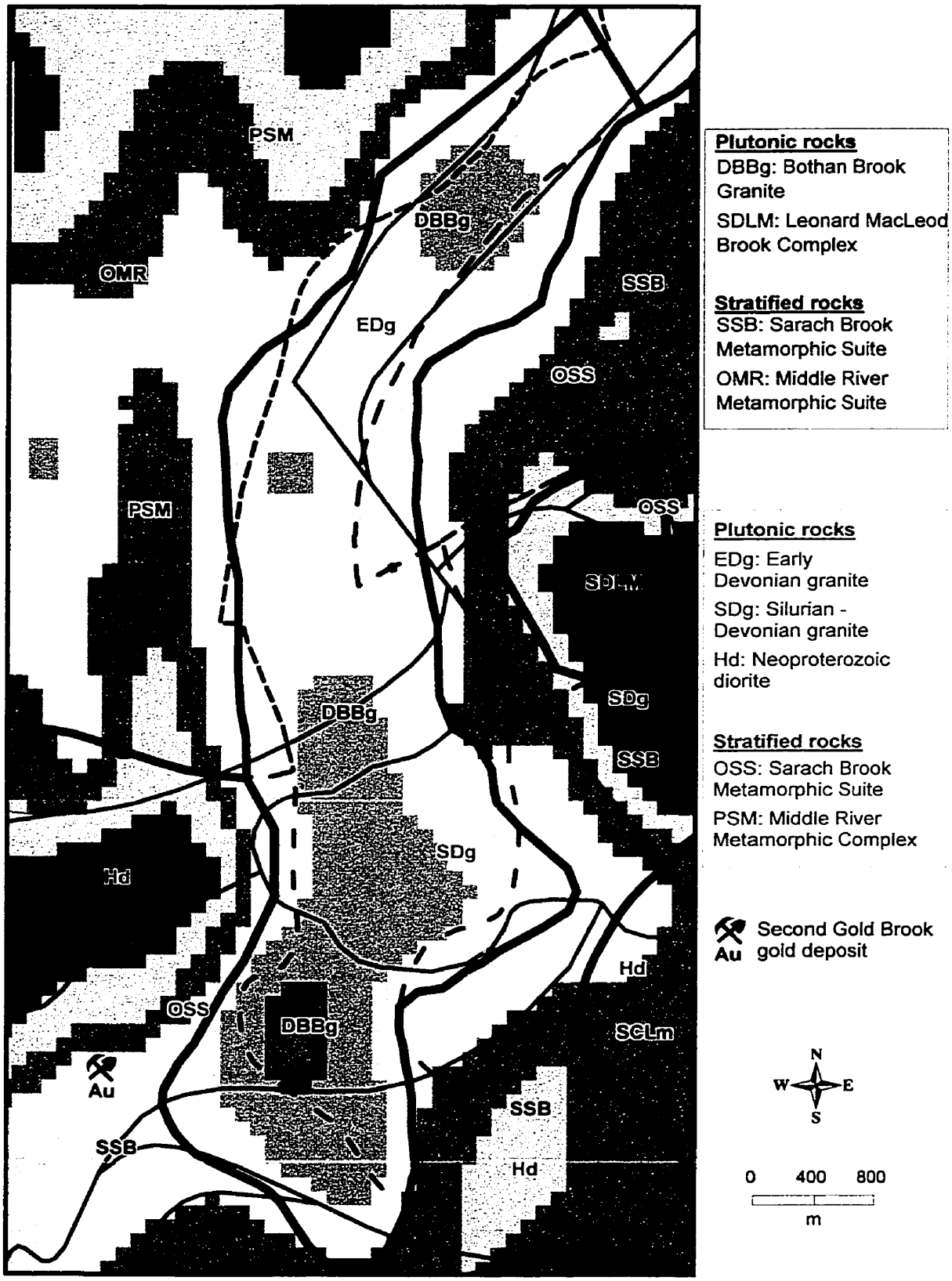

Fig. 5.1 Radiometric classification overlain by geology. Red lines and units are from Keppie (2000), taken from Lynch and Lafrance (1996). Dashed lines and units are from Barr et al. (1992). The solid lines are the contacts proposed here, using units of Barr et al. (1992).

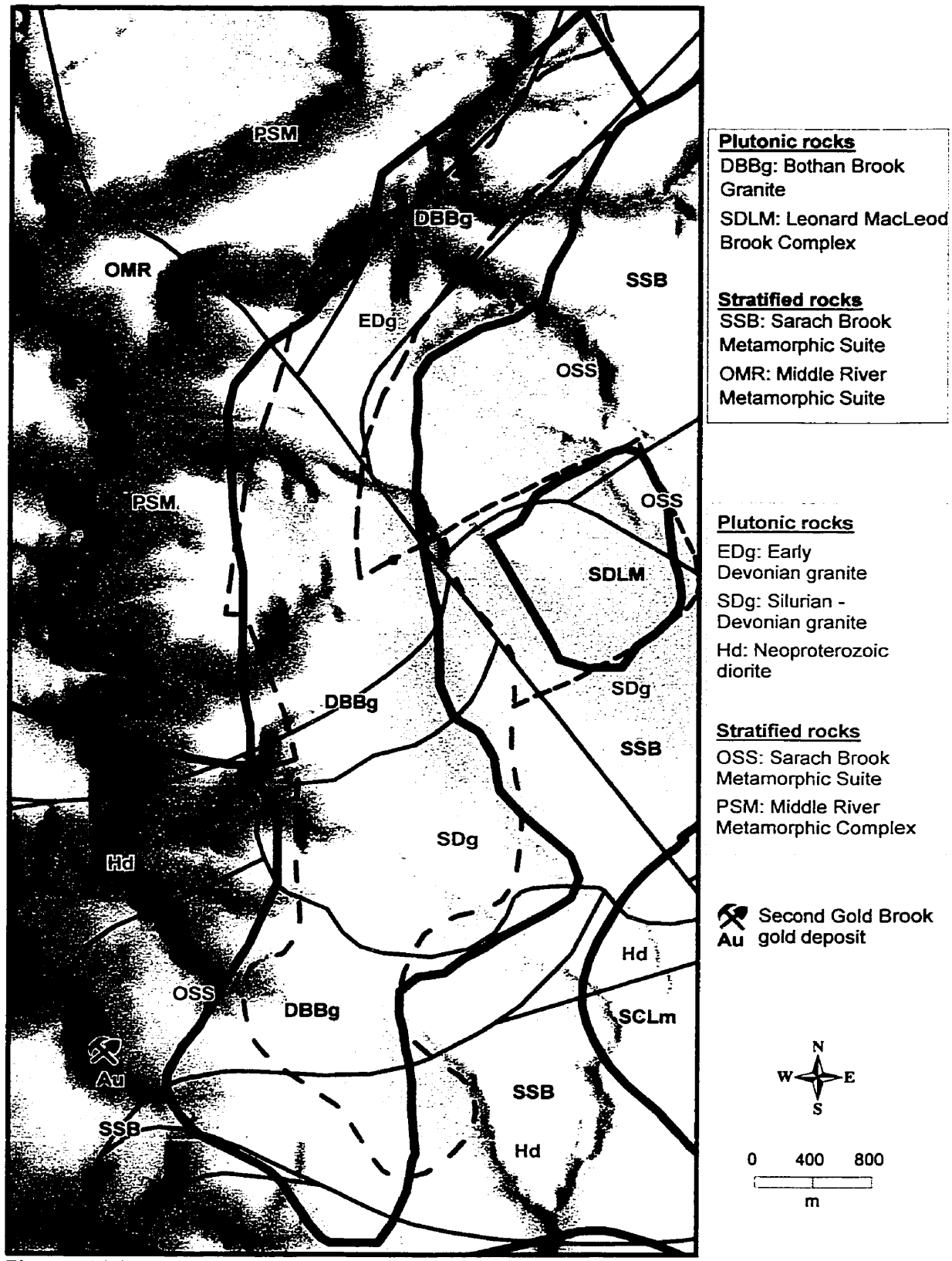

Fig. 5.2 Digital elevation model overlain by geology. Red lines and units are from Keppie (2000), taken from Lynch and Lafrance (1996). Dashed lines and units are from Barr et al. (1992). The solid lines are the contacts proposed here, using units of Barr et al. (1992).

compiled from Lynch and Lafrance (1996). The solid black contacts are modified based on the GIS imagery from those of Barr et al. (1992), which are also shown in the dotted black line. The modified geological interpretation is essentially the same as that of Barr et al. (1992). Differences between the two interpretations are subtle and could be attributed to scale problems, such as manual digitizing errors and differences in map projections. Outcrop control for the Bothan Brook Granite and the eastern part of the Sarach Brook Metamorphic Suite is good, as also shown on the unpublished map of O'Neill (1996).

However, the interpretation contrasts with that on the published map of Keppie (2000), compiled from Lynch and Lafrance (1996), which shows stratified units crossing the highly potassic Bothan Brook Granite. In the central part of figures 5.1 and 5.2, the red lines show a granitic body (SDg) sinistrally offset and a younger pluton (EDg) to the north separated by the stratified units of the Middle River Metamorphic Complex (PSM). South of the granitoid body, Keppie (2000) and Lynch and Lafrance (1996) interpreted that the stratified rocks of the Sarach Brook Metamorphic Suite and a Neoproterozoic diorite unit cross Bothan Brook Granite; this interpretation is not consistent with the GIS imagery.

An important implication of the new interpretation is that the Second Gold Brook gold mine is much closer to the pluton than previously suggested, and is clearly in the contact metamorphic aureole of the granite (Fig. 5.1 and 5.2).

5.3 Strike-slip basins of the Gillanders Mountain Area

Constructing the detailed DEM for the study area and integrating it with various geophysical data provided a fresh outlook on regional structural interpretations. As a result, a "strike-slip basin" model has been developed to explain the distribution of units and topography in the Gillanders Mountain area (Fig. 5.4, 5.5). It is a simple model, but possibly explains the island-like appearance of Sugarloaf and Gillanders mountains (Fig 5.3). The model was derived as a result of noticing on the image of VGM fused with DEM that Gillanders Mountain has strong magnetic signatures and that the lowland to the east (Middle River area) has a rhombic shape with low magnetic amplitude. By cutting and pasting selected areas using a paper copy of the VGM fused with DEM, it was noted that after cutting out the Carboniferous units, Gillanders Mountain fitted well in the Margaree Valley. Consequently, further examination was carried out.

The occurrence of large faults within this area has been known for a long time (e.g. Cameron 1966). West of the Gillanders Mountain area, a zone of intense shear marks, the trace of a possible extensional detachment fault termed the Ainslie Detachment by Lynch and Giles (1995) (Fig. 5.4, 5.5). This detachment was mapped by Giles et al. (1997) throughout the Carboniferous units as a bedding-parallel fault, listric faults and smaller detachment faults. Giles et al. (1997) applied the term Hollow Fault system to the series of northeasterly- trending faults extending from the Colindale - Mabou Harbour area northeasterly to Margaree Centre and beyond to Sugarloaf Mountain (A on Fig. 5.3). The Cobequid-Hollow Fault System has been shown to be a dextral strike-slip system, movement on which was responsible for development of the Carboniferous Stellarton Graben as a small pull-apart basin (Yeo and Gao 1987).

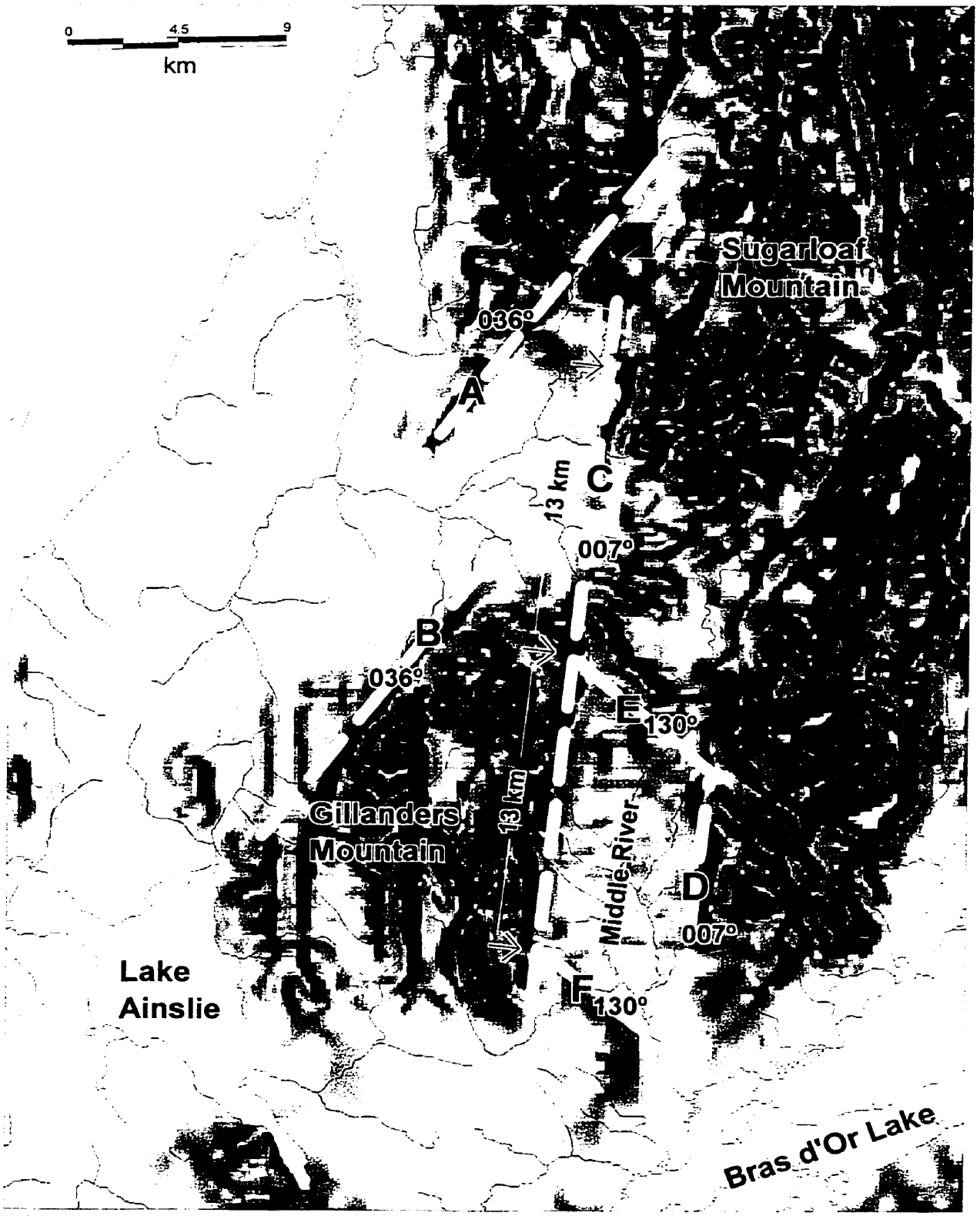

Figure 5.3 Grayscale vertical gradient magnetic data gridded at 100 m cell size and illuminated from the northwest (azimuth 315°, inclination 45°). White dashed lines represent lineament orientations.

Figure 5.4 DEM overlain by faults (black lines) modified from Barr et al. (1992) and Lynch et al. (1997). Red lines and arrows show possible development of a pull-apart basin.

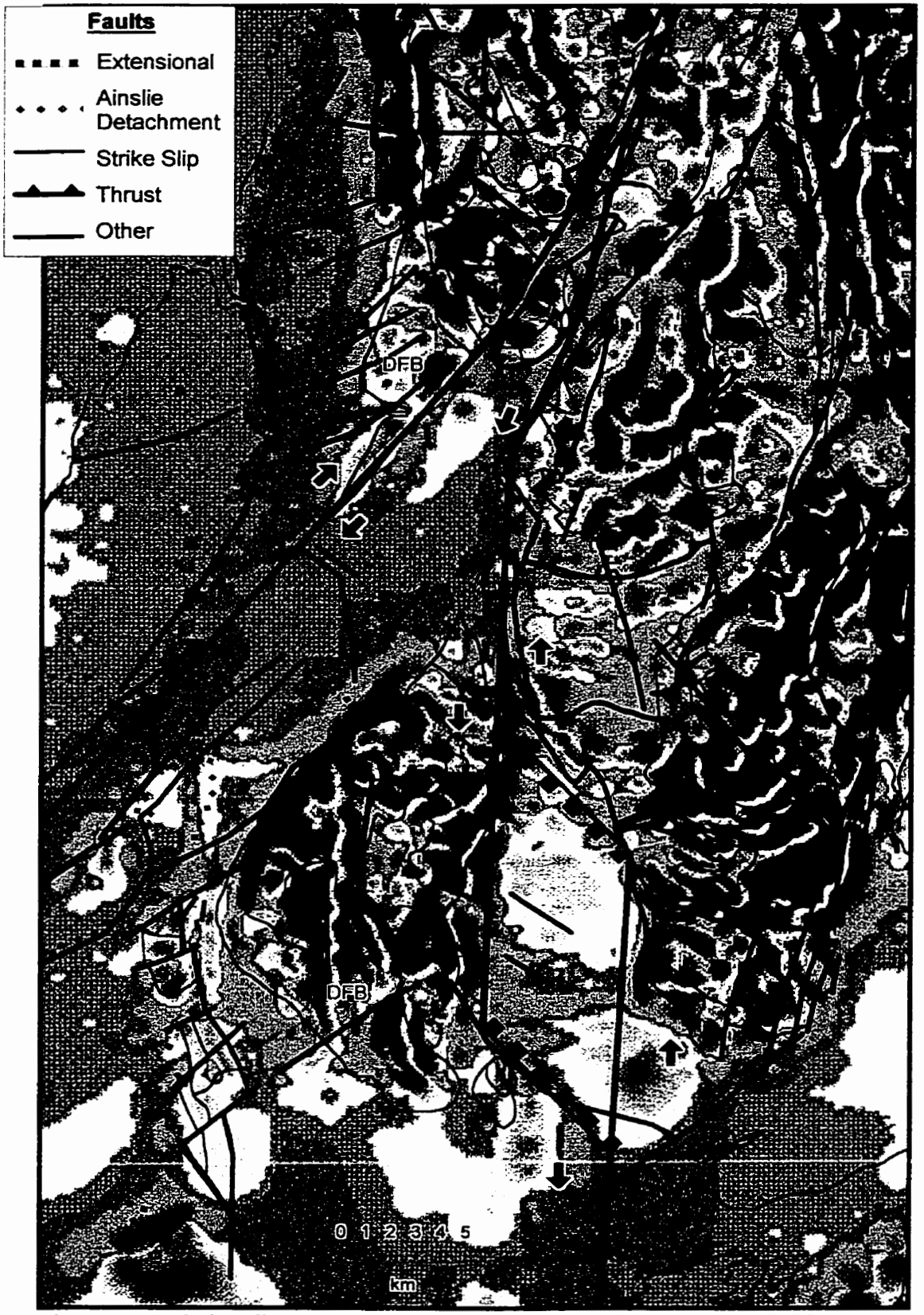

Figure 5.5 Vertical gradient magnetic data overlain by faults (black lines) modified from Barr et al. (1992) and Lynch et al. (1997). Red line and arrows show possible development of a pull-apart basin.

As a result of previous studies, the large northeasterly-trending faults in the Margaree valley (or Hollow Fault system) have been interpreted as strike-slip faults with a dextral sense of movement within the model (Fig. 5.4 and 5.5). Figure 5.3 shows the relationship and geometry of the major bounding magnetic breaks along the Carboniferous units. At this point, without looking at the geology, in order for this model to work, simple geometry should work also. By moving Gillanders Mountain northward along the C axis, line A and B would fit at 36°, and line E and F at 130°. From this outlook there would be approximately 13 km movement along the C axis. In any respect, the 7° trend of line C is well constrained and very straight. The magnetic data and DEM clearly show the 7° linear break between adjacent rock units, showing that the Middle River Metamorphic Suite and the Belle Côte Road Gneiss do not correlate directly across to Gillanders Mountain.

By using a dextral sense of movement along the Hollow Fault system, the block of Gillanders Mountain can be moved sinistrally along strike-slip fault C. Consequently, there should be a similar strike-slip fault at line D forming a pull-apart basin in the Middle River area, where the 130° trending line E and F would be extensional faults (Fig 5.4 and 5.5). The Ainslie Detachment by Lynch and Giles (1995) could also be explained by this model, because the area west of Gillanders Mountain would be an extensional detachment fault with a dextral component. On the eastern side of the pull-apart, sinistral movement could explain the thrust faults in the Leonard MacLeod Brook Complex, as well as the curvilinear fabrics in the Middle River and Sarach Brook metamorphic suites.

As the strike-slip basins evolved through time and space, the surrounding area may have been strongly modified as a result of significant translation along the principal strike-slip faults (C and D; Fig. 5.3). For example, where the strike-slip basin encountered releasing bends (changes in strike of the principal fault that generate local transtension) it underwent subsidence and extension, forming the Middle River basin, and where it encountered restraining bends (changes in strike of the principal fault that generate local transpression), uplift and erosion may have occurred in the area of the Leonard MacLeod Brook Complex and the Middle River and Sarach Brook metamorphic suites.

Furthermore, by moving the block including Gillanders Mountain north to the Margaree Valley, geological units should also correlate. First, the stratigraphy, lithology, age, and petrochemical characteristic of the Fisset Brook Formation (DFB) in the Cheticamp area are very similar to those in the Gillanders Mountain-Lake Ainslie area (Barr and Peterson 1998). Devonian granitoid rocks in the Gillanders Mountain area have also been correlated with plutons of the Sugarloaf Mountain area and possibly parts of the Margaree and Salmon Pool plutons farther north (S.Barr, pers. comm. 2001). Although the eastern units of the Gillanders Mountain area do not appear to correlate with Middle River or Sarach Brook metamorphic suites to the east, they have some similarity to units in the Leonard MacLeod Brook Complex (O'Neill 1996), consistant with the model.

More work is needed to investigate whether or not such a model is possible and its broader implications for the region, as well as the timing of such movements in relationship to Carboniferous sediment deposition.

5.4 Major faults and the Aspy-Bras d'Or terrane boundary

The most evident and well known structure within the study area is the Aspy Fault. Many workers extended this fault across the Cheticamp River gorge to connect with similar faults in Margaree Valley, west of Sugarloaf and Margaree plutons. However, the DEM and magnetic data suggest that the West Margaree Valley fault terminates in the Belle Côte Road Gneiss south of the Cheticamp River and may not connect with the Aspy Fault. The 3D view of the VGM fused with DEM (Fig. 5.6a) suggests that the north-trending southern part of the Aspy Fault converges toward a major north-trending structure that appears to merge with the "zone of structural complexity" in the southeastern highlands. The 3D-image also shows that the Black Brook Granitic Suite and associated units east of the Aspy Fault have a unique topographic expression compared to the surrounding areas (e.g. Cameron Brook Granodiorite). The Black Brook Granitic Suite area is the only part of the highlands where there is a constant linear slope measured at 2° up toward the highest elevation in the area of the Park Spur Granite (maximum elevation 531 m). The indication that this block was tilted to the northeast suggests a scissors-like displacement along the Aspy fault. It is proposed that east-west lineaments in the Black Brook Granitic Suite could be related to near-vertical master joints formed by regional bending of the crust, possibly related to the intrusion of the pluton.

One of the disputed questions in the Cape Breton Highlands is the position of the boundary between the Aspy and Bras d'Or terranes, and the significance of the boundary (Lin 1993, 1995; Chen et al. 1995; Lynch et al 1993; Lynch and Tremblay 1992). This study corroborates that a major change in rock character occurs across the

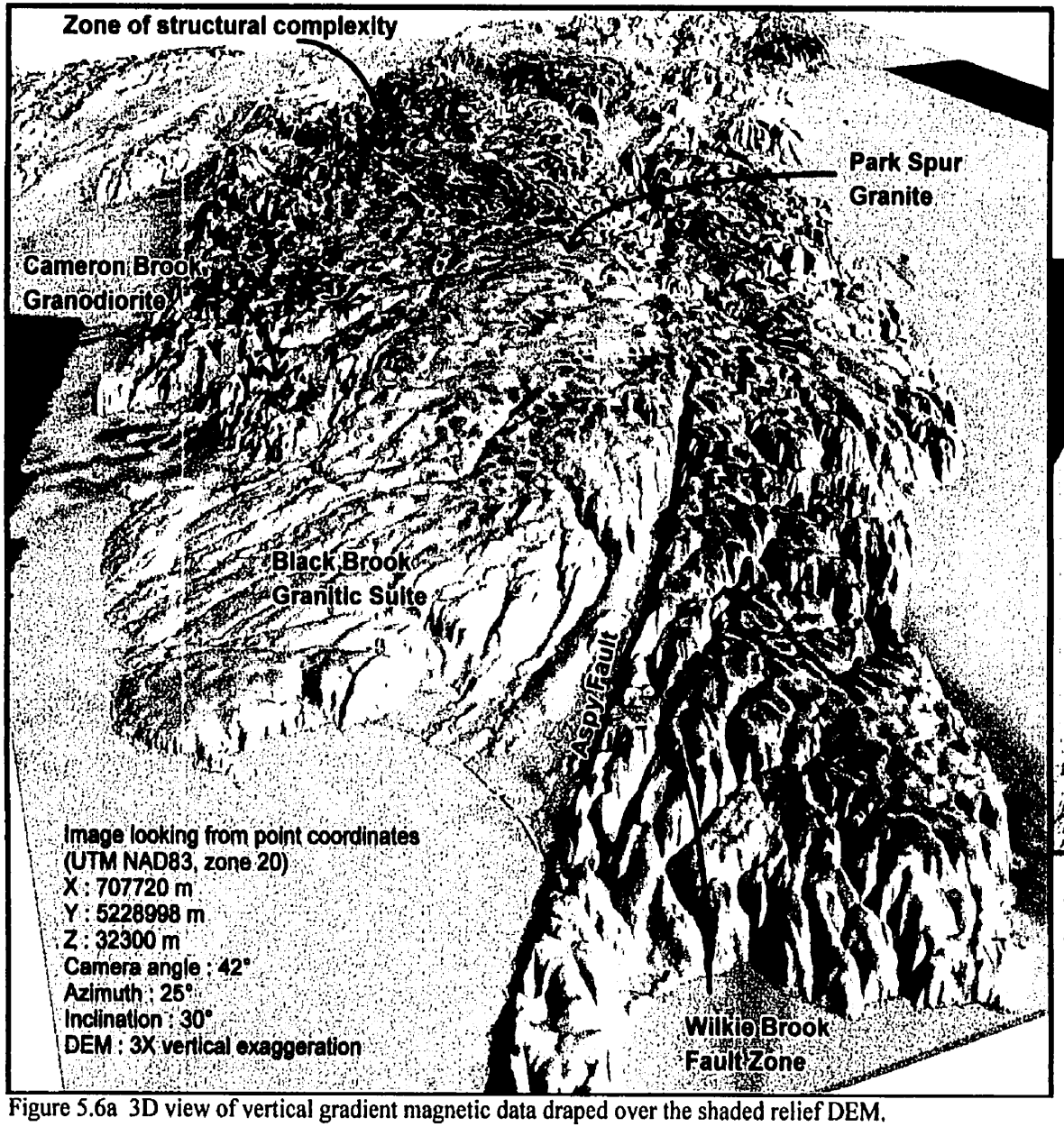

Figure 5.6a 3D view of vertical gradient magnetic data draped over the shaded relief DEM.

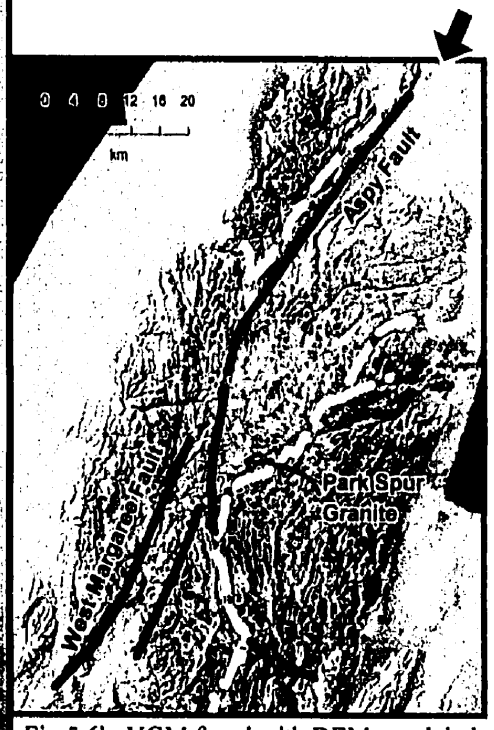

Fig 5.6b VGM fused with DEM overlain by terrane boundaries (white dashed lines) and major structural lineaments in black.

Eastern Highlands Shear Zone of Barr and Raeside (1989). The data are also consistent with the modification by Barr and Raeside (1998) that placed the Clyburn Brook Formation in the Aspy terrane rather than the Bras d'Or terrane. However, the precise position of the terrane boundary in the Clyburn Brook area remains enigmatic (Fig 5.7). Magnetic data suggest that the boundary is located north of the Clyburn Brook Formation and Cameron Brook Granodiorite, inferring that intrusion of the granodiorite may have somehow displaced the boundary.

The position of the boundary to the west in the area of the Park Spur Granite is also uncertain. This area is one of convergence for many of the major linear structures, as well as the proposed boundary between the Aspy and Bras d'Or terranes (Fig 5.6a, b). Barr and Raeside (1989) placed the boundary in a north-east and then north-trending zone of mylonite that separated rocks of the Jumping Brook Metamorphic Suite on the northwest from the Bateman Brook Metamorphic Suite on the southeast. However, McMullin et al. (1993) re-interpreted the area to be part of the McMillan Flowage Formation, and moved the terrane boundary to the west. Mengel et al. (1991) showed the presence of a major north-trending mylonite zone (Southern Highland Shear Zone) which they considered to be a more major structure than the EHSZ. The Southern Highland shear zone (SHSZ) of Mengel et al (1991) has similar kinematics and has been traced by Lin (1992) in his detailed study of the area, into the EHSZ. Similar to Barr and Raeside (1989), Lin (1992) treated the shear zone as part of the EHSZ. The VGM fused with DEM and radiometric images do not resolve the question because of the converging lineaments and similarity of magnetic and radiometric signatures of the units.

The southwestern boundary part of the Aspy and Bras d'Or terrane boundary appears to be well constrained from the geology, as well as on the images, although it seems to be offset and to splay across to form the "bow-tie" appearance in the "zone of structural complexity". A possible explanation for the complexity in this area is that the West Branch North River granite intruded the EHSZ, as possibly did the Cameron Brook Granodiorite.

The combined geological and remote sensing databases also provide new insight concerning the possible relationship between major regional structural features and known gold occurrences in the Cape Breton Highlands. A project aimed at investigating this type of relationship was initiated (Mengel et al. 1991), but no follow up was completed on a regional scale. Figure 5.7 shows the location of gold (Au) occurrences in the highlands. Most are in close proximity to the Eastern Highland Shear Zone and the "zone of structural complexity". Further detailed studies in understanding the nature of the terrane boundary between the Aspy and Bras d'Or terranes and the " zone of structural complexity" might provide more insight on the kinematics and extent of tectonic features on a terrane scale.

For example, in the eastern part of the Bras d'Or terrane gold-bearing mineralization occurs in an auriferous sericitized zone in the SW extension of the Eastern Highland shear zone (Mengel et al. 1991). The grayscale DEM on figure 5.7 shows convincing east-west lineaments associated with the gold deposits. An understanding of the detailed structural setting and history of these east-west lineaments could be valuable in predicting more mineralized zones.

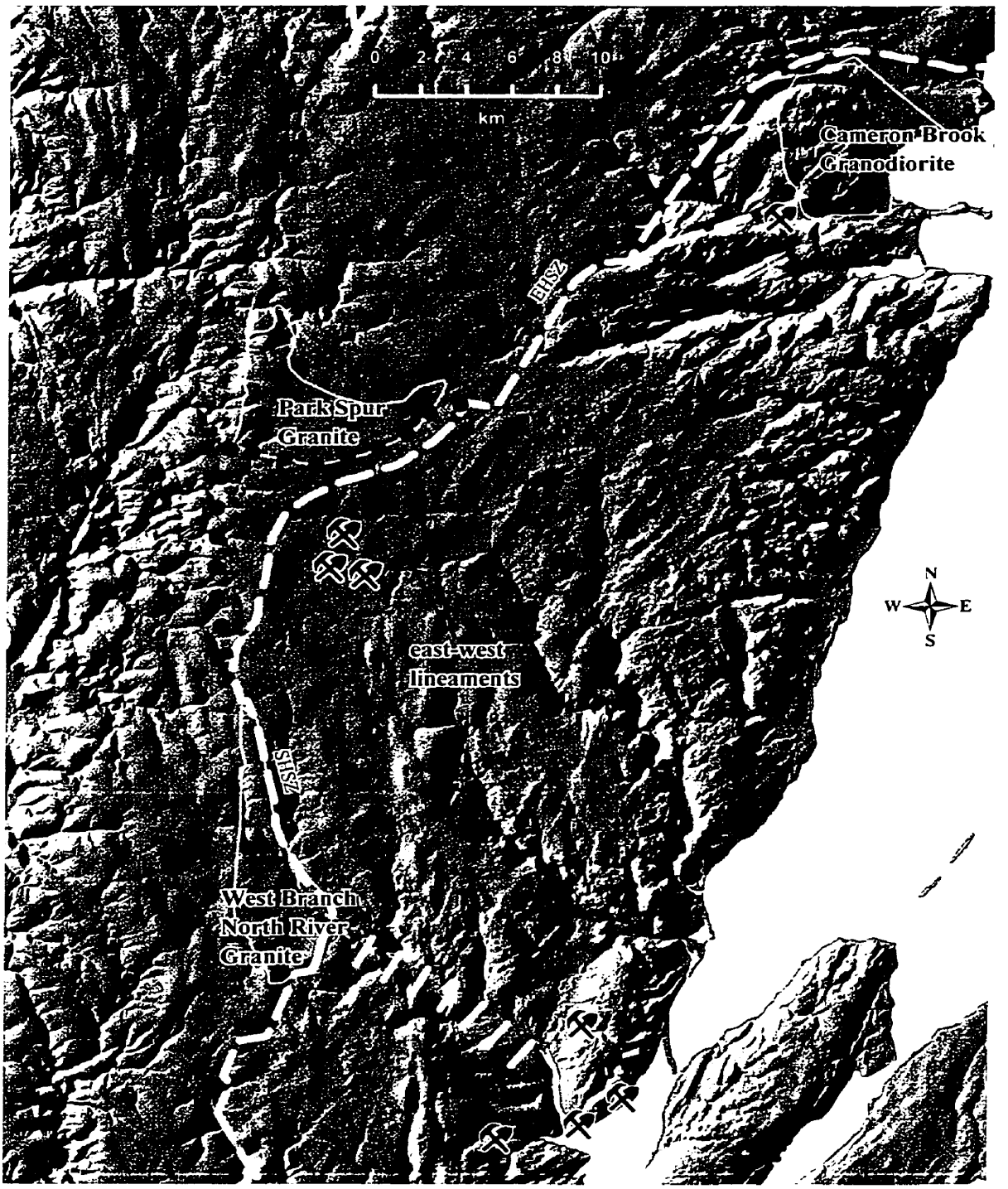

Figure 5.7 Grayscale shaded relief DEM illuminated from the northwest (azimuth 300°, inclination 30°). Broken line represents terrane boundary from Barr et al. (1992). White dashed lines represent the "zone of structural complexity".

Chapter 6. Conclusions and Implications for Future Studies

6.1 Conclusions

1) The basis for the project was the construction of the high-resolution digital elevation model (DEM) for the Cape Breton Highlands. With the DEM, the angle and inclinations of the artificial light source were manipulated, thus selectively enhancing or suppressing geomorphologic and structural features having a particular orientation. The colour-coded shaded DEM illuminated from the west (270°) at an inclination of 45° was the main DEM used. Colour coding the DEM was important in recognising elevation differences within the plateau. The grayscale-shaded relief DEM illuminated from multiple orientations and inclinations provided the best structural information.

2) Radarsat S7 and S2 were not as useful as the DEM because they are less flexible in terms of artificial illumination and manipulating and have lower resolution, although they provide similar topographic information. The images were used in a few places to check the quality of surface expression of the DEM. Also together with the Landsat TM, the Radarsat S7 was very important in delineating surface water such as lakes and man-made reservoirs, as well as sphagnum bogs.

3) The Landsat TM was useful for geomorphologic information and imaging man-made feature such as roads. As such, it was an excellent navigation tool during the ground-truthing process, used in conjunction with the Global Positioning System (GPS). Fortunately, the U.S. government had discontinuing the intentional

degradation of the GPS signals available to the public from the 1st of May 2000, so the accuracy of the inexpensive GPS instrument used in this study was normally better than ±10 metres compared to the previous accuracy of ± 100 m. During the process of ground-truthing, the Landsat TM was used on a laptop computer in the vehicle as a backdrop image in the GIS, and hooked up to the GPS. This process was very efficient to recognise spatial understanding between geological features in a regional and local sense. Although a bit dated (1992 and 1986) the Landsat TM images were adequate for this purpose.

4) Data integration using colour display transformations and IHS (Intensity, Hue and Saturation) modelling was an effective way to provide combined information from two separate images. The vertical gradient magnetic fused with elevation model was the most important image to provide lithological and structural information, although the total field magnetic fused with Radarsat assisted the previous image. Gravity data fused with elevation models provided an understanding of the spatial relationship of the gravity data in relation to the major structural trends. Similarly, the gravity data fused with vertical gradient magnetic data show the correlation between the denser rock units in relation to the magnetic trends.

5) Perspective 3D-images generated using the Landsat TM and the vertical gradient magnetic fused with the digital elevation model provided an interesting outlook on the regional trends, especially to show the Aspy fault converging to the "zone of structural complexity".

6) An unsupervised classification of airborne gamma-ray spectrometry data was devised as an aid in interpreting the radiometric data. The radiometric data were shown to correlate well with known rock unit compositions. The classification grouped the radiometric data into 15 classes making it manageable to illustrate variations in the proportions of potassium, thorium and uranium. An image was produced that showed the compositional differences between rock units, especially plutons.

Examination of the above images in conjunction with published geological maps showed the following interpretations :

7) Mesoproterozoic rocks of the Blair River Inlier generally have high total magnetic field and variable vertical gradient magnetic pattern. Based on the limited data available, the gravity response for this area is moderately high for the Cape Breton Highlands. The radiometric signature of the area is dominated by low eU, eTh, and K and contrasts with that of the surrounding Carboniferous units and units of the adjacent Aspy terrane. The differences are consistent with the distinctive rock types in the BRI, which differ from those of the Aspy terrane. Lineaments derived from Radarsat and DEM trend mainly northeast to north-northeast, a pattern not readily apparent from the geological maps or the VGM and radiometric images.

8) The part of the Bras d'Or terrane in the study area is characterised by strong northeast-trending anomalies in the east and more disrupted but mainly north-trending anomalies in the west. Most of the Bras d'Or terrane is characterised by radiometric low eU, eTh and K and has the highest Bouguer gravity values in the study area. In contrast to the tonalite and diorite units in the middle of the area, the eastern edge of the terrane has higher K and eTh and lower gravity values, consistent with presence of granite plutons in that area. Lineaments derived from DEM and Radarsat indicate a dominant northeasterly trend consistent with the geological and magnetic trends.

9) The northeastern part of the Aspy terrane is characterised by a gradual elevation change from the lowest in the northeast along the coastline of the Black Brook Granitic Suite to highest in the southwest. This elevated plateau has variable radiometric signatures as a result of numerous bogs and swamps. Magnetic trends are variable, gravity values are moderate to the west and low in the northeast, related to the change from metavolcanic to granitoid units. This area has been divided into two domains representing different lineament orientation. The southeast part of the area, mainly underlain by the Black Brook Granitic Suite, is characterised by east-to ENE-trending topographic linears, whereas the northwestern part has mainly northeast-trending linears. The presence of different phases in the Black Brook Granitic Suite were corroborated by the radiometric classification.

10) The Aspy terrane in the central and western Cape Breton Highlands shows strong NNE and moderate NW lineament orientations. The NNE lineaments are related to the Margaree Fault system extending SW past the study area. The NW lineaments are related to NW-trending faults cutting through Carboniferous units, the Devonian Fisset Brook Formation, and Proterozoic Cheticamp pluton. The Radarsat image shows an E-W lineament related to the Cheticamp River Gorge that can be traced in a straight line across the highlands to Ingonish through Cheticamp Flowage and Ingonish River. The radiometric classification is very effective to differentiate the Margaree, Taylors Barren, and West Branch North River granitic plutons from surrounding units. Sparse gravity data give some control between the plutons mentioned above and surrounding rocks. Radarsat S7, but more so Radarsat S2 and the DEM, provide a dramatic outlook on the topographic linears and slopes. The VGM fused with DEM, and TFM fused with Radarsat S7 categorises particular lithological and structural patterns within specific regional blocks.

11) Magnetic, gravity and DEM data differentiated the southwestern part of the Aspy terrane including the Mabou Highlands, Gillanders Mountain, and the southern tip of the Cape Breton Highlands compared to the surrounding Carboniferous units. The detailed DEM for the study area and integrating it with various geophysical data provided a fresh outlook on regional structural interpretations. As a result, a "strike-slip basin" model has been developed to explain the distribution of units and topography in the Gillanders Mountain Area.

12) As a result of this study, a new digital geological map and associated geological unit database were produced. The geological map of Barr et al. (1992) appears to provide the best agreement with the image datasets, and was used as the base for the revised map.

6.2 Future Studies

This study was dependent on acquiring a variety of information sets from different sources. The GIS was a way both to collect and store data, and, more importantly, to spatially analyse the relationships among the collected data. The ability to combine datasets and simultaneously interpret the spatial relationship between various sources of information on a qualitative basis allowed for more comprehensive geological interpretations.

Organising the information within the GIS does not just represent digital information, hardware and software, but provides a basis for controlled data management and information dissemination. All the information collected was useful, but it was the combination of all the data together that resulted in the enhanced interpretations. This project and datasets can be regarded as a foundation that can be built upon to further geological knowledge of the Cape Breton Highlands.

The unsupervised classification of radiometric data was useful for this study, the next step would be to produce a supervised classification where geochemical sample data points could be used a basis for the selection of spectral classes and then one could assess variation within different lithological units as well as different phases within the plutons. It will be important to establish a database of the geochemical samples within

the GIS for the Cape Breton Highlands. Such a database will provide better spatial control on the different geophysical properties of particular units, for example.

The construction of the Bouguer gravity image was valuable in separating density domains on a regional scale within the highlands, even though the data are sparse. More gravity data are needed for the Cape Breton Highlands, Gillanders Mountain area, and the Mabou Highlands. Enhanced gravity data in the Park Spur Granite and Clyburn Brook areas would probably provide better insight on the terrane boundary problem. Having better gravity for these areas could provide a good opportunity to understand the geological units, not only in map view, but at depth. Gravity 3D-modelling would help to show if the terrane boundary between the Aspy and Bras d'Or continues at depth.

It is also important for the onshore data utilized in this study to be correlated to data in the surrounding offshore areas (e.g., Pascucci et al. 2000). Such studies could resolve current uncertainties and controversies about the correlation of terranes in Cape Breton Island to those in Newfoundland to the northeast and the mainland part of the Appalachian orogen to the southwest.

References

Barr, S.M. and Macdonald, A.S., Arnott, A.M., Dunning, G.R. 1995. Field relations, structure, and geochemistry of the Fisset Brook Formation in the Lake Ainslie – Gillanders Mountain area, central Cape Breton Island, Nova Scotia. Atlantic Geology, **31**: 127-139.

Barr, S.M., and Jamieson, R.A. 1991. Tectonic setting and regional correlation of Ordovician-Silurian rocks of the Aspy Terrane, Cape Breton Island, Nova Scotia. Canadian Journal of Earth Sciences, **28**: 1769-1779.

Barr, S.M., and Peterson, K.C.A. 1998. Field relationships and petrology of the Late Devonian Fisset Brook Formation in the Cheticamp area, western Cape Breton Island, Nova Scotia. Atlantic Geology, **34**: 121-132.

Barr, S.M., and Raeside R.P. 1989. Tectono-stratigraphic terranes in Cape Breton Island, Nova Scotia: Implications for the configuration of terranes in the northern Appalachian Orogen, Geology, **17**: 822-825.

Barr, S.M., and Raeside, R.P. 1986. Pre-Carboniferous tectonostratigraphic subdivisions of Cape Breton Island, Nova Scotia. Maritime Sediments and Atlantic Geology, **22**: 252-263.

Barr, S.M., and Raeside, R.P. 1994. Relationship between the Aspy and Bras d'Or "terranes" in the northeastern Cape Breton Highlands, Nova Scotia: Discussion. Canadian Journal of Earth Sciences, **31:** 1384-1385.

Barr, S.M., and Raeside, R.P. 1998. Petrology and tectonic implications of Silurian(?) metavolcanic rocks in the Clyburn Brook area and on Ingonish Island, northeastern Cape Breton Island, Nova Scotia. Atlantic Geology, **34**: 27-37.

Barr, S.M., Jamieson, R.A., Raeside R.P. 1992. Geology, Northern Cape Breton Island, Nova Scotia. Geological Survey of Canada, Map 1752A, scale 1:100 000.

Barr, S.M., Macdonald, A.S. 1989. Geology of Mabou Highlands (NTS Sheet 11k/03 west half), Nova Scotia. Nova Scotia Department of Mines and Energy, Map 89-1.

Barr, S.M., Raeside, R.P., Miller, B.V., and White, C.E. 1995. Terrane evolution and accretion in Cape Breton Island, Nova Scotia. *In* Current perspectives in the Appalachian-Caledonian Orogen. *Edited by* J.P. Hibbard, C.R. van Staal, and P.A. Cawood. Geological Association of Canada, Special Paper 41, 391-407.

Barr, S.M., Raeside, R.P., and White, C.E. 1998. Geological correlations between Cape Breton Island and Newfoundland. Canadian Journal of Earth Sciences, **35**: 1252-1270.

Bonham-Carter, G.F. 1994. Geographic Information Systems for Geoscientists: Modelling with a GIS. Elsevier Science Inc., New York, pp. 120-125.

Cameron, H.L. 1966. The Cabot Fault Zone. in Continental Drift, The Royal Society of Canada Special publication, **09**: 129-140.

Chen, Y.D., Lin, S., and van Staal, C.R. 1995. Detrital zircon geochronology of a conglomerate in the northeastern Cape Breton Highlands: implications for the relationships between terranes in Cape Breton Island, the Canadian Appalachians. Canadian Journal of Earth Sciences, **32**: 216-223.

Currie, K.L. 1987. Relations between metamorphism and magmatism near Cheticamp, Cape Breton Island, Nova Scotia, Geological Survey of Canada. Paper 85-23, 66p.

Darnley, A.G. and Ford, K.L. 1987. Regional Airborne Gamma-ray Surveys: a Review; *in* Exploration '87 Proceedings, Geophysical Methods, Advancements in the State of the Art.

Desjardins, R., Iris, S., Roy, D.W., Lemieux, G.H. and Toutin, T. 2000. Éfficacité des données de RADARSAT-1 dans la reconnaissance des linéaments: un bilan. Canadian Journal of Remote Sensing, **26**: 537-548.

Drury, S.A. 1993. Image Interpretation in Geology. Chapman & Hill, London. pp. 217.

Earth Resource Mapping Inc., 2000. http://www.ermapper.com.

Giles, P.S., Hein, F.J. and Allen, T.L. 1997. Bedrock geology of Port Hood-Lake Ainslie (11K04, 11K03, 11F13), Cape Breton Island, Nova Scotia: Geological Survey of Canada Open File 3253; 1:50000 map with marginal notes.

Grant, J.A., 1993. SurView: a Microsoft Windows 3.x Application for Viewing Geophysical Survey Data, Geological Survey of Canada, Open File 2661, List 1025.

Grecco, L. E., and Barr, S. M. 1999. Late Neoproterozoic granitoid and metavolcanic rocks of the Indian Brook Area, southeastern Cape Breton Highlands, Nova Scotia. Atlantic Geology, **35**: 43-57.

Harris, J., Murray, R., and Hirose, T. 1990. IHS Transform for intergration of Radar imagery with other remotely sensed data. Photogrammetric Engineering and Remote Sensing, **56**: 1631-1641.

Harris, J.R. 1989. Clustering of gamma-ray spectrometer data using a computer image analysis system. *In* Statistical Applications in the Earth Sciences, *Edited* by Agterberg, F.P. and Bonham-Carter, G.F. Geological Survey of Canada, Paper 89-9, pp. 19-31.

Harris, J.R., Bowie, C., Renez, A.N. and Graham, D. 1994. Computer-Enhancement Techniques for the Integration of Remotely Sensed Geophysical, and Thematic Data for the Geosciences. Canadian Journal of Remote Sensing, **20**: 210-221.

Horne, R.J. 1995. Geology of the South-Central Cape Breton Highlands, Inverness and Victoria Counties. Nova Scotia Department of Natural Resources, Minerals and Energy Branch, Paper 95-2.

Howells, K., and Clarke, E.D. 1995. Reprocessing of Nova Scotia Gravity Data from the NSRFC gravity database (1952-1988). Mineral Resources Division, Nova Scotia Department of Natural Resources, OFR 95-005.

Keppie, J.D. 2000. Geological Map of the Province of Nova Scotia , version 1, scale 1: 500 000, Nova Scotia Department of Natural Resources, Minerals and Energy Branch.

Keppie, J.D., Dallmeyer, R.D. and Krogh, T.E. 1992. U-Pb and $^{40}Ar/^{39}Ar$ mineral ages from Cape North, northern Cape Breton Island: implications for accretion of the Avalon Composite Terrane. Canadian Journal of Earth Sciences, 29, 277-295.

Keppie, J.D. 1990. Comment on "Tectonostratigraphic terranes in Cape Breton Island, Nova Scotia: Implications for the configuration of the northern Appalachian orogen". Geology, **18**: 669-670.

Lillesand, Thomas M., and Kiefer, Ralph W. 1994. Remote sensing and image interpretation. John Wiley & Sons, Inc 3rd edition, 549p.

Lin, S. 1992. The Stratigraphy and structural geology of the southeastern Cape Breton Highlands National Park and its implications for the tectonic evolution of Cape Breton Island, Nova Scotia. Ph.D. thesis, University of New Brunswick, Fredericton New Brunswick.

Lin, S. 1993. Relationship between the Aspy and Bras d'Or "terranes" in the northeastern Cape Breton Highlands, Nova Scotia. Canadian Journal of Earth Sciences, **30**: 1773-1781.

Lin, S. 1995. Structural evolution and tectonic significance of the Eastern Highlands shear zone in Cape Breton Island, The Canadian Appalachians. Canadian Journal of Earth Sciences, **32**: 545-554.

Lin, S., and van Staal., C.R. 1997. Comment on "Tectonic burial thrust emplacement, and extensional exhumation of the Cabot nappe in the Appalachian hinterland of Cape Breton Island, Canada, Tectonics, **16**: 702-706.

Lister, K. J. 1998. Petrography and tectonic implications of the Silurian Sarach Brook Metamorphic suite, southern Cape Breton Island, Nova Scotia B.Sc. Honours thesis, Acadia University, Wolfville, N.S.

Lynch G., and Tremblay, C. 1992. Imbricate thrusting, reverse-oblique shear, and ductile extensional shear in the Acadian Orogen, central Cape Breton Highlands, Nova Scotia; *in* Current Research, Part D, Geological Survey of Canada, Paper 92-1D, p. 91-100.

Lynch, G. 1996. Tectonic burial, thrust emplacement, and extensional exhumation of the Cabot nappe in the Appalachian hinterland of Cape Breton Island, Canada, Tectonics, **15**: 94-105.

Lynch, G. 1997. *Reply*: Comment on "Tectonic burial thrust emplacement, and extensional exhumation of the Cabot nappe in the Appalachian hinterland of Cape Breton Island, Canada, Tectonics, **16**: 707-712.

Lynch, G., and Brisson, H. 1996. Bedrock geology, Whycocomagh (11F/14), Geological Survey of Canada, Open File 2917, Scale 1:50 000.

Lynch, G., and Giles, P.S. 1995. The Ainslie Detachment: a regional flat-lying extensional fault in the Carboniferous evaporitic Maritimes Basin of Nova Scotia, Canadian Journal of Earth Sciences, **33**: 169–181.

Lynch, G., and Lafrance, B. 1996. Bedrock geology, Baddeck (11K/02), Geological Survey of Canada, Open File 2488, Scale 1:50 000.

Lynch, G., Barr, S.M., Houlahan, T., and Giles, P. 1997. Geological Compilation, Cape Breton Island, Nova Scotia. Geological Survey of Canada, Open File 3159, scale 1:250 000.

MacDonald, C. K. 1996. Petrography, Geochemistry, and Structure of the Taylors Barren Pluton, Cape Breton Island, Nova Scotia B.Sc. Honours thesis, Acadia University, Wolfville, N.S.

McMullin, D.W.A., Barr, S.M., and Raeside, R.P. 1993. A re-interpretation of the "Bateman Brook Metamorphic Suite", Cape Breton Highlands, Nova Scotia, as sheared, fault-bounded blocks of other units. Atlantic Geology, 29, 43-50.

Mengel, F., Godue, R., Sangster., A., Dubé, B., and Lynch, G. 1991. A progress report on the structural control of gold mineralization in the Cape Breton Highlands: *in* Current Research, Part D; Geological Survey of Canada, Paper 91-1D, p. 117-127.

Miller, B.V., Dunning, G.R., Barr, S.M., Raeside, R.P., and Jamieson, R.A. 1996 Magmatism and Metamorphism in a Grenvillian Fragment: U-Pb and Ar/Ar Ages from the Blair River Complex., Northern Cape Breton Island, Nova Scotia, Geological Society of America Bulletin, **108**: 127-140.

Miller, B. 1997. Geology, geochronology and tectonic significance of the Blair River Complex, Northern Cape Breton, Nova Scotia. Ph.D. Thesis Dalhousie University, Halifax, Nova Scotia.

Miller, B. V., and Barr, S.M. 2000. Petrology and Isotopic Composition of a Grenvillian Basement Fragment in the Northern Appalachian Orogen: Blair River Inlier, Nova Scotia, Canada. Journal of Petrology, **41:** 1777-1804.

Murphy, J.B., Keppie, J.D., Nance R.D., and Dostal, J. 1990. The Avalon Composite terrane of Nova Scotia. *In* Avalonian and Cadomian geology of the North Atlantic. *Edited by* R.A. Strachan and G.K. Taylor. Blackie, Glasgow, 195-213.

Northwood Geoscience Ltd. 1999. Vertical Mapper User Guide, version 2.6. Nepean, Ontario, Canada.

O'Beirne-Ryan, A.M. and Jamieson, R.A. 1986. Geology of the West Branch North River and the Bothan Brook plutons of the south-central Cape Breton Highlands, Nova Scotia, in Current Research, Part B, Geological Survey of Canada, Paper 86-1B, 191-200.

O'Beirne-Ryan, A.M., Barr, S.M., and Jamieson, R.A. 1986. Contrasting petrology and age of two megacrystic granitoid plutons, Cape Breton Island, Nova Scotia; *in* Current Research, Part B, Geological Survey of Canada, paper 86-1B, 179-190.

O'Leary, D.W., Friedman J.D., and Pohn H.A., 1976. "Lineament, Linear and Lineation: Some Proposed New Standards for Old Terms". Geological Society of America Bulletin, **87**: 1463-1469.

O'Neill, Michael 1996. Geology of the Leonard MacLeod Brook area, Cape Breton Island, Nova Scotia. M.Sc. thesis, Acadia University, Wolfville, N.S.

Pascucci, V., Gibling, M.R., and Williamson, M.A. 2000. Late Paleozoic to Cenozoic history of the offshore Sydney Basin, Atlantic Canada. Canadian Journal of Earth Sciences, **37**: 1143-1165.

Price J.R. 1997. The Geology of the Belle Côte Road orthogneiss and First Brook gneiss, Cape Breton Highlands, Nova Scotia, Canada. M.Sc. thesis, Dalhousie University, Halifax, Nova Scotia.

Price J.R., Barr, S.M., Raeside, R.P., and Reynolds P.H. 1999. Petrology, tectonic setting, and $^{40}Ar/^{39}Ar$ (hornblende) dating of the Late Ordovician – Early Silurian Belle Côte Road orthogneiss, western Cape Breton Highlands, Nova Scotia. Atlantic Geology, **35**: 1-17.

Raeside, R.P., and Barr, S.M. 1990. Geology and tectonic development of the Bras d'Or suspect terrane, Cape Breton Island, Nova Scotia. Canadian Journal of Earth Sciences, **27**: 1371-1381.

Raeside, R.P., and Barr, S.M. 1992. Geology of the northern and eastern Cape Breton Highlands, Cape Breton Island, Nova Scotia. Geological Survey of Canada, Paper 89-14, 39p.

Robinson, E. S. and Çoruh, C. 1988. Basic Exploration Geophysics. John Wiley & Sons, Toronto. 562p.

Simon, B. 1993. How Lossy Compression Shrinks Image Files, PC Magazine, July. **12**: 371-375.

Singhroy, V.H., Ellis, T.J., and Janes, D. 1985. Interpretation of Enhanced TM Data for Medium-Scale Geological Mapping in Glaciated Forested Terrains: Ontario Case Study. Proceedings of the ERIM Fourth Thematic Conference, Remote Sensing for Exploration Geology. 531-538.

Singhroy, V., R. Slaney, P. Lowman, Harris, J., and Moon, W. 1993. Radarsat-1 and Radar Geology in Canada. Canadian Journal of Remote Sensing, **19**: 338-351.

Slaney, R. 1981. Landsat Images of Canada – A geological Appraisal. Geological Survey of Canada Paper 80-15, 102p.

Smith, P.K., and O'Reilly, G.A. 1994. Gold Mineralization in the Cape Breton Highlands, Nova Scotia. Nova Scotia Department of Natural Resources, Minerals and Energy Branch, Open File Report 94-023.

Stea, R.R., Conley, H., and Brown, Y. 1992. Surficial Geology Map of the Province of Nova Scotia , version 1, 1997, scale 1:500 000, Nova Scotia Department of Natural Resources Minerals and Energy Branch.

Waldron, J.W.F., Gillis, K.S., Naylor, R.D., and Chandler, F.W. 1995. Structural investigations in the Stellarton pull-apart basin, Nova Scotia; in Current Research, 1995-D; Geological Survey of Canada, pp. 19-25.

Webster, T.L. 1996. Remote sensing and geographic information system analysis of the St. Marys Basin and surrounding areas, central Nova Scotia. M.Sc. thesis, Acadia University, Wolfville, N.S.

Webster, T.L., Murphy, J.B. and Barr, S.M. 1998. Anatomy of a terrane boundary: An integrated structural, GIS and remote sensing study of the Late Paleozoic Avalon-Meguma terrane boundary, mainland Nova Scotia, Canada. Canadian Journal of Earth Sciences, **35**: 787-801.

Yaowanoiyothin, W. 1988. Petrology of the Black Brook Granitic Suite and associated gneiss, northeastern Cape Breton Highlands. Nova Scotia M.Sc. thesis, Acadia University, Wolfville, N.S.

Yaowanoiyothin, W., and Barr S.M. 1991. Petrology of the Black Brook Granitic Suite, Cape Breton Island, Nova Scotia. Canadian Mineralogist, **29**: 499-515.

Yeo, G., and Gao, R.-X. 1987. Stellarton Graben: an upper Carboniferous pull-apart basin in northern Nova Scotia; Canadian Society of Petroleum Geologists, Memoir 12, pp. 299-309.

Appendix A

Geological map units in alphabetical order.

BEDCD	UNIT NAME	AGE
c	Carboniferous rocks	Carboniferous
ЄCSg	Cape Smokey Granite	Cambrian
ЄKMg	Kellys Mountain Leucogranite	Cambrian
ЄSAg	St. Anns Leucogranite	Cambrian
DBBg	Bothan Brook Granite	Devonian
DBGg	Black Brook Granitic Suite	Devonian
DCAMg	Andrews Mountain Granite	Devonian
DCBg	Cameron Brook Granodiorite	Devonian
DCLC	Lowland Cove Formation	Devonian to Carboniferous
DCSg	Sugarloaf Granite	Devonian to Carboniferous
DCWSg	Wilkie Sugarloaf Granite	Devonian to Carboniferous
DFB	Fisset Brook Formation	Devonian
Dg	Unnamed Granite	Devonian
DGAg	Grande Anse Granite	Devonian
DGMg	Gillanders Mountain Granite	Devonian
DGMs	Gillanders Mountain Syenogranite	Devonian
DMBg	McLean Brook Granite	Devonian
Dmd	Microdiorite, occuring as dykes	Devonian
DMGg	Margaree Pluton	Devonian
DMM	MacMillan Mountain Volcanics	Devonian
DNH	Neils Harbour Gneiss	Devonian
DPBd	Port Ban Diorite	Devonian
DPBg	Pleasant Bay Granite	Devonian
DPSg	Park Spur Granite	Devonian
DSPg	Salmon Pool Granite	Devonian
DWBg	West Branch North River Granite	Devonian
DWBgd	West Branch North River Granodiorite	Devonian
HBB	Bateman Brook Gniess	Neoproterozoic
HCGq	Gisborne Flowage Quartz Diorite	Neoproterozoic
HCTd	Timber Lake Dioritic Suite	Neoproterozoic
HDMq	Morrison Brook Quartz Monzonite	Neoproterozoic to Cambrian
HSCgd	Snake Cat Lake Granodiorite	Neoproterozoic
OMR	Middle River Metamorphic Suite	Ordovician to Silurian
OSBCogn	Belle Côte Road Orthogneiss	Ordovician to Silurian
OSCN	Cape North Group	Ordovician to Silurian
OSCNgn	Cape North Group	Ordovician to Silurian
OSCNm	Cape North Group	Ordovician to Silurian
OSCNp	Cape North Group	Ordovician to Silurian
OSGBgd	Glasgow Brook granodiorite	Ordovician to Silurian
OSGMm	Gillanders Mountain Metamorphic	Ordovician to Silurian
OSGMp	Gillanders Mountain Metamorphic	Ordovician to Silurian
OSGMs	Gillanders Mountain Metamorphic	Ordovician to Silurian

OSJBa	Faribault Brook Metavolcanics	Ordovician to Silurian
OSJBb	Barren Brook Schist	Ordovician to Silurian
OSJBc	Dauphinee Brook Suite	Ordovician to Silurian
OSJBd	Corney Brook Schist	Ordovician to Silurian
OSJBe	George Brook Amphibolite	Ordovician to Silurian
OSMP	Money Point Group	Ordovician to Silurian
OSMPm	Money Point Group	Ordovician to Silurian
OSMPp	Money Point Group	Ordovician to Silurian
OSPB	Pleasant Bay Complex	Ordovician to Silurian
SCB	Clyburn Brook Formation	Silurian
SDCLgn	Cheticamp Lake Gniess	Silurian to Devonian
SDCLp	Cheticamp Lake Gniess	Silurian to Devonian
SDGBg	Gulch Brook Granite	Silurian to Devonian
SDLM	Leonard MacLeod Brook Complex	Silurian to Devonian
SDLMg	Leonard MacLeod Brook Granite	Silurian to Devonian
SDm	Mylonite	Devonian
SDMAg	Middle Aspy River Granitic Orthogneiss	Silurian to Devonian
SDMGct	McDonald Glen Brook Formation	Silurian to Devonian
SDMGVS	McDonald Glen Brook Formation	Silurian to Devonian
SDTg	Taylor Barren Pluton	Silurian
SFBd	Fox Back Ridge Diorite	Silurian
Sli	Ingonish Island Rhyolite	Silurian
SRRS	Red Ravine Syenite	Silurian
SSB	Sarach Brook Metamorphic Suite	Ordovician to Silurian
SSBg	Sammys Barren Granite	Silurian
Ych	Charnockite in BRI	Mesoproterozoic
YDBa	Delaneys Brook Anorthosite	Mesoproterozoic
YLBS	Lowland Brook Syenite	Mesoproterozoic
YOBgn	Otter Brook gneiss	Mesoproterozoic
YPC	Polletts Cove River Gneiss	Mesoproterozoic
YPCgn	Polletts Cove River Gneiss	Mesoproterozoic
YPCm	Polletts Cove River marble	Mesoproterozoic
YRRa	Red River Anorthosite Suite	Mesoproterozoic
YSBgn	Sailor Brook Gneiss	Mesoproterozoic
YSRa	Salmon River Anorthosite	Mesoproterozoic
Z	Unnamed granitoid rock	Neoproterozoic
ZBBg	Birch Plain Granite	Neoproterozoic
ZBBgd	Beinn Bhreagh Granodiorite	Neoproterozoic
ZBR	Barachois River Formation	Neoproterozoic
ZBRgd	Baddeck River Granodiorite	Neoproterozoic
ZCMBq	Morrison Brook Quartz Monzonite	Neoproterozoic to Cambrian
ZCMg	Cross Mountain Granite	Neoproterozoic
ZCmy	Mylonite in BRI	Devonian to Carboniferous
ZCPg	Cheticamp Pluton	Neoproterozoic
ZD	Unnamed granitoid rock	Neoproterozoic to Devonian
ZDGMd	Gillanders Mountain Diorite	Neoproterozoic to Devonian
ZGCg	Goose Cove Brook Granite	Neoproterozoic
ZGFqd	Gisborne Flowage Quartz Diorite	Neoproterozoic
Zgn	Unnamed gneiss	Neoproterozoic

ZGR	George River Metamorphic Suite	Neoproterozoic
ZIBg	Indian Brook Granite	Neoproterozoic
ZIBgd	Indian Brook Granodiorite	Neoproterozoic
ZIRt	Ingonish River Tonalite	Neoproterozoic
ZKBg	Kerrs Brook Granite	Neoproterozoic
ZKMd	Kellys Mountain Dioritic Rocks	Neoproterozoic
ZKMgn	Kellys Mountain Gneiss	Neoproterozoic
ZKRd	Kathy Road Dioritic Suite	Neoproterozoic
ZMFa	McMillan Flowage Formation	Neoproterozoic
ZMFb	McMillan Flowage Formation	Neoproterozoic
ZMFc	McMillan Flowage Formation	Neoproterozoic
ZMFd	McMillan Flowage Formation	Neoproterozoic
ZMFe	McMillan Flowage Formation	Neoproterozoic
ZMHd	Middle Head Leucodiorite	Neoproterozoic
ZMHt	Mabou Highlands leucotonalite	Neoproterozoic
ZMMq	Murray Mountain Quartz Monzodiorite	Neoproterozoic
ZNBt	North Branch Baddeck River Leucotonalite	Neoproterozoic
ZNGg	New Glen Granite	Neoproterozoic
ZRB	Roper Brook Amphibolite	Neoproterozoic
ZSGMd	Gillanders Mountain Diorite	Neoproterozoic to Silurian
ZSgn	Unnamed gneiss	Neoproterozoic to Silurian
ZSP	Sight Point Group	Neoproterozoic
ZSPig	Sight Point Group	Neoproterozoic
ZSPit	Sight Point Group	Neoproterozoic
ZSPms	Sight Point Group	Neoproterozoic
ZSPp	Sight Point Group	Neoproterozoic
ZWCd	Wreck Cove Dioritic Suite	Neoproterozoic